NOTICE

The quality of this microform is heavily dependent upon the quality of the original thesis submitted for microfilming. Every effort has been made to ensure the highest quality of reproduction possible.

If pages are missing, contact the university which granted the degree.

Some pages may have indistinct print especially if the original pages were typed with a poor typewriter ribbon or if the university sent us an inferior photocopy.

Reproduction in full or in part of this microform is governed by the Canadian Copyright Act, R.S.C. 1970, c. C-30, and subsequent amendments.

AVIS

La qualité de cette microforme dépend grandement de la qualité de la thèse soumise au microfilmage. Nous avons tout fait pour assurer une qualité supérieure de reproduction.

S'il manque des pages, veuillez communiquer avec l'université qui a conféré le grade.

La qualité d'impression de certaines pages peut laisser à désirer, surtout si les pages originales ont été dactylographiées à l'aide d'un ruban usé ou si l'université nous a fait parvenir une photocopie de qualité inférieure.

La reproduction, même partielle, de cette microforme est soumise à la Loi canadienne sur le droit d'auteur, SRC 1970, c. C-30, et ses amendements subséquents.

A STUDY OF PHYSICAL AND BIOLOGICAL MECHANISMS OF CRYOINJURY AND CRYOPROTECTION OF HUMAN ERYTHROCYTES IN FREEZING PRESERVATION

Dayong Gao

A Thesis

in

The Department

of

Mechanical Engineering

Presented in Partial Fulfilment of the Requirements
for the Degree of Doctor of Philosophy at
Concordia University
Montreal, Quebec, Canada

March 1991

ISBN 0-315-64708-6

ABSTRACT

A STUDY OF PHYSICAL AND BIOLOGICAL MECHANISMS OF CRYOINJURY AND CRYOPROTECTION OF HUMAN ERYTHROCYTES IN FREEZING PRESERVATION

Dayong Gao, Ph.D.
Concordia University, 1991

In freezing preservation of biological cells, low temperature is used to keep cells dormant but potentially alive. However, there is an apparent contradiction between the purpose of the preservation and experimental findings that the cells are often injured by the freezing process itself. This thesis presents a study of the mechanisms of cryoinjury of cells and its prevention taking the human erythrocyte as the cell model and glycerol as a cryoprotective agent (CPA).

The major aspects of the investigation include (a) establishing an optimization technique to evaluate the separate effect of each of the influencing factors (e.g. cooling rate, warming rate, concentration of the CPAs, cell density, storage temperature, etc.) and their coupled interactions on the cryoinjury of cells; (b) studying the effect of some important experimental parameters on the characteristics of the freezing process in the cell suspension, including the temperature distribution throughout the sample, the movement of the interface between the frozen and unfrozen solutions, the generation

of thermal stress in the frozen cell suspension, and the crush of the frozen cell suspension; (c) evaluating the effect of mechanical interaction between the ice and cell membrane on the damage to the cell membrane during the freezing process; (d) investigating the functions of glycerol in protecting cells from the cryoinjuries caused by "thermal stress effect" and "osmotic shock", respectively.

From these investigations, some important mechanisms of cryoinjury and cryoprotection are verified or revealed. Optimal conditions for cryopreservation of the human erythrocytes have been determined, and important properties which a good CPA candidate should have are recommended. Furthermore, a general optimization technique used to seek the optimal cryopreservation conditions for a biological system has been developed.

ACKNOWLEDGEMENTS

I wish to express my sincere appreciation to my Ph.D. thesis supervisor, Dr. Sui Lin, for initiating the project and providing continued guidance and support throughout the investigation and the thesis preparation.

I am very grateful to Dr. J.A. Kornblatt of Department of Biology, Concordia University, for his excellent guidance and providing facilities and materials throughout the biological experiments of my Ph.D. project.

A special acknowledgement is due to Dr. F.M. Guttman of Department of Pediatric Surgery, Montreal Children's Hospital, McGill University for his continued interest in my Ph.D. project and providing facilities and materials in freezing preservation of the human erythrocytes.

I am grateful to Mr. D. Edgell, and Ms. E. Nuguid of Montreal Children's Hospital, Mr. C. Lamarche of the Physical Workshop of Department of Physics, Mr. J. Elliott and Mr. J. Sarruf of the Mechanical Engineering Laboratory at Concordia University for their expert technical assistances.

I am thankful to Mr. P. Chen of Department of Mathematics and Dr. D. Fairbairn of Department of Biology at Concordia University for their suggestions in the statistical analysis of the experimental data.

I appreciate very much Dr. P.F. Watson of Royal Veterinary College, University of London, U.K. for his suggestions and comments in preparing this thesis.

To my late grandmother, Xianfang Fu Gao, my father, Jia Gao and mother, Zhenping Zuo, for their helps and encouragement throughout my research work, I would like to extend my deep appreciation.

Finally an expression of deep love and gratitude is reserved for my dearest wife, Chi Liu for loving patience and support in all phases of this work.

To My Dear Wife, Chi Liu

CONTENTS

LIST OF FIGURES

LIST OF TABLES

CHAPTER 1

INTRODUCTION

Freezing preservation of living cells and tissues has been utilized in many medical, agricultural and industrial applications, such as, blood banking for transfusion, semen preservation for artificial insemination, organ preservation for transplantation, embryo preservation for embryo transfer, and food storage, etc. However, there is an apparent contradiction between cryopreservation and the experimental finding that a part of the preserved cells or tissues are often injured by freezing process itself. This contradiction has greatly limited the application of the freezing technique to the preservation of biomaterials.

The new era of the cryopreservation of biomaterials started in 1949 when Polge [1] accidentally found the function of glycerol in protecting rooster spermatozoa from cryoinjury. Since that time, many different compounds have been found to be glycerol-like cryoprotective agents (CPAs) [2]. By using the CPAs, successful cryopreservation protocols have been defined for some cell-types and tissues. Unfortunately, these successes currently cannot be extended to many other cell-types or tissues because of the lack of the understanding of the mechanisms of both cryoinjury and cryoprotection [3].

1.1. Survival of Cells in Vitro

1.1.1. Survival of Cells in Artificial Solutions

Usually, cells and tissues removed from warm-blooded animals can be kept alive only for a short time at the normal temperature of the animal in an artificial solution designed to provide some of the essential features of the environment within the animal [4]. Conditions that are usually controlled include temperature, pH, total osmotic pressure, glucose concentration, partial pressure of oxygen and carbon dioxide, and individual concentrations of various ions. Processes that take place within living cells can be broadly classified into two groups. First, there are physical processes identical to those that take place in nonliving systems, such as, passive diffusion of a solute down a concentration gradient. Secondly, there are biochemical processes that are the distinguishing feature of living material. The biochemical processes proceed by using metabolic energy, and often enzymatic catalysts are involved. Both the physical and biochemical processes are maintained by proper environmental conditions. The length of time for which different cells will live in vitro depends on the accuracy with which the more important characteristics of their normal environment have been mimicked. Especially, the provision of biochemical substrates to cells and removal of metabolic waste products from cells are two of the most important factors

determining the duration of cell survival.

1.1.2. Importance of Water for Cell Survival

The majority of living cells contain about 75-80% (by weight) of water which is very important for the cell's life. Water is the substrate that transports essential nutrients and waste products within living organisms. Each cell, and organelle within a cell, requires a critical balance of water so that it can function properly. In metabolism, water is the necessary reagent in any process that involves hydrolysis, condensation and redox reactions (i.e. most biochemical reactions). Many of the important chemical properties of macromolecules (e.g. nucleotides and proteins, etc.) in biological system, including conformational stability and biochemical specificity, depend on the interaction of their constituent groups with the surrounding solvent medium. These interactions are, in turn, markedly influenced by the structural features of liquid water and by structural changes in water caused by solutes and changes in temperature.

1.1.3. Survival of Cells in Low Temperature

The major effect of reduced temperatures on any system is the reduction of molecular motion which, for biological systems, has important consequences. The inhibitory effects of low temperatures on the biochemical and physical processes provide the basic means for achieving long-term cryosurvival or cryopreservation of cells and tissues. In

the extreme temperature reduction to absolute zero (-273.16°C) brings to a halt of all molecular motion and causes reactions or processes to cease. In practice, no changes of biological importance occur at temperature below -150°C [5]. However, cooling below 0°C but over -150°C brings about dramatic changes in biological systems, especially if the water in the intra- and extracellular media freezes and separates as ice, giving rise to a series of changes which may be lethal to cells. Therefore an understanding of the properties of water and its solutions is fundamental for the study of the cryoinjury in cryopreserved cells.

1.2. Water and Solutions

1.2.1 Water Structure

To a good approximation the structure of H_2O molecule can be regarded as a sphere of radius 0.282nm which has embedded in it two positive and two negative charges, placed at the vertices of a regular tetrahedron, as shown in Fig.1.1(a). The positive charges can be identified with those of the two hydrogen atoms and the negative charges with those of the two lone pairs of electrons in the electronic structure. The H_2O molecule thus has the ability to form four hydrogen bonds [6], with two proton donor and two proton acceptor sites. The spatial disposition of these sites gives rise to a three-dimensional hydrogen bonded network, with each oxygen atom surrounded by four other

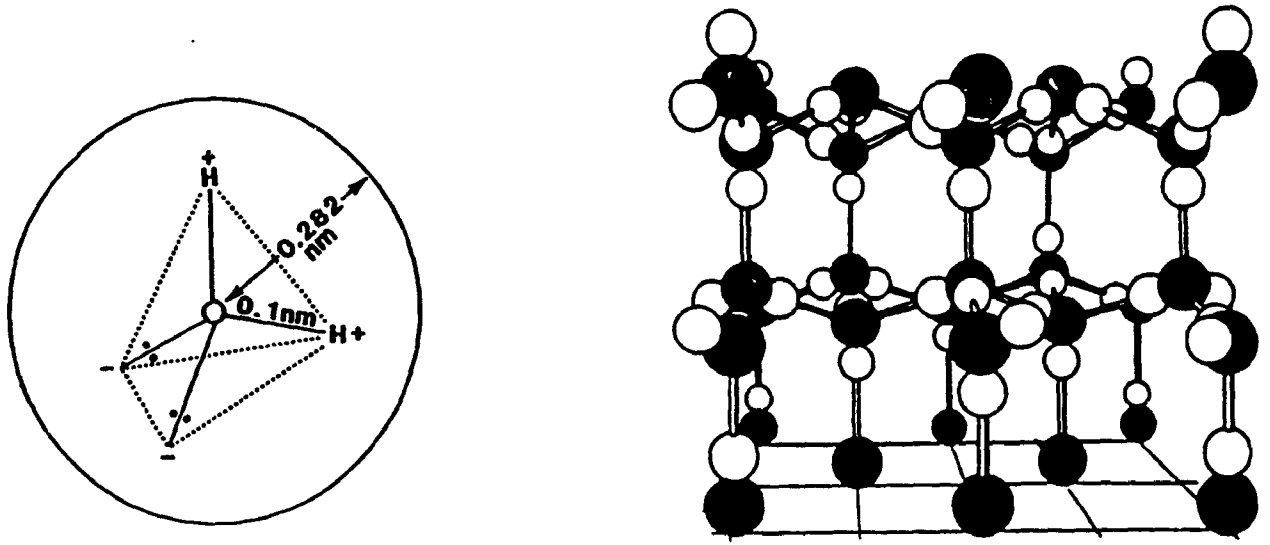

Figure 1.1: (a) The four-point-charge model of the water molecule. The oxygen atom is placed at the center of a regular tetrahedron, the vertices of which are occupied by two positive (hydrogen atoms) and two negative (lone electron pairs) charges, the O-H distance being 0.1 nm. The distance of closest approach of two molecules (van der Waals radius) is 0.282 nm.

(b) Crystal structure of 'ordinary' ice (Ih), showing the regular hexagonal lattice of oxygen atoms (dark circles) with one hydrogen atom (light circle) lying on each O-O axis. Each oxygen atom is thus hydrogen bonded to four other oxygen atoms, placed at the vertices of a regular tetrahedron.

oxygen atoms and with a hydrogen atom placed on each O-O axis. Ordinary hexagonal ice is the ideal manifestation of such an arrangement (Fig. 1.1(b)).

The ability of water to form and to accept hydrogen bonds (H-bonds) has important consequences for the cryopreservation of cells. The most important consequence is that water can bind both to cryoprotective agents and to the macromolecules on cell membranes through H-bonds, contributing to the stability of the tertiary and quaternary structures of the macromolecules [7].

1.2.2. Freezing of Water and Its Solutions

The phase or state of a substance (vapor, liquid, or solid) is dependent on temperature, pressure, and volume (Fig.1.2(a)) [15]. Figure 1.2(b) shows the effects of temperature and pressure on the phase of water with volume kept constant. At atmospheric pressure and 0°C, the liquid and solid phases are equilibrium. The "freezing point", 0°C, is actually the temperature at which ice and liquid water can coexist. Usually, when the temperature of water is lowered below the freezing point, water supercools rather than beginning to freeze immediately [7]. The diagram in Fig.1.2(b) also illustrates that the vapor pressure of supercooled water (dashed extension, smoothly continuous with steam line) is greater than the vapor pressure of ice (hoar frost line), and an increase of pressure lowers the freezing point of water.

Water may solidify by vitrification or crystalliza-

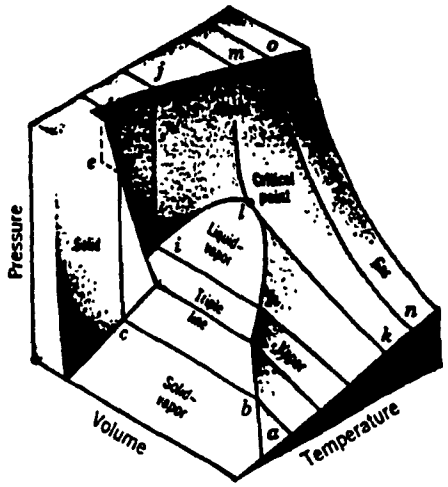

(a)

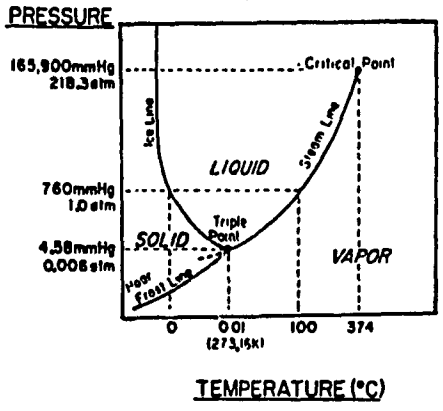

(b)

Figure 1.2: Phase diagram of water (not to uniform scale).
(a) The three-dimensional phase diagram illustrates the effect of varing temperature, pressure and specefic volume on the three phases of water: soloid, liquid, and vapor.

(b) The phase diagram of water kept at a constant volume.

tion. The term vitrification applies to the formation of an amorphous solid instead of crystal with organized structure, exhibiting a glassy appearance. The vitrification of water could be achieved by a ultra-rapid cooling [8], which quickly stops molecular motion without allowing sufficient time for a more organized structure to form.

For the ice-crystallization, a nucleating agent must be present. This agent can be water molecules clumped together via hydrogen bonds, or insoluble crystalline impurities which either appear crystallographically similar to ice or can interact with hydrogen binding sites of water [9]. The potential of an agent to cause nucleation is dependent upon its size and the temperature. As the temperature decreases below 0°C, the size requirement to initiate ice formation decreases. At -35°C, molecular aggregates of water can act as its own nucleators. Therefore, theoretically it is possible to supercool water to -35°C if nucleation particles are absent [10].

The physicochemical properties of liquid water change dramatically and discontinuously at its freezing point. For example, at 0°C the heat capacity (C_p) decreases by 50% if the water freezes. If the water is able to supercool, then C_p curve exhibits no discontinuity [11]. Similar effects are observed for most other physical properties, e.g. density and compressibility [12].

The properties of aqueous solutions are greatly affected by the solutes which dissolve into water.

Particularly, the so-called colligative properties [13] of a solution are functions of the number of solute molecules per unit volume of solution. These properties are the osmotic pressure, the freezing point, the boiling point and the vapor pressure of a solution. With an increase of the mole concentration of the solutes, the osmotic pressure and the boiling point of a solution increase, and the vapor pressure and the freezing point decrease. Ideally, the freezing point of a solution at atmospheric pressure is decreased by 1.86°C if the concentration of solute is increased by one mole.

Once freezing starts, water in a solution first freezes and separates as ice. At some temperature below the freezing point of a solution, complete solidification of both solvent and solute occurs. This temperature is termed the eutectic point of the solution. Thus, between the freezing point of a solution and the eutectic point there exists a mixture of ice, water and solutes. The dissolved solutes cannot become incorporated into the crystalline structure of ice. This implies that the concentration of solutes increases in the water which remains in liquid form. As solute concentration increases with decreasing temperature, the solubilities of different solutes are altered and nonhomogeneous precipitation results, significantly altering the pH of the existing solution [14]. Besides, the rate of cooling and warming has important consequences during the freezing and thawing of a

solution. Within a solution, the number of ice nuclei that form after freezing has been initiated, the rate at which they grow and the size they attain are all dependent upon the cooling rate at which heat is removed from the immediate environment. If water is slowly cooled below 0°C, ice crystals will develop around few nuclei that form first. As the temperature continues to fall, the crystals that are formed grow larger, rather than other new crystals being initiated because it is energetically more difficult to start a crystal than to promote the growth of a preexisting crystal [15]. Thus, with slow cooling rate, one obtains a small number of very large crystals. With a rapid cooling rate, however, the temperature quickly falls into a range where nuclei are more plentiful and there is insufficient time for the growth of large crystals; a myriad of very small crystals characteristically results. However, very small crystals, thermodynamically less stable than larger crystals because of their higher surface energies [16], are subject to recrystallization. Recrystallization is defined as the process by which crystals fuse with other crystals and thereby minimize their surface energies [17].

During warming, the rate at which ice crystals melt and the opportunity for crystal growth or recrystallization will depend on the warming rate at which heat is pumped into the system. A slow warming process enhances recrystallization [18].

For the freezing and thawing of a biological system, the cooling and warming rates are influenced by both the temperature gradients outside the biological system and the gradients within it, as determined by the thermal conductivity and specific heat of the system both in the liquid and frozen states, by its latent heat of fusion and by the overall geometry of the system. The effect of cooling and warming rates on the cryoinjury of cells will be discussed in the following sections.

1.3. Proposed Mechanisms of Cryoinjury

In the cryopreservation of cells, the methods of achieving the inhibition of cellular activity by low temperature are determined by principles of thermodynamics and heat transfer. Cellular responses to freezing are governed by physical and chemical properties of both the biological and physical systems involved, and they tend to establish a new set of equilibrium conditions, those of normal physiology having been disrupted. In principle, the cryopreserved cells may be injured by any physiologically abnormal alterations taking place in extra- or intracellular solutions during the cryopreservation.

Based on previous research work [19,20,21], it is known that the cryoinjury of cells occurs mainly during the cooling and warming processes rather than during the low-temperature storage period. The currently proposed mechanisms of cryoinjury in cells can be conceptualized as "Solution Effects", "Intracellular Ice-crystallization and

Recrystallization" , "Packing Effects" and "Thermal Stress Effects", etc.

1.3.1. Solution Effects

"Solution effects" concerns the cryoinjury of cells resulting from the alteration of concentration of solutes, especially, electrolytes in the extra- and intracellular solutions during the slow cooling and quick warming processes.

In the cooling process, when the temperature falls below the freezing point of the extracellular solution, water will first precipitate from the solution as ice. Once ice begins to form, the concentration of all dissolved substances in the residual extracellular liquid will increase. The concentrated extracellular medium makes a difference of osmotic pressure between extra- and intracellular solutions, which results in withdrawal of intracellular water from cells.

Lovelock [22] proposed that the increased concentration of solutes and the removal of water has deleterious effects on the lipid protein complexes of cell membranes, weakening them and increasing lipid and phospholipid losses. The cell is rendered permeable to cations and swells, eventually rupturing. Mazur [20] refered to Lovelock's theory on the concentrating solutes as "solution effects". He suggested that solution effects on cells are greatly enhanced in a slow cooling process during which the

time of the exposure of cells to a highly concentrated solution is prolonged. In consequence, the dehydration of cells is severe, the cell membrane becomes permeable to ions, and the extracellular ions penetrate into the cell. If the following warming process is very quick, the melting of ice will suddenly dilute the extracellular solution. In this case, the extracellular water will abruptly transport into the dehydrated cells, which causes the osmotic shock of cells i.e. the rupture of cell membrane (Fig.1.3). Smith [23] suggested that as the temperature falls and water is drawn out of cells, the solution becomes saturated with respect to the solute. A further decrease in temperature causes the solute to precipitate out at the eutectic point of that solution.

In contrast, Meryman [24] proposed that slow freezing injury in most cells is a result of decreased intracellular volume beyond a critical volume. As the cell reduces in size in response to increasing osmolarity, the compression of the contents enhances the resistance to further shrinking. This results in a hydrostatic pressure difference across the cell membrane, incurring cell membrane damage. Williams [25] measured the amount of water loss in several different cells at minimal temperatures. It was found that the amount of water loss, approximately 64% of cell volume was near equal for all cell types.

The dehydration of cells also results in abnormal cross-linking of intracellular structures. Levitt [26]

-GENERALLY ACCEPTED MECHANISM OF CRYOINJURY

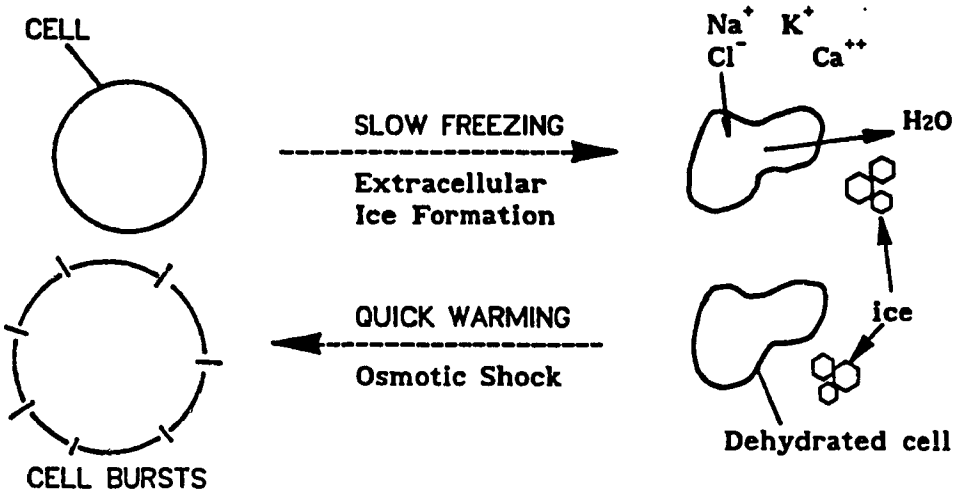

Figure 1.3: "Solution Effect". In the slow cooling process, the extracellular water first precipitates from solution as ice. Therefore, the concentration of extracellular solutes will increase, resulting in dehydration of cells. If the following warming rate is very quick, the melting of ice will suddenly dilute the extracellular solution, inducing the "osmotic shock" of cells.

theorized that loss of water from the protoplasm brings protein molecules into apposition, presenting the opportunity for the formation of new chemical bonds previously too distant and rigidly structured in hydrated form to permit combination. Thawing would have a disruptive force on the new combination, permitting unfolding and denaturation. Kendrew [27] showed that in myoglobin, the exterior of the protein is encased in a hexagonal water lattice, while the interior exhibits clathrate-like, pentagonal water structures. Karow and Webb [28] explained slow freezing injury as a consequence of the extraction of this bound water from cellular structures for incorporation into ice crystals, denuding proteins of lattice-arranged bound water essential to cell integrity.

Rall et al [29] observed that the survival of red blood cells correlated with salt concentration during freezing. Fishbein and Winkert [30] froze solutions of the enzyme catalase. Increased NaCl concentration was damaging to the enzyme; freezing in KCl solutions was less deleterious, suggesting that loss of activity of enzyme was due to acidification of the solution during slow cooling. Weist and Steponkus [31] found that red blood cells behave as osmometers in solutions as high as 3.5M salt concentration without reaching a minimum cell volume. Reports on the effects of dehydration of nucleated cells do not support the minimum cell volume hypothesis [32, 33].

Evidence that membrane fluidity is important for the

survival of the frozen and thawed cells was provided by Kruuv et al [34]. Yeast cells grown on different sources of fatty acids, which altered membrane fluidity, showed different rates of survival after freezing and thawing. Mironescu [35] found no correlation between cell size and survival after exposure of Chinese Hamster cells to hypertonic solutions. Close correlation was found between survival and loss of cellular K^+, assumed due to the onset of membrane leakage. Griffiths [33] assessed freezing damage to Chinese Hamster cells using specific radiochemical markers. Cell death was linked to a loss of membrane integrity, increased permeability to cations, and loss of cytoplasm.

Fahy [36] presented phase diagrams and analytic equations to determine the freezing point and the concentration of solutes in the unfrozen ternary systems NaCl-Water-Glycerol and NaCl-Water-Dimethylsulfoxide.

Although there are different explanations for the cryoinjury of cells caused by solution effects, it is generally accepted that slow cooling and quick warming enhance solution effects. If solution effects are the only reason for the cryoinjury of cells in freezing preservation, increasing the cooling rate still further would maintain good survival of cells. In fact, however, there is an optimal cooling rate for each cell-type. A faster cooling rate produces a rapid decline in the survival of cells [37] as shown in Fig. 1.4. This

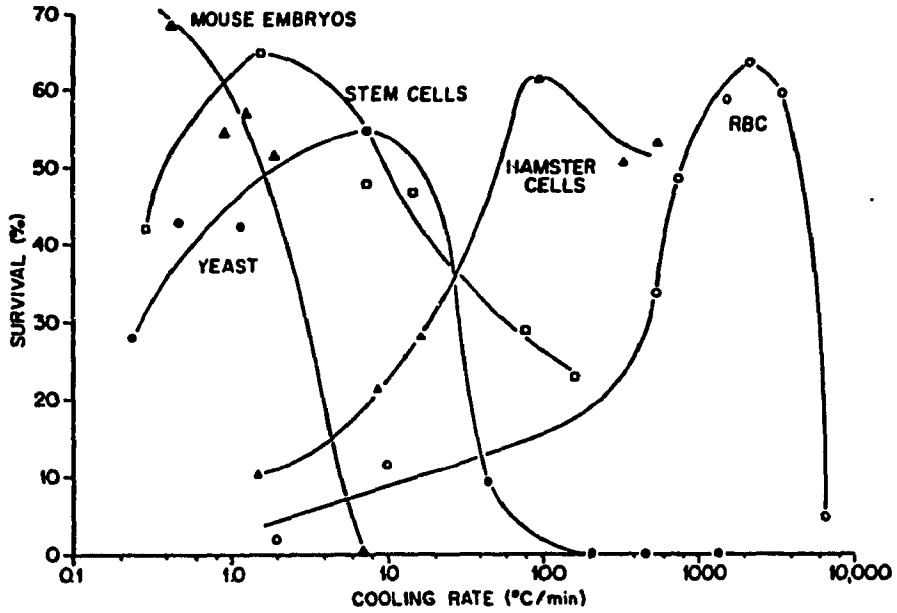

Figure 1.4: Relationship between survival and cooling rate in five types of cells. Stem cells refer to mouse marrow stem cells (adapted from Mazur [23]).

potentially indicates that there must be other mechanisms causing the cryoinjury.

1.3.2. Intracellular Ice-crystallization and Recrystallization

Mazur suggested a "two-factor" hypothesis [20] i.e. there might be two factors affecting the survival of the cells in freezing preservation. One factor is the "Solution Effects" discussed. Another one is the formation and growth of ice-crystals inside cells, which is mainly caused by quick freezing and slow warming processes.

The probability of intracellular ice-crystallization depends on the amount of water remaining in the cells at any temperature during cooling below the freezing point of water. Between -5 and -15°C, ice forms in the external medium, whereas the intracellular water remains unfrozen and supercooled, due to the fact that the plasma membrane block the growth of ice crystals into the cell [38]. In a rapid cooling process, the main events which take place in a biomaterial are the same as those in a slow cooling process which has been discussed. The important difference is that in a rapid cooling process, there is not enough time for the cell to lose sufficient supercooled water to reach osmotic equilibrium with its environment. The cell water continues to supercool and freezes interiorly [39] as shown in Fig.1.5.

Smith et al. [40] observed no intracellular ice-crystals in slowly frozen red blood cells. Rapatz and

-GENERALLY ACCEPTED MECHANISM OF CRYOINJURY

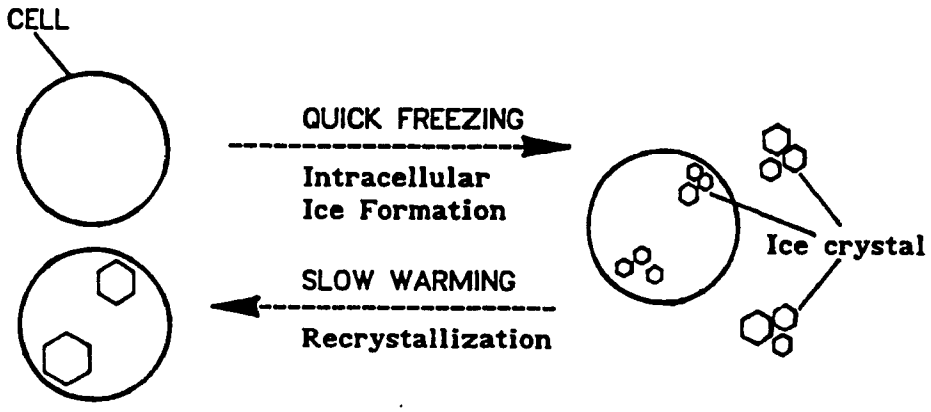

Figure 1.5: "Intracellular Icecrystallization and Recrystallization".
In the quick cooling process, there is no time for cell dehydration. Therefore, the intracellular ice forms. If the following warming rate is very slow, the growth of the intracellular ice, i.e. recrystallization will occur.

Luyet [41], using electron microscopy, found no ice crystals inside red cells after slow cooling but observed intracellular ice after rapid freezing.

Using freeze-fracture and etching technique, Mazur [42] and Fujikawa [43] provided strong experimental data for membrane damage of the cells caused by formation of intracellular ice.

Mazur [44] noted that yeast cells cooled at 100°C/min contained 79% of their original water at -50°C. He proposed that the value for the critical cooling rate which will produce intracellular crystallization is a function of the ratio of cell volume to cell surface area, and the cell permeability to water. Large spherical cells, and cells with low permeability to water, require a cooling rate lower than the critical rate of smaller, or more permeable cells.

Mazur [42] presented a series of equations which allow one to calculate the extent of supercooling in cells as a function of the cooling rate, the given cell permeability to water, its temperature coefficient, the initial osmolarity of the cell and the ratio of cell volume to surface area. To prevent intracellular freezing the water content of the cell must approach an equilibrium before intracellular ice formation occurs. In this way the probability of intracellular ice formation with cooling rate was calculated for yeast and human red cells. When the calculated survivals were compared with actual experimental

survival curves, the drop in survival coincided with an increase in the probability of intracellular freezing [42]. Leibo et al [45] observed the same pattern in unfertilized mouse ova (Fig.1.6) using a cryomicroscope which allows visualization of the ovum during controlled freezing processes.

Farrant et al [46] froze Chinese Hamster cells using a two-step cooling technique. Cells cooled rapidly to, and held at, a temperature just above that at which intracellualr nucleation occurs tolerate a second rapid cooling step to -196°C and rewarming. This suggested that the cells were sufficiently dehydrated at the holding temperature and contained few ice nuclei. Cells cooled to and held at a higher temperature in the first step contain ice nuclei, killing the cells. It was concluded that cell damage correlated with the total amount of ice formed per cell.

Fujikawa [43] studied membrane damage of human erythrocytes by freeze-fracture and freeze-etching techniques. The results were consistent with a direct damaging effect of intracellular ice crystals. He suggested that ice formation in direct contact with a membrane causes bilayer membrane molecular disruption which results in post-thaw hemolysis.

The effect of rate of warming on cell survival is strongly influenced by the prior rate of cooling. In almost all cases examined, cells that are cooled at supraoptimal

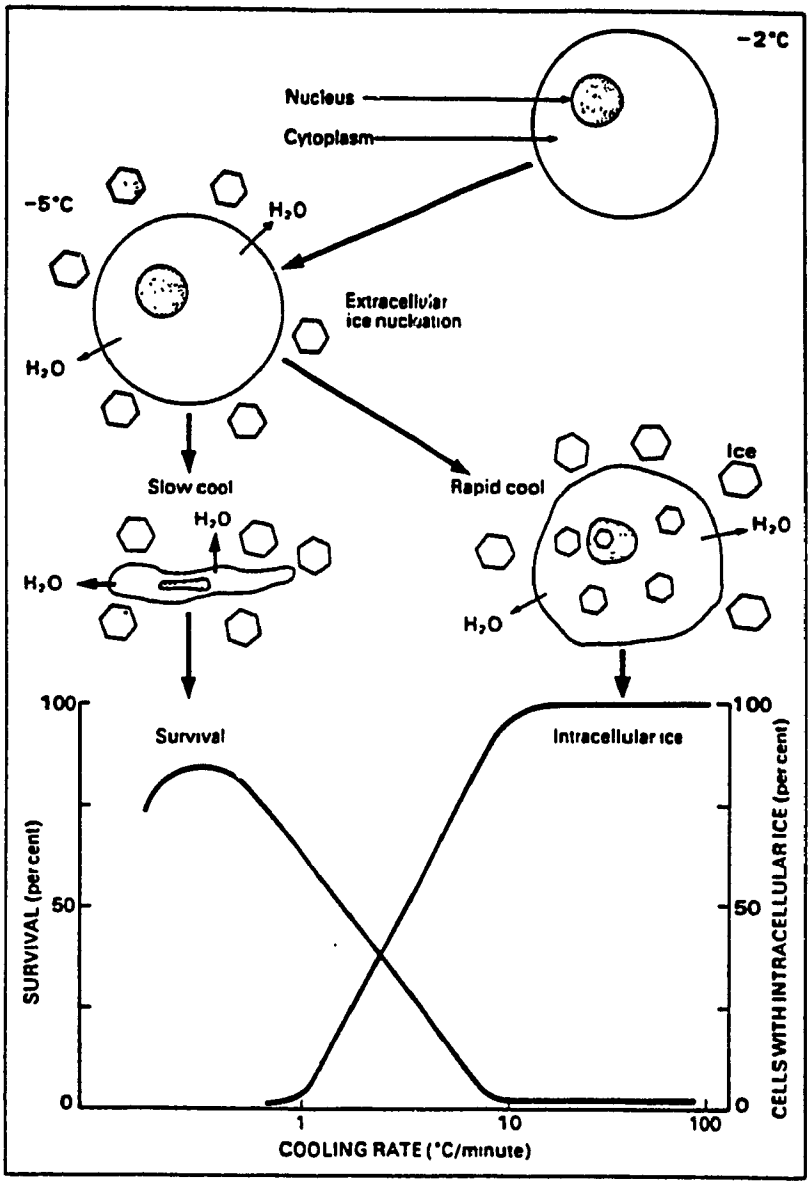

Figure 1.6: The illustration shows the behaviour of mouse ova at various subzero temperatures when cooled slowly and rapidly. The graph illustrates the decrease in survival which coincides with the increase in the number of embryos containing intracellular ice. (adapted from Leibo [31])

rates (i.e. rates sufficient to reduce intracellular ice) survive better when warming is rapid than when it is slow. Mazur and Schmidt [47] investigated the effect of warming rate on yeast and hamster cells. It was found that the high sensitivity of rapidly cooled cells to slow warming results from the growth of intracellular ice crystals, i.e. recrystallization, to a damaging size by grain growth (small crystals disappearing as large ones grow). If warming is rapid, time does not permit the recrystallization to occur before the melting point is reached. As described above, Farrant [46] provided evidence that the critical factor is not only the size of intracellular crystals, but also the amount per cell which is allowed to achieve equilibrium during warming. A rapid warming process does not allow this amount of ice to be achieved.

The "two-factor" hypothesis has been considered as the classic basis for interpreting the cryoinjury of biomaterials in freezing preservation. Generally speaking, a slow cooling and quick warming process enhances "Solution Effects"; while a quick cooling and slow warming causes intracellular ice-crystallization and recrystallization. However, because of the complexity of cryoinjury in biomaterials, the "two-factor" hypothesis cannot explain other damage of cells during the freezing/thawing process. Recently, "Packing Effect" and "Thermal Stress Effect" on the cryoinjury of cells have been invoked.

1.3.3. Packing Effect

In 1970 and 1976, Nei [48,49,,50] investigated the survival of red cells during slow freezing at near-zero temperature. It was found that when the specimens were cooled, extracellular ice columns grew and advanced gradually, leaving enclosed unfrozen channels. Although a few cells are individually surrounded by ice columns, most cells were displaced and confined in the channels as shown in Fig. 1.7. As the temperature was lowered, the channels of unfrozen solution were narrowed and the confined cells became tightly packed. Some of the cells thus packed together were hemolysed during the freezing process down to $-10^{\circ}C$ and most of the remaining cells were also hemolysed during the warming process from $-10^{\circ}C$ to $0^{\circ}C$. It was also indicated that for the fixed cooling and warming process, the hemolysis of the cells increased with the increase of the initial cell concentration (i.e. number of cells per unit volume of cell suspension). Based on the experimental results and observations, Nei predicted that mechanical interactions between the packed cells and between the cells and ice walls may play important role in causing cryoinjury of the cells.

Mazur [51] suggested that the survival of human red cells during slow freezing at 2% hematocrit is dependent more on the magnitude of the unfrozen fraction in the sample than on the salt concentration in that unfrozen fraction. The cell damages may be mainly due to the shear

-GENERALLY ACCEPTED MECHANISM OF CRYOINJURY

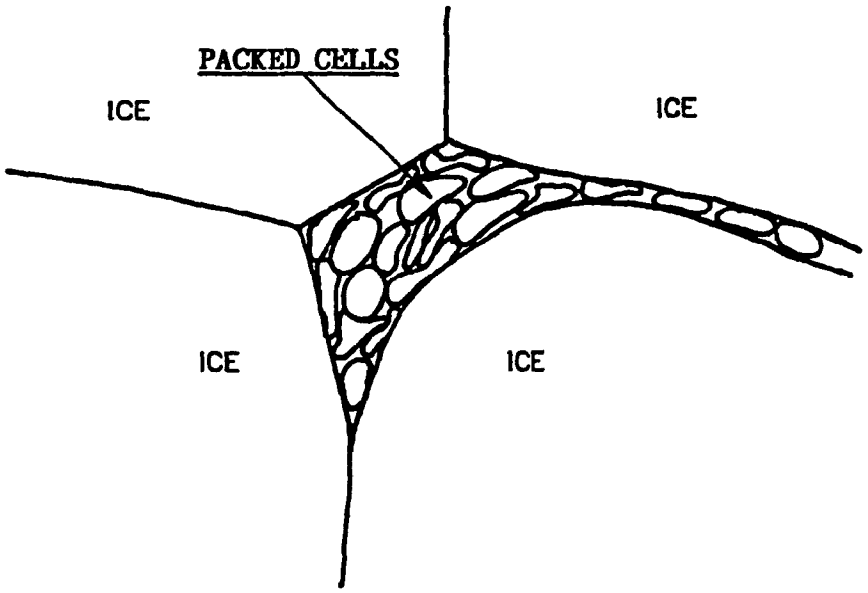

Figure 1.7: "Packing Effect". During the cooling process of a cell suspension, the cells will be highly packed in the unfrozen solution between ice walls. The interactions among the packed cells, and between the cells and ice walls may cause injury of cell membrane.

stress or cell deformation induced by interaction between cell and ice wall. But at high hemotocrits (40% or 60%), cell survival became dependent on both the unfrozen fraction and the salt concentration. He pointed out that when freezing occurs at high hematocrit, increasing numbers of cells are presumably brought into contact with their neighbors, i.e. highly packed. The interaction between packed cells may cause mechanical damage or membrane fusion damage. In 1984, Pegg [52,53] further investigated the effect of cell concentration on the cryoinjury of the human erythrocytes and invoked a "Packing Effect" i.e. "an inverse dependence of cell survival upon the proportion of the initial sample volume that is occupied by the cells."

1.3.4. Thermal Stress Effect

It is well known that the volume change of a solid material depends on the temperature and the thermal expansion coefficient of the solid. The thermal expansion coefficient varies with different materials.

One of the causes of mechanical stresses in a solid is nonuniform heating or cooling. When the temperature is raised or lowered, the elements of a body expand or contract. Such expansions or contractions generally are not uniform and hence cannot proceed freely in the body because of both the nonuniform temperature distribution in the body and the different material compositions of the body elements. Therefore mechanical stresses are set up in the body. This type of stress is so-called thermal stress. For

example, the fracture of glass when a surface is rapidly heated is attributable to the thermal stress.

It is obvious that the freezing process of a biomaterial during cryopreservation is a nonuniform cooling process. As shown in Fig.1.8, during the cooling process, the temperature at the outer part of a frozen biomaterial is lower than that at the inner part before the thermal equilibrium state is achieved. Therefore thermal stresses will be generated in the frozen biomaterial.

The effect of high thermal stress on the survival of biomaterials in cryopreservation was first emphasized by Rubinsky in 1980 [54]. Using a sphere as an organ model and water as a freezing medium, He calculated the thermal stresses inside the frozen organ during the freezing processes by computer simulation. He hypothesized that the higher the thermal stress, the worse the survival of cells.

Using cryo-electron microscope, Gupta [55] observed the serious deformation of erythrocyte membrane in frozen solution. Bank [56] observed a change in the ice structure during warming and its influence on the cell damage. Fujikawa and Miura [57] showed experimentally that the plasma membrane ultrastructural changes caused by thermal stress in the formation of extracellular ice was a primary cause of freezing injury in fruit-bodies of basidiomycetes. Using a freezing-etching technique, Fujikawa [43] demonstrated ultrastructural changes of the erythrocyte membrane caused by freezing process. Hornblower and Meryman

-GENERALLY ACCEPTED MECHANISM OF CRYOINJURY

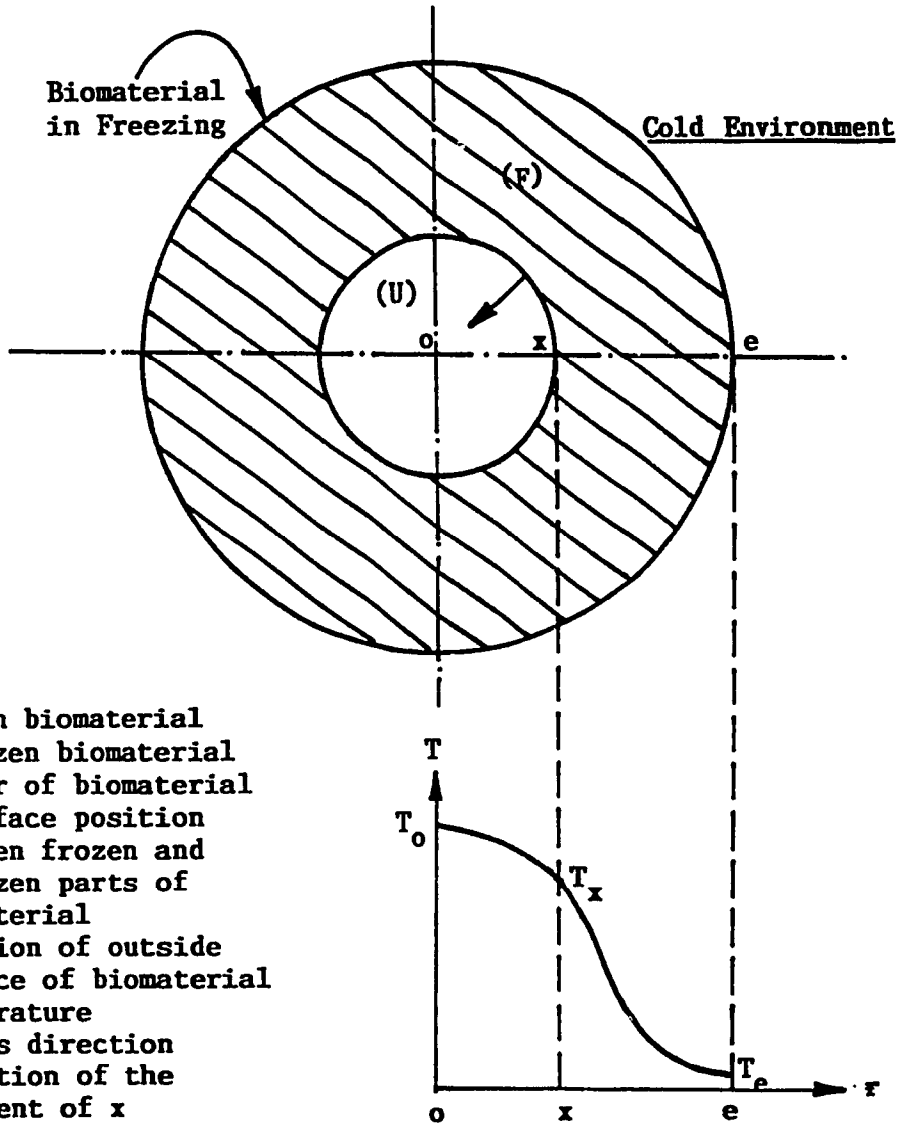

Figure 1.8: "Thermal Stress Effect". In freezing, the temperature distribution inside a frozen biomaterial is nonuniform, resulting in high thermal stresses in the biomaterial.

[58] noted the influence of the container material on the hemolysis of red cells after freezing and thawing.

In addition to the proposed four mechanisms of the cryoinjury described above, the experimental research also indicated that the dissolved gas inside the biomaterial [59], the kind of CPAs in use, the concentration of CPAs, the method with which a CPA is added and withdrawn from biomaterials [60], and the toxicity of CPAs themselves to biomaterials [61], etc, might also affect the survival of cells during the cryopreservation.

1.4. Cryoprotection

Based on the proposed mechanisms by which the freezing can damage cells, it is obvious that the cryoinjury of cells results originally from the conversion of the extra- and intracellular water into ice. Therefore, a direct and effective mode of preventing the cryoinjury of cells is to prevent the ice crystallization or reduce the amount of ice formation.

1.4.1. High Pressure Technique

A way to prevent ice crystallization is by the use of high pressure. The freezing point of water can be depressed to about -22°C by increasing the pressure to 2000 atm. This technique has been used alone and in conjunction with other protective procedures for the preservation of the biomaterials [62]. Unfortunately, apart from the technical

problems involved, it seems that pressures of this order can themselves cause baroinjury to living cells, particularly to the structure of cell membrane [63]. Several possibilities might be considered to explain its effects on the membrane components of living cells: (a) electromechanical breakdown due to membrane compression [64]; (b) pressure-induced phase transitions of the lipids in the membrane bilayer; (c) membrane compression leading protein units to reach completely through the membrane, and (d) breakdown of structured water around ions [65] and membrane components, such as proteins and phospholipids, changing reversibly or irreversibly the three-dimensional organization of these molecules.

1.4.2. Vitreous Technique

Another way of preventing the crystallization is by vitrification i.e. to cool the biological systems so rapidly that there is no time for the water molecules to assume an ice-like configuration before the temperature is below the glass transition point or, if micronuclei do form, that there is not enough time for them to grow. Luyet [66] predicted that if water in living cells could be vitrified, the viability of the system would be maintained. However, the attainment of this vitreous state in the absence of CPAs requires cooling rates of greater than 5000°C/sec [8]; these are probably impossible to obtain for the freezing preservation of majority of biomaterials.

1.4.3. Cryoprotective Agents (CPAs)

Since the epoch-making discovery of the beneficial function of glycerol against the cryoinjury in 1949 [1], the most feasible and effective means to reduce cryoinjury in cells has been the use of CPAs.

There are marked differences of the major functional groups and compositions of compounds that have cryoprotective efficiency. The list includes alcohols, amides, glycols, high-molecular-weight polysaccharides, mono- and disaccharides, proteins, inorganic salts, and several synthetic high molecular weight compounds of various chemical compositions. Figure 1.9 shows the commonly used CPAs which have been traditionally classified into two broad categories [67] according to their ability to penetrate the cell membrane.

(1) Penetrating Agents:

Penetrating agents, such as, glycerol and dimethylsulfoxide (DSMO) can penetrate the cell membrane and have relatively small molecular weight (200 or less);

(2) Non-penetrating Agents:

The nonpenetrating agents have molecular weights of approximately 10,000 to 150,000, and cannot penetrate the cell membrane.

The penetrating ability of a CPA is not only dependent on its molecular weight and size, but also on functional groups on the molecule; lipid-water partition coefficient; the permeability coefficient of the membrane to that agent;

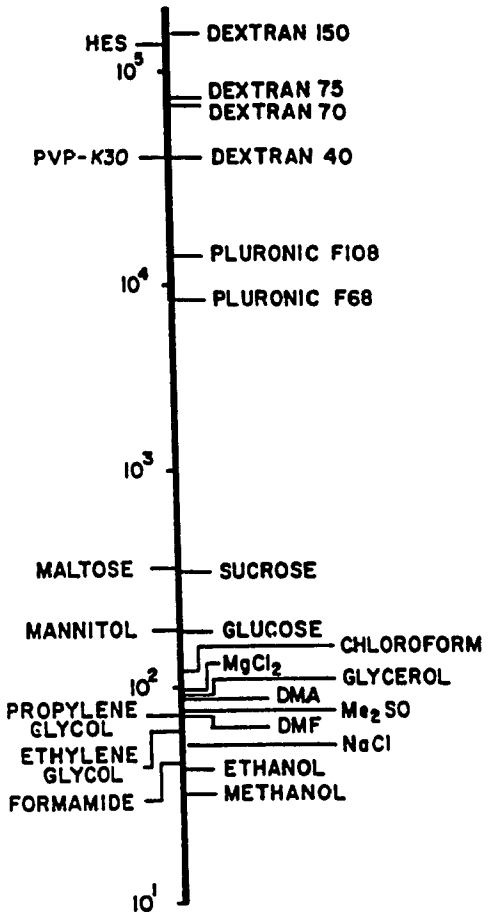

Figure 1.9: The commonly used cryoprotective agents (CPAs). The permeating CPAs, which have the greatest efficacy and applicability, have molecular weights in a narrow range near 100, despite their markedly different chemical structures. Non-permeating CPAs have reported mean molecular weights of approximately 10,000 to 150,000. Abbreviation: DMA, dimethylacetamide; DMF, dimethylformamide; Me2SO i.e. DMSO, dimethylsulfoxide; PVP, polyvinylpyrrolidine; HES, hyrdroxyethyl starch.

and the temperature at which the agent is administered [68].

Even though the mechanism of CPAs in preventing cryoinjury is not known clearly, several explanations of the mode of action of the CPAs have been put forth. Lovelock [69] found that the permeability of the cryprotectant was most important when using glycerol in a red cell system. Using Ca^{++} as a inhibitor for glycerol penetration through cell membrane, he found that if glycerol was able to penetrate the red cell, it had a protective effect. If Ca^{++}-treated red cells were exposed to glycerol, the cells became dehydrated, but were not protected against freezing damage. He proposed that the mechanism of cryoprotection afforded by glycerol and other permeating CPAs was based on a colligative action: the addition of these compounds to a biological system depresses colligatively the freezing point of the extra- and intracellular solutions and, once freezing has begun, reduces the mole fraction of solutes (primarily electrolytes) remaining in the non-frozen solution. At the same time the amount of ice that forms at a given sub-zero temperature is reduced. He concluded that an effective cryoprotectant should have low toxicity, be highly soluble, and a good cell permeator. Using these criteria, Lovelock and Bishop [70] were able to predict the effectiveness of DMSO as a CPA. In support, Meryman [71] demonstrated that 4M ammonium acetate, a CPA without demonstrable eutectic

point will protect the human red blood cell; whereas ammonium chloride, with a eutectic of -15.8°C, will not protect. The buffering effect was supported by Rasmussen and Mackenzie [72] who determined that the water-DMSO trihydrate has a eutectic point of -63±1°C. Meryman et al. froze human red cells in the presence of methanol, ethanol, glycerol, DMSO, ammonium acetate, sucrose and PVP. They showed that the action of the CPAs was purely colligative in the case of penetrating CPAs. The percentage of hemolysis was a function of the salt concentration. In addition, studies with sucrose and PVP indicated no cryoprotective function.

Luyet and Keane [73] attributed protection to a partial dehydration of the tissue. They suggested that characteristic chemicals having properties of easy penetration, low toxicity, efficiency of binding water and a low eutectic temperature could serve as CPA.

Further studies have cast doubt on the necessity of cellular penetration for cryoprotection. Mazur et al [74] studied the survival bovine red cells as a function of the permeation of glycerol and sucrose, and of human red cells under similar conditions [75]. For both cell types, varying intracellular glycerol concentration did not confer significantly greater protection to cells, indicating that extensive permeation is not required. Freezing cells with the nonpermeant, sucrose, conferred similar protection, but attempts to remove sucrose were deleterious.

Leibo and Mazur [37] indicated that glycerol permeation is not a requirement for protection in the eight-celled mouse embryo. A 20-second exposure to glycerol afforded the same protection as a 60-minute exposure. Furthermore, a 20-second exposure prior to freezing gave the same protection at 1, 10, 20, or 37°C. Taylor et al. [76] studied the permeability of glycerol and DMSO in hamster ovarian cells before cooling to -196°C. They found that glycerol may be regarded as a non-permeant at 2°C with a 30-minute incubation period; while DMSO was considered to be a good permeator under all conditions. Leibo et al [77] measured the cell volume of eight-celled mouse embryos photographically. Even after 90 minutes at 0°C, embryos in DMSO solution did not regain their original volume unless diluted back to original osmolarity. They concluded that DMSO permeates the cell very slowly, if at all, at 0°C, and thus protection does not require permeation.

Using a two-step cooling procedure, McGann [78] compared survival of Chinese Hamster ovary cells frozen with a penetrating agent, DMSO, and a non-penetrating agent, hydroxyethyl starch (HES). As the DMSO concentration was increased, the holding temperature for maximal survival decreased. Increasing the concentration of HES did not alter the holding temperature for maximal survival. Glycerol added to the cells at 20°C exhibited a pattern similar to DMSO; however, if added at 0°C, permeation of the cell was poor, and the pattern was similar to HES. He

concluded that both penetrating and non-penetrating agents protect by colligative action, allowing cell survival by decreasing the volume of water and reducing the likelihood of intracellular ice. Penetrating agents reduce cell water content at temperatures low enough to reduce the deleterious effects of increased solute concentration during slow cooling. Non-penetrating agents act by withdrawing water osmotically from the cell at higher temperatures suggesting little protection from increased solute concentration. In the latter case, slow cooling may be hazardous.

Lovelock's colligative theory does not, however, explain how nonpenetrating compounds, such as, sucrose, polyvinylpyrrolidone (PVP), or dextran act as cryoprotective agents. Furthermore, it does not explain the specificity of low molecular weight CPAs, since all of them will reduce the salt concentration during freezing. The latter objection, however, may in part be due to some intrinsic toxicity of different molecules. The fact that cryoprotective ability of the CPAs varies between different tissues is probably due to the interrelationship between physical factors and biological variability. The solubility of the agent, the eutectic changes it produces in a given system, the viscosity and temperature all affect the diffusion of the agent in a system, and its protection. Keane [79] suggested that hydrogen binding of the agent can be one factor of its variability. Karow [80] believed that

the hydrogen binding of CPAs may be related to the 'pseudo toxic' effect of glycerol, DMSO and dextran on cardiac muscle. He defined two effects of cryoprotectants: an intrinsic toxicity related to the chemistry of the cryoprotective agent, and a non-specific toxicity related to the concentration, the temperature of administration, and the duration of the exposure to the cryoprotective agent.

Several hypotheses have been proposed to explain the mechanism of protection of non-penetrating agents against cryoinjury in cells. Farrant [81] suggested that a polymer such as PVP may exhibit enhanced colligative properties at higher concentrations and may protect cells by lowering the external salt concentration at a given subfreezing temperature in a manner similar to penetrating CPAs. ..shwood-Smith et al [82] and Williams [25] noted that the cryoprotective properties reside in the ability of non-penetrating CPAs to alter the physical properties of solutions during freezing process rather than in direct effects on cell membranes. Korber and Scheiwe [83], on the basis of thermal analysis, suggested that a certain portion of water is absorbed by HES and kept from freezing. In their hypothesis, the protective action of HES against solution effects is attributed to its water absorptive capacity and to kinetics, rather than to a postponement of lethal solution effects to lower temperatures. MacKenzie [84] observed that polymers suppress the formation of salt

eutectics whose presence can be lethal.

Other theories have been suggested to explain the action of CPAs in different freezing systems, especially in view of the protective effect on the cell membrane. The hydrogen bonding theory [85] could account for the specificity of the CPAs. X-ray diffraction studies demonstrated that there is vitreous ice in rapidly frozen solutions of known cryoprotectants. The growth rate of ice in supercooled liquids with a variety of solutes is correlated with the mole equivalent of potential hydrogen binding sites provided by the solutes [86]. Multiple binding sites increase the protective action [87]. It is theorized that the CPAs establish hydrogen bonds with water, reducing the amount of water available for ice crystal incorporation, and promote the formation of vitreous ice. Karow and Webb [28] further indicated that hydrogen binding may act by stabilizing the hydration lattice surrounding proteins and reducing the probability of protein denaturation by desiccation during freezing. Slow cooling allows sufficient time for water lattices around proteins to grow and strengthen, thus providing protection. According to Meryman [68], at -20°C, 1 mole of glycerol binds 2 moles of H_2O and 1 mole of DMSO binds 3 moles of H_2O. Miller et al [88] tested the CPAs' ability to act as hydroxyl radical scavengers, which would prevent oxidation of protein sulfhydryl groups to intermolecular disulfide bonds. They found that both cryoprotectant and

scavenger efficiency decreased in the same order within a homologous series.

In a cell-free system, Tsutsayeva et al. [152] studied the mechanism of action of low temperature and cryoprotective agents on immune antitoxic antitetanus sera and globulins frozen in the presence and absence of polyethylene oxide. They suggested that the cryoprotective effect was due to the formation of a protective coat preventing protein dehydration precipitated by contact with ice; glycerol could protect through interaction of its hydroxyl groups with polar amino acid residues on the protein surface. Korber and Scheiwe [83] investigated the cryoprotective properties of HES by differential thermal analysis. They hypothesized that the protective action of HES differs from the colligative effect attributed to DMSO or glycerol because of its water absorptive capacity. Williams and Harris [89] studied the distribution of cryoprotective agents into lipid interfaces, and proposed that they protect cells by interaction with the plasma membrane by virtue of surface activity and/or distribution into membrane lipid. Barnett [90] found that glycerol and DMSO inhibit Na^+-K^+ ATPase of pig kidney medulla due to interactions with membrane lipids. Both agents lower the lipid transition temperature and increase membrane fluidity, rendering the membrane resilient to osmotic stress.

Alternate theories of cryoprotection do not reduce the

importance of a colligative action. They may serve to identify certain characteristics of agents which aid in freeze-thaw protection of cells in conjunction with the abiiity to prevent intracellular ice-crystallization and delay solute concentration. Cell water volume, sodium concentration, and potassium concentration were measured in human red cells under hypertonic conditions equivalent to freezing at -37°C with NaCl [91], sucrose, and DMSO [92]. It was found that the mass of cell water reached minimal values of approximately 40% of total cell water under isotonic conditions with sucrose and NaCl, while exposure to DMSO resulted in only a transient loss of cell liquid which attained near normal volumes after 5 or 10 minutes. It was shown that sucrose did not permeate the cell in the hypertonic solution, but labelled DMSO did enter the cell and replaced a certain proportion of cell water. Studies found that the onset of cation leakage occurred at approximately 1500, 2050, and 5350 milliosmoles for NaCl, sucrose and DMSO respectively. It was concluded that a cation leak developed at approximately 2000 milli- osmoles, and penetrating agents prevented cell shrinkage and cation leaks, postponing these damaging effects to higher osmolarities.

Alterations of membrane structure of Chinese Hamster Ovary cells under hypertonic conditions were observed by Mironescu and Seed [32] using scanning electron microscopy. Exposure to 2600 mOsm/kg NaCl produced minimal

changes. Above 2600 mOsm/kg, the microvilli and blebbing of the membrane were reduced, and cell locomotion ceased. At 7550 mOsm/kg, the cells were devoid of normal surface detail, and exhibited small perforations. With DMSO, at 7550 mOsm/kg, microvilli, blebs and ruffling activity were still present. Substituting sucrose as the hyperosmotic agent produced membrane changes, but were not the same as those produced with NaCl. The authors concluded that increased solute concentration dramatically altered surface microprojections of cells. The extent of alteration was mediated by the osmolality, duration of exposure and type of solute, and was mitigated by DMSO, suggesting an ability of DMSO to protect cells from hyperosmotic damage in addition to a colligative effect. Further studies failed to correlate survival of cells with cell size or sodium content [35], but found a close correlation with potassium loss suggesting that DMSO may regulate K^+ loss from the cell, which may be protective at low temperature in hypertonic medium.

In summary, the possible functions by which CPAs prevent cells or tissues from cryoinjury can be described as follows:

(1) Preventing "solution effect" by a colligative action by
    (a) reducing the concentration of electrolyte in biological system during the cryopreservation;
    (b) reducing cell dehydration;
    (c) reducing the fraction of solution frozen at any

given subzero temperature.

(2) Stabilizing the structure of macromolecules on cell membranes and preventing their denaturation through
   (a) hydrogen bond binding;
   (b) acting as a hydroxyl radical scavenger.

(3) Enhancing vitrification of cell water and preventing icecrystallization.

(4) Preventing cation leakage into the cells.

From the previous research on the function of CPAs in preventing the cryoinjury, it is generally accepted that most effective CPAs are those which can penetrate the cell membrane, i.e. penetrating agents which prevent both extra- and intra-cellular ice-crystallization. Two most cryoprotective and universally used penetrating CPAs are glycerol and DMSO. Therefore, the investigation of the cryoprotective function of glycerol and DMSO is particularly important to further reveal the cryoprotective mechanism of CPAs. In the present study, glycerol is employed both as a cryoprotectant and a research model.

1.5. Research Models

1.5.1. Glycerol

Glycerol is the simplest trihydric alcohol. It is colourless, viscous liquid, odorless when pure and has a sweet taste [93]. It is neutral to indicators. Its empirical formula, $C_3H_8O_3$, indicates the molecular weight,

92.09. This molecular weight is one of the smallest among all cryoprotective compounds used. Glycerol dissolves in water at any proportion, and the viscosity of its aqueous solution greatly increases with the reduction of temperature. Its structural formula, shows it to have two primary and one secondary hydroxyl groups. Its chemical nature is that of an alcohol, but because of the multiple hydroxl groups, it possesses possibilities for more than the usual number of reactions and derivatives. Being one of the basic precursor molecules of biochemistry, glycerol plays an important role in biochemical reactions, including the synthesis of lipids [94]. As one of the most important cryoprotective agents, glycerol presents a much lower chemical toxicity to cryopreserved biomaterials than does DMSO [95].

1.5.2. Human Erythrocyte

The human erythrocyte (red blood cell) is used as a research model of cryopreserved cells in the present study because of its simplicity in biology.

A mature human erythrocyte has no nucleus and contains no intracellular organelles. Essentially a bag of hemoglobin with relatively few other proteins, its function is to transport oxygen from lung to the tissues and carbon dioxide back to the lung [94]. Red blood cells can be obtained conveniently and in large quantities. Cryoinjury of the cells after freezing preservation usually can be quantified by measuring the release of hemoglobin.

An erythrocyte normally adopts the shape of a biconcave disk 7 μm in diameter as shown in Fig.1.10(a). Just as any other cells, the cytoplasm of an erythrocyte is bounded by a plasma membrane. Traditionally, the diameter of the erythrocyte is measured with the light microscope, with the cell lying flat on a glass slide, and the size and shape of the cell are measured with the cell hanging on edge [96]. Since the measurements with the light microscope have an uncertainty of approximately 0.5μm, Evans and Fung [97] used a dual-beam interference microscope to create image hologram of red cells, thereby improving the resolution of the light microscope by an order of magnitude. They measured the size of the human erythrocyte and described the cell shape by a mathematical formula.

The cytoskeleton of human erythrocyte forms a shell that lies under the entire plasma membrane and is attached to it at many points (Fig.1.10(b)). It is this structure that gives the membrane considerably mechanical strength, elasticity and flexibility [98, 99]. The original experiments and analyses indicate that the erythrocyte can be mechanically modeled as a thin elastic membrane [100,101,102]. The membrane has little resistance to bending [103] and a very large resistance to an increase in area [102]. It readily elongates in shear at constant surface area [101, 102]. It is "totally anisotropic: a continuum in two dimensions, and molecular character in the third dimension" [104]. It "behaves like a two-dimensional

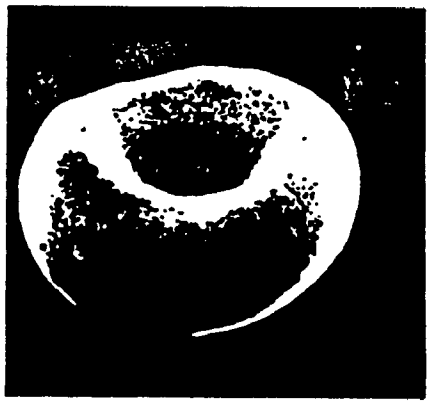

(a)

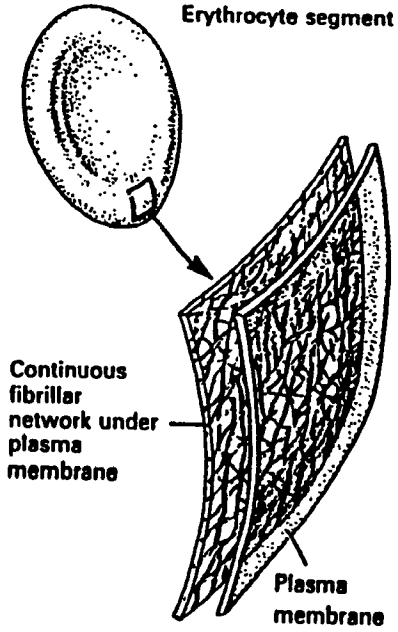

(b)

Figure 1.10: (a) The scanning electron micrograph of a normal disk-shaped human erythrocyte; the surface not visible is also concave. (adapted from Lux [116])
(b) Human erythrocyte contains a fibrillar cytoskeleton that underlies the entire plasma membrane and is attached to it at many points.

version of a soft, but nearly incompressible material [102].

Despite their variable composition, all biological membranes are thought to be constructed on a common pattern. Figure 1.11 shows the lipid-globular protein mosaic model of membrane structure [98]. All membranes contain a phospholipid bilayer as the basic structure unit. All phospholipids are amphipathic molecules: they have a hydrophobic portion and a hydrophilic portion. The primary physical forces for organizing biological membranes are the hydrophobic interactions between the fatty acyl chains of lipid molecules. These interactions result in the formation of a phospholipid bilayer, a sheet containing two layers of phospholipid molecules whose polar head groups face the surrounding watery surface while the fatty acyl chains form a continuous hydrophobic interior. Embedded in the membrane and attached to its surfaces are proteins which are very important for both structure and function of cells. They first catalyze biochemical reactions; secondly, receive signals from extracellular surroundings and transmit them to the cell interior; thirdly, act as anchors for cytoskeletal components and for components of extracellular matrix; and fourthly, control the passage of certain substances into and out of cells [98]. Because of the importance of the plasma membrane, damage to the cell membrane is usually lethal. During cryopreservation, as the first barrier of the cell to encounter the effects of

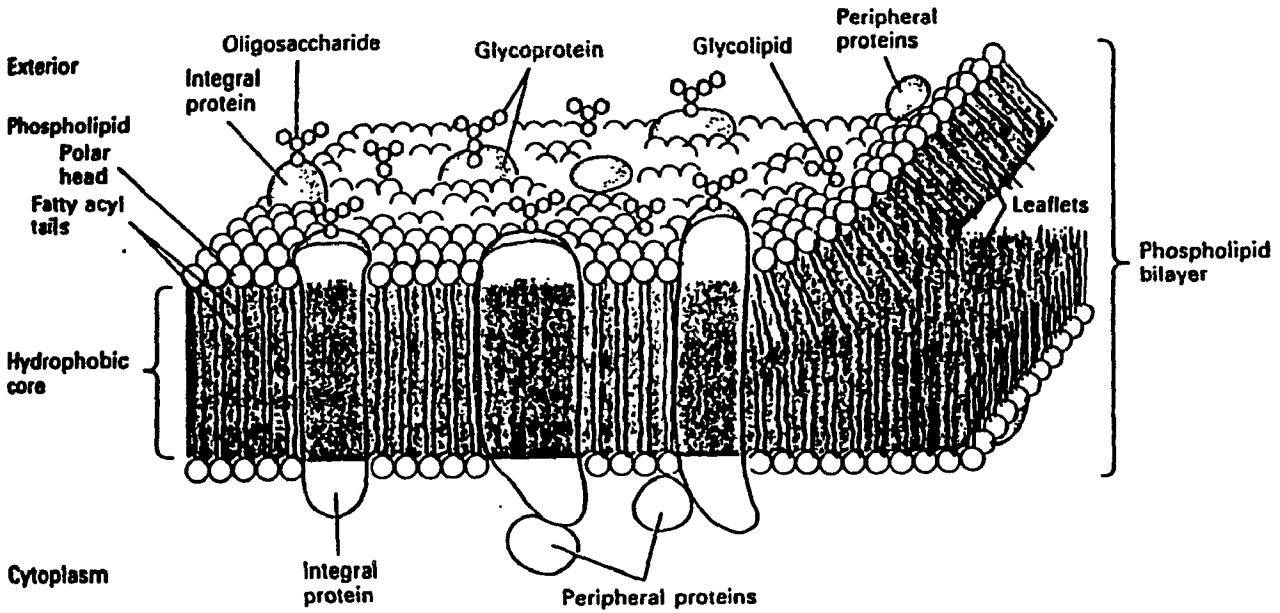

Figure 1.11: A general model of the structure of biological membranes. a phospholipid bilayer constitutes the basic structure. The hydrophobic tails of the fatty acyls from the middle of the bilayer, while the polar, hydrophilic heads of the phospholipids line both surfaces. Each half of the bilayer constitutes a leaflet. The integral proteins have one or more their regions embedded in the lipid bilayer, interacting with the fatty acyl chains in the hydrophobic cores. Peripheral membrane proteins are merely associated with the membrane by specific protein-protein interaction. Oligosaccharides and bound mainly to membrane proteins, forming glycolipids. Because proteins are visualized as free to move laterally in the two-dimensional lipid fluid, this model is often termed the fluid mosaic model of membrane.

extracellular freezing, the cell membrane is therefore a most sensitive and obvious site for the primary freezing injury in the cells.

1.6. Objective of Present Study

The imperative to use cryopreserved biological materials has highlighted a great concern that many cell-types and tissues have not been successfully cryopreserved by the freezing techniques and CPAs which are currently used. Therefore, a further study on the mechanisms of both cryoinjury and cryoprotection is required in order to develop new freezing techniques and CPAs.

The major purposes of this study are fourfold as follows: (a) establishing an optimization technique to evaluate the separate effect of each of the influencing factors (e.g. cooling rate, warming rate, concentration of the CPAs, cell density, storage temperature, etc.) and their coupled interactions on the cryoinjury of cells; (b) studying the effect of important experimental parameters on the characteristics of the freezing process in the cell suspension, including the temperature distribution throughout the sample, the movement of the interface between the frozen and unfrozen solutions, the generation of thermal stress in the frozen cell suspension, and the crush of the frozen cell suspension; (c) evaluating the effect of mechanical interaction between the ice and cell membrane on the damage to the cell membrane during the

freezing process; (d) investigating the functions of glycerol in protecting cells from the cryoinjuries caused by "thermal stress effect" and "osmotic shock", respectively.

From these investigations, important mechanisms of cryoinjury and cryoprotection are verified or revealed. Optimal conditions for the cryopreservation of human erythrocytes have been determined, and important properties which a good CPA candidate should have are recommended. Furthermore, a general optimization technique used to seek the optimal cryopreservation conditions for a biological system has been developed.

CHAPTER 2

SEPARATE EFFECTS OF INFLUENCE FACTORS AND THEIR COUPLED INTERACTIONS ON CRYOINJURY OF HUMAN ERYTHROCYTES

NOMENCLATURE

A	cooling rate, °C/min
B	warming rate, °C/min
C	hematocrit, %
D	molarity of glycerol in cell suspension, M
E	holding temperature, °C
f	degree of freedom
H	percentage hemolysis, %
S	sum of squares
V	mean squares
Y	transformed data of percentage hemolysis

Greek Symbols

ε	experimental error

2.1. Introduction

In cryopreservation of the human erythrocytes, there are at least five influence factors which affect the survival of the cells. They are the cooling rate, the warming rate, the hematocrit of the cell suspension, the concentration of cryoprotectant, and the holding

temperature at which the frozen cells are kept. In order to find an optimal condition for the cryopreservation, one usually has to test hundreds of combinations of the influence factors. This practically takes a long period of time and costs a lot of money. In addition, for some biomaterials, such as, mammalian eggs, embryos and human organs, etc., it is very difficult to obtain a sufficient number of the samples to support such a great number of tests.

Theoretically, even though the cryoinjury of the preserved cells is a function of all influence factors, some of the influence factors are potentially more significant for the cryoinjury than the others. Therefore, an optimal cryopreservation condition for the survival of cells may be achieved by properly controlling these more significant factors. Unfortunately, the extent of cryoinjury (e.g. percent hemolysis of the erythrocytes) of cells can be measured only after the freezing and thawing processes. In other words, the cryoinjury measured is a total consequence caused by all influence factors and their coupled interactions. Up to now, no effective method has been found to estimate the separate effect of each of the influence factors and their coupled interactions on the cryoinjury of the cells. Therefore, the relative significance or importance of the influence factors on the cryoinjury has not been known clearly.

In this chaper, an optimum seeking technique,

Fractional Factorial Design [105,106,107], is used to design experiments. The separate effect of each of the influence factors and their coupled interactions on the cryoinjury of the erythrocytes are evaluated by statistical analysis. Furthermore, the optimal combination of the factors for the survival of the cryopreserved cells is determined.

2.2. Experimental Materials and Methods

2.2.1. An Overview

In order to establish the best conditions for maintenance of any biological process, theoretically speaking, one should scan a countless number of conditions which are related to the process. This is clearly an impossible task. It is feasible, nevertheless, to establish a set of good or very good conditions that will permit the achievement of homeostasis. To determine the good conditions for cold preservation of red blood cells, we examined five interacting factors which potentially contribute to the cell's cryoinjury. The factors are cooling rate (section 2.2.3), warming rate (section 2.2.3), hematocrit (section 2.2.2), holding temperature (section 2.2.3), and glycerol concentration (section 2.2.2). Each factor was tested at three different levels, for instance, the hematorit at 2%, 11%, 60%. The tests, of which 243 are possible, can be evaluated by measuring the extent of hemolysis. We avoid testing all the possible combinations of the five interacting factors at each of the three levels. Instead, we chose 27 combinations using

the Fractional Factorial Design (section 2.2.4, Table 2.2 and 2.4) and determined the extent of hemolysis for these 27 selected combinations of the five factors.

The experimental data were evaluated by an analysis of variance (Table 2.6, and 2.7). A quantity, V_k (Mean Square) is calculated; it is this value that is used to determine the relative importance of each of the factors and their coupled interactions. The resultant data allow us to state the optimal combination of the factors and levels which will produce the least cryoinjury of the cells.

2.2.2. Preparation of Cell Suspensions

Human blood was obtained from the Red Cross Blood Bank of Montreal and stored at 4°C for not more than 3 days. The red blood cells were washed three times in Phosphate-buffered Saline (PBS) containing 1.86mM $NaH_2PO_4 \cdot H_2O$, 8.4mM Na_2HPO_4, 0.15M NaCl and pH 7.4. Then, the red cells were suspended at a hematocrit of about 15% in 1M, 2M, and 4M glycerol in PBS respectively. The suspensions were stored 24 hours at 4°C and then washed twice in the homologous diluant. The hematocrit was then accurately measured using a microhematocrit centrifuge at 12000g. Two aliquots were diluted appropriately to yield final hematocrits of 2% and 11%. The remainder was concentrated by centrifugation until the measured hematocrit was 60±2%. The maximum g force used in this preparation was 1500g.

2.2.3. The Cooling and Warming Procedures

Eight samples (0.8 ml for each) of the same cell suspension were used for each test. Four of them were placed into four stainless steel tubes (capacity of 0.8±0.1 ml) for the freezing and thawing tests; two of them were used as unfrozen controls, and the remaining two were totally lysed to determine total hemoglobin content. A copper-constantan thermocouple was placed into one of the samples in the stainless steel tubes; the temperature change of the sample was recorded by an automatic temperature recorder built into a cooling/warming rate controlled device (Controller and Cooling Chamber, Model No. CRF-4 FTS SYSTEMS, INC.). The cooling/warming rates that are reported here are average rates which were measured between -10°C and -60°C. Outside these limits the reported rates may differ from the actual rates.

(a) Cooling Rate:

(1) At -0.5°C/min. with a relative error of 10%. A holder containing 4 samples was placed into the cooling/warming rate controlled device. The heat exchanger was 2L of stirred ethanol. The cooling process stopped when the temperature of the sample reached -75°C.

(2) At -140°C/min. with a relative error of 3.5%. A holder containing 4 samples was lowered into a cooling bath of stirred ethanol at -75°C.

(3) At -850°C/min. with a relative error of 2.3%. A holder containing 4 samples was immersed in a tank

containing liquid nitrogen at -196°C.

After the cooling process, the frozen samples were either directly thawed, or held at -75°C or -196°C for one and a half hours before being thawed.

(b) Warming Rate:

(1) At 0.5°C/min. with a relative error of 10%. The four tubes containing the samples were allowed to warm in the cooling/warming rate controlled device. The warming process stopped when the temperature of the sample reached 20°C.

(2) At 25°C/min. with a relative error of 12%. The samples were thawed in the room air at 20°C.

(3) At 200°C/min. with a relative error of 7.5%. The samples were thawed in a stirred water bath at 35°C.

2.2.4. Design of the Experiment

The five factors with three different levels in the present study are shown in Table 2.1. Mathematically, there are 243 combinations of the five factors with three different levels. Therefore, 243 tests are required to determine the effects of the factors on the cryoinjury of the cells and to obtain the best one of the 243 combinations for the survival of the cells. By using the Fractional Factorial Design [105,106,107], only 27 of the 243 tests need to be performed. The 27 tests were chosen as required by the design table (Table 2.2) [106,107]. To set up the matrix for five interacting factors, we follow the

Table 2.1: Experimental Factors with three levels:

Level	Cooling rate (A)	Warming rate (B)	Hematocrit (C)	conc. of glycerol (D)	Holding* temperature (E)
1	-0.5°C/min.	+0.5°C/min.	2%	1M	-75°C
2	-140°C/min.	+25°C/min.	11%	2M	-
3	-800°C/min.	+200°C/min.	60%	4M	-196°C

* The holding temperature is the temperature at which the frozen cells are kept for one and a half hours. Level 2 of the holding temperature condition is "no holding" i.e. the frozen samples are thawed immediately without holding.

distribution shown in Table 2.2; for a different number of factors, a similar procedure is followed.

In Table 2.2, we use the following shorthands: capital letter A is cooling rate, B is warming rate, C is hematocrit, D is concentration of glycerol, and E is holding temperature condition. The numbers 1,2, and 3 in columns 1, 2, 5, 7, and 9 express the three different levels of the factors set in the columns. For example, from row 10 in Table 2.2, the five factors in the 10th test are, cooling rate at level 1 (-0.5°C/min), warming rate at level 2 (+25°C/min), hematocrit at level 1 (2%), concentration of glycerol at level 2 (2M), and holding condition at level 3 (kept at -196°C for one and a half hours). In summary, columns 1, 2, 5, 7, and 9 in Table 2.2 are used for setting/designing the factors, as well as used for the statistical analyses of the main effects of the factors. The remaining columns in Table 2.2 will be used for statistical analyses of the coupled interactions between the factors. The interaction between the cooling rate, A, and the warming rate, B, is expressed by AxB. Similar expressions, AxC, AxD, AxE, BxC, BxD, BxE, CxD, CxE, and DxE are used for the other interactions.

2.2.5. Measurement of Hemolysis

Cell damage was quantified by measuring the percent hemolysis as follows: the thawed samples (tested) from each stainless steel tube were centrifuged at 15,000g. Drabkin's [108] solution (0.77mM potassium cyanide, 0.61mM

Table 2.2: Original table of the Fractional Factorial Design

Test No. (i)	1 B	2 A	3	4	5 C	6	7 E	8	9 D	10	11	12	13	Results
1	1	1	1	1	1	1	1	1	1	1	1	1	1	
2	1	1	1	1	2	2	2	2	2	2	2	2	2	
3	1	1	1	1	3	3	3	3	3	3	3	3	3	
4	1	2	2	2	1	1	1	2	2	2	3	3	3	
5	1	2	2	2	2	2	2	3	3	3	1	1	1	
6	1	2	2	2	3	3	3	1	1	1	2	2	2	
7	1	3	3	3	1	1	1	3	3	3	2	2	2	
8	1	3	3	3	2	2	2	1	1	1	3	3	3	
9	1	3	3	3	3	3	3	2	2	2	1	1	1	
10	2	1	2	3	1	2	3	1	2	3	1	2	3	
11	2	1	2	3	2	3	1	2	3	1	2	3	1	
12	2	1	2	3	3	1	2	3	1	2	3	1	2	
13	2	2	3	1	1	2	3	2	3	1	3	1	2	
14	2	2	3	1	2	3	1	3	1	2	1	2	3	
15	2	2	3	1	3	1	2	1	2	3	2	3	1	
16	2	3	1	2	1	2	3	3	1	2	2	3	1	
17	2	3	1	2	2	3	1	1	2	3	3	1	2	
18	2	3	1	2	3	1	2	2	3	1	1	2	3	
19	3	1	3	2	1	3	2	1	3	2	1	3	2	
20	3	1	3	2	2	1	3	2	1	3	2	1	3	
21	3	1	3	2	3	2	1	3	2	1	3	2	1	
22	3	2	1	3	1	3	2	2	1	3	3	2	1	
23	3	2	1	3	2	1	3	3	2	1	1	3	2	
24	3	2	1	3	3	2	1	1	3	2	2	1	3	
25	3	3	2	1	1	3	2	3	2	1	2	1	3	
26	3	3	2	1	2	1	3	1	3	2	3	2	1	
27	3	3	2	1	3	2	1	2	1	3	1	3	2	
I_j														
II_j														
III_j														
S_j														

Potassium ferricyanide and pH 7.2) was prepared; an aliquot of each supernatant fluid was mixed with 4ml Drabkin's solution in order to convert hemoglobin into cyanmethemoglobin. 100 μl, 50 μl and 20 μl of the supernatant fluid with 2%, 11%, and 60% hematocrits were used respectively. The unfrozen controls (blank) and totally lysed (standard) samples were treated in the same way. The absorbance (Abs.) of the mixture of the supernatant with the Drabkin's solution was measured at a wave length of 540nm in a spectrophotometer. The percent hemolysis was defined as:

$$\text{Percent Hemolysis} = \frac{\text{Abs.(tested)} - \text{Abs.(blank)}}{\text{Abs.(standard)} - \text{Abs.(blank)}}$$

2.3. Experimental results and Statistical Analysis

The experimental results (percent hemolysis) from the 27 tests are shown in the last column in Table 2.3. The statistical analysis for the results is based upon the theory of the analysis of variance. The assumptions underlying the analysis of variance are:

(1) Experimental errors are random, independently and normally distributed about zero mean and with a common variance;

(2) Effects induced by the influence factors and their interactions on the experimental data are additive, and the following data structure is commonly assumed,

Table 2.3: The 27 tests designed by using Table 2.2, and the experimental results (percentage hemolysis, mean ± SEM).

Test No.	(A) Cooling rate (°C/min)	(B) Warming rate (°C/min)	(C) Hematocrit (%)	(D) Concentration of glycerol (*M*)	(E) Holding temperature (°C)	(H_t) Result (percentage hemolysis)
1	−0.5	+0.5	2	1	−75	35.00 ± 0.11
2	−0.5	+0.5	11	2	no holding	2.02 ± 0.10
3	−0.5	+0.5	60	4	−196	9.49 ± 1.50
4	−140	+0.5	2	2	−75	43.05 ± 1.12
5	−140	+0.5	11	4	no holding	53.95 ± 0.12
6	−140	+0.5	60	1	−196	99.45 ± 1.21
7	−800	+0.5	2	4	−75	77.86 ± 1.08
8	−800	+0.5	11	1	no holding	80.79 ± 1.25
9	−800	+0.5	60	2	−196	81.87 ± 1.22
10	−0.5	+25	2	2	−196	28.00 ± 1.11
11	−0.5	+25	11	4	−75	3.98 ± 0.92
12	−0.5	+25	60	1	no holding	100.00 ± 0.81
13	−140	+25	2	4	−196	83.95 ± 1.01
14	−140	+25	11	1	−75	28.00 ± 0.77
15	−140	+25	60	2	no holding	27.65 ± 2.16
16	−800	+25	2	1	−196	62.12 ± 1.19
17	−800	+25	11	2	−75	74.61 ± 0.38
18	−800	+25	60	4	no holding	97.21 ± 0.71
19	−0.5	+200	2	4	no holding	11.29 ± 0.75
20	−0.5	+200	11	1	−196	67.76 ± 0.74
21	−0.5	+200	60	2	−75	58.09 ± 3.09
22	−140	+200	2	1	no holding	25.00 ± 1.12
23	−140	+200	11	2	−196	19.61 ± 1.77
24	−140	+200	60	4	−75	33.43 ± 1.91
25	−800	+200	2	2	no holding	75.86 ± 0.73
26	−800	+200	11	4	−196	17.39 ± 0.23
27	−800	+200	60	1	−75	59.01 ± 1.71

Note. The combination of the five factors in each test above is from Table 2.

$$X_{ijklmn} = \bar{u} + A_i + B_j + C_k + D_l + E_m + + A_i \times B_j + A_i \times C_k + A_i \times D_l + A_i \times E_m + B_j \times C_k + B_j \times D_l + B_j \times E_m + C_k \times D_l + C_k \times E_m + D_l \times E_m + \varepsilon_{ijklmn}$$

where the interactions among three or more than three influence factors are omitted, and

X_{ijklmn}: experimental result generated from the test involving the influence factors A, B, C, D, and E at the levels i, j, k, l, and m, respectively. "n" means the *n*th repeated test.

$\bar{u}$: general mean of the experimental results.

A_i: main effect of factor A at level i.

B_j: main effect of factor B at level j.

C_k: main effect of factor C at level k.

D_l: main effect of factor D at level l.

E_m: main effect of factor E at level m.

$A_i \times B_j$: interaction between A_i and B_j; The similar expressions $A_i \times C_k$, $A_i \times D_l$, $A_i \times E_m$, $B_j \times C_k$, $B_j \times D_l$, $B_j \times E_m$, $C_k \times D_l$, $C_k \times E_m$, and $D_l \times E_m$, are used for the other interactions at the corresponding levels.

ε_{ijklmn}: experimental error.

In order to use Analysis of Variance on percentage data, one needs to make a suitable transformation of percentage such that the assumptions inherent in such an analysis can be better satisfied [109]. Here we used Arcsine

Transformation [109] to transform the percent hemolysis, H_i (i is the sequence number of the selected tests in Table 2.2, varying from 1 to 27); the transformed data Y_i (= $\text{Arcsin}(\sqrt{H_i/100})$) are shown in the last column of Table 2.4. In Table 2.4, I_j, II_j, and III_j (j is from 1 to 13) are the summations of the transformed data from the tests which respectively involve level 1, 2, and 3 of the factor set in column j. For instance: the factor B is set in column 1, and I_1 is the summation of the transformed data from the first nine tests, which involve level 1 of the factor B.

$$I_1 = Y_1 + Y_2 + Y_3 + Y_4 + Y_5 + Y_6 + Y_7 + Y_8 + Y_9$$

$$= 36.27 + 8.17 + 17.94 + 41.01 + 47.27 + 85.75 + 61.93 + 64.01 + 64.80 = 427.15$$

In Table 2.4, S_j is defined as follows:

$$S_j = 9 \times (\overline{I}_j - \overline{Y})^2 + 9 \times (\overline{II}_j - \overline{Y})^2 + 9 \times (\overline{III}_j - \overline{Y})^2$$

$$= (I_j^2 + II_j^2 + III_j^2)/9 - G^2/27$$

Where $\overline{I}_j = I_j/9$, $\overline{II}_j = II_j/9$, $\overline{III}_j = III_j/9$

$$\overline{Y} = G/27$$

$$G = \sum Y_i = 1234.49$$

In the above equations, $\overline{I}_j$, $\overline{II}_j$, and $\overline{III}_j$ are called the Variety-Means, S_j is called the Sum of Squares which

Table 2.4: The 27 selected tests from the 243 possible tests by using the Fractional Factorial Design technique, and the experimental results (percentage hemolysis)

Test No. (i)	1 B	2 A	3 A × B	4 A × B	5 C	6 A × D	7 E	8 A × C	9 D	10 A × E	11 A × C	12 A × D	13 A × E	Percentage hemolysis (Hi)	Transformed data (Yi)
1	1	1	1	1	1	1	1	1	1	1	1	1	1	35.00 ± 0.11	36.27
2	1	1	1	1	2	2	2	2	2	2	2	2	2	2.02 ± 0.10	8.17
3	1	1	1	1	3	3	3	3	3	3	3	3	3	9.49 ± 1.50	17.94
4	1	2	2	2	1	1	1	2	2	2	3	3	3	43.05 ± 1.12	41.01
5	1	2	2	2	2	2	2	3	3	3	1	1	1	53.96 ± 0.12	47.27
6	1	2	2	2	3	3	3	1	1	1	2	2	2	99.45 ± 1.21	85.75
7	1	3	3	3	1	1	1	3	3	3	2	2	2	77.86 ± 1.08	61.93
8	1	3	3	3	2	2	2	1	1	1	3	3	3	80.79 ± 1.25	64.01
9	1	3	3	3	3	3	3	2	2	2	1	1	1	81.87 ± 1.22	64.80
10	2	1	2	3	1	2	3	1	2	3	1	2	3	28.00 ± 1.11	31.95
11	2	1	2	3	2	3	1	2	3	1	2	3	1	3.98 ± 0.92	11.51
12	2	1	2	3	3	1	2	3	1	2	3	1	2	100.00 ± 0.81	90.00
13	2	2	3	1	1	2	3	2	3	1	3	1	2	83.95 ± 1.01	66.38
14	2	2	3	1	2	3	1	3	1	2	1	2	3	28.00 ± 0.77	31.95
15	2	2	3	1	3	1	2	1	2	3	2	3	1	27.65 ± 2.16	31.72
16	2	3	1	2	1	2	3	3	1	2	2	3	1	62.12 ± 1.19	52.01
17	2	3	1	2	2	3	1	1	2	3	3	1	2	74.61 ± 0.38	59.74
18	2	3	1	2	3	1	2	2	3	1	1	2	3	97.21 ± 0.71	80.38
19	3	1	3	2	1	3	2	1	3	2	1	3	2	11.29 ± 0.75	19.63
20	3	1	3	2	2	1	3	2	1	3	2	1	3	67.76 ± 0.74	55.40
21	3	1	3	2	3	2	1	3	2	1	3	2	1	58.09 ± 3.09	49.66
22	3	2	1	3	1	3	2	2	1	3	3	2	1	25.00 ± 1.12	30.00
23	3	2	1	3	2	1	3	3	2	1	1	3	2	19.61 ± 1.77	26.28
24	3	2	1	3	3	2	1	1	3	2	2	1	3	33.43 ± 1.91	35.32
25	3	3	2	1	1	3	2	3	2	1	2	1	3	75.86 ± 0.73	60.57
26	3	3	2	1	2	1	3	1	3	2	3	2	1	17.39 ± 0.23	24.65
27	3	3	2	1	3	2	1	2	1	3	1	3	2	59.01 ± 1.71	50.19
I_j	427.15	320.53	346.11	327.84	399.75	447.64	377.58	389.04	495.58	480.81	388.72	515.75	347.89		
II_j	455.64	395.68	442.90	490.85	328.98	404.96	431.75	407.84	373.90	367.54	402.38	404.44	468.07		
III_j	351.70	518.28	445.48	415.80	505.76	381.89	425.16	437.61	365.01	386.14	443.39	314.30	418.53		
S_j	641.03	2214.20	712.94	1479.32	1759.17	247.29	194.14	133.29	1182.73	819.94	179.90	2262.86	810.65		

Note. The transformed data Yi = arcsin ($\sqrt{Hi/100}$).

corresponds to the variation of the Variety-Means, and $\bar{Y}$ is the mean of all transformed data.

For example, for the 5th column, j = 5,

$$I_5 = Y_1 + Y_4 + Y_7 + Y_{10} + Y_{13} + Y_{16} + Y_{19} + Y_{22} + Y_{25}$$

$$= 36.27 + 41.01 + 61.93 + 31.95 + 66.38 + 52.01 + 19.63 + 30.00 + 60.57$$

$$= 399.75$$

Similarly one can obtain:

$II_5 = 328.98$

$III_5 = 505.76$

Hence, one can get:

$$S_5 = (I_5^2 + II_5^2 + III_5^2)/9 - G^2/27$$

$$= 1759.17$$

Using a Fractional Factorial Design in any experiment, there is aliasing of the factors' main effects and their coupled interactions. This simply means that a particular Sum of Squares (S_j) in the Analysis of Variance can be attributed to more than one effect or interaction. Table 2.5 indicates the aliasing present in this experimental design used in Table 2.2. In order to determine which effect is really significant it is often reasonable to assume, from physical or biological point of view, certain interactions to be negligible in size. With the aliases presented in Table 2.5, some will turn out to

Table 2.5: Aliasing of main effects and interactions between two factors in the experimental design used in Table 2.2.

No. of column in Table 2.	1	2	3	4	5	6	7	8	9	10	11	12	13
Aliasing of Main Effects and interaction	B	A			C		E		D				
	ExC		AxB CxD	AxB ExD	ExB	AxD BxC ExC ExB	BxC	AxC BxD		AxE BxD	AxC ExD	AxD	AxE CxD

NB. Where AxB is used to express the interaction between the factor of cooling rate (A) and the factor of warming rate (B). Similar expressions are used for the other interactions.

be negligible while the others will not be so. In that which follows, it will be shown how to determine which aliases fall into which category.

In the cold preservation of living cells, most changes in cell structure are directly or indirectly caused by lowering of the temperature i.e. the freezing process. The freezing process is practically controlled by the cooling rate. From previous cryobiological research it is known that the cooling rate is a dominant factor affecting the survival of the cells. First, the cooling rate dramatically affects the degree of supercooling of the cell suspension and the morphology of ice formation (e.g. the vitrification and ice-crystallization) which play important roles in the cryoinjury [110,111,112,113,114]. Additionally, the cooling rate also strongly affects the cryoinjury of the cells caused from the 'Solution Effect' and 'Packing Effect' [20,41,52]. Therefore, the coupled interactions between the cooling rate and each of the other factors should be investigated in the statistical analyses. These coupled interactions are A×B, A×C, A×D, and A×E. Each of them is potentially important but only A×B and A×D actually are (vide infra).

The research work of Mazur, Pegg and Nei [48,115, 116] indicated that the hematocrit of cells is related to the cryoinjury caused by the 'Packing Effect' which mainly takes place in the freezing process but not in the warming process. Hence, the interaction between the warming rate

and the hematocrit (B×C) may be neglected in the statistical analysis. Because the original concentration of glycerol will be changed or redistributed during the freezing process [29,36], the interaction between the warming rate and the original concentration of glycerol (B×D) may also be neglected.

From practical experience, holding temperatures below -50°C in short-term cold perservation of cells, such as a few hours, make almost no difference for cryoinjury of cells if the other experimental factors remain unchanged. In a first analysis, therefore, all the interactions between the holding temperature and each of the other factors, except the cooling rate, may be neglected.

In summary, the five interactions B×C, B×D, E×B, E×D, and E×C are neglected in the statistical analysis. The remaining aliases, the main effects, and the interactions between two factors are shown in the top row of Table 2.4. Interactions among three or more than three factors are, as usual, neglected in the statistical analysis. The statistical analysis of the experimental data in Table 2.4 is presented in Table 2.6. We treat each term A, B ... , and A×E as though it were pure but, each term contains, hidden, those interactions that were deemed negligible. Most importantly, the A×B term of column 3 and A×E term of column 13 contain C×D terms that may not be ignored. As a first approach, the interaction term C×D is neglected in the present study. The further studies are required to

Table 2.6: Statistical Analysis

Number of column in Table 4.	Factors and Interactions (k)	sum of Squares (S_k)	Degree of Freedom (f_k)	Mean Squares ($V_k = S_k/f_k$)
1	B	641.03	2	320.52
2	A	2214.20	2	1107.10
3&4	AxB	2192.26	4	548.01
5	C	1759.17	2	879.59
6&12	AxD	2510.15	4	627.54
7	E	194.14	2	97.07
8&11	AxC	313.19	4	78.30
9	D	1182.73	2	591.37
10&13	AxE	1630.59	4	407.65

NB. Where $S_B = S_1$, $S_A = S_2$, $S_{A\times B} = S_3 + S_4$, $S_C = S_5$, $S_{A\times D} = S_6 + S_{12}$, $S_E = S_7$, $S_{A\times C} = S_8 + S_{11}$, $S_D = S_9$, $S_{A\times E} = S_{10} + S_{13}$.

determine whether this interaction is really negligible in comparison with the other interactions.

In Table 2.6, V_k is called the Mean Squares and defined as:

$$V_k = S_k / f_k$$

where S_k is Sum of Squares and f_k is Degree of Freedom [105,107].

In the Analysis of Variance, the Mean Squares, V_k, indicates the relative significance of each main effect of the factors and their interactions. The larger is the value of the Mean Squares, the more significant is the corresponding main effect or interaction. Because the importance of the analysis is the relative significance among the main effects and interactions, a few relatively small values of the Mean Squares may be considered to be caused by the experimental errors and hence can be taken as the "Error Mean Squares"** which will be used in statistical significance tests. In Table 2.6, the values of the Mean Squares of factor E and interaction AxC are 78.30 and 97.07, which are the relatively small values in

---

** *This procedure to determine the Error Mean Squares is not totally rigorous. The Error Mean Squares can be determined rigorously based on the total original experimental data by the standard statistical method. However, this rigorously determined value of Error Mean Squares does not change the relative significance among the main effects and the interactions in the significance tests.*

comparison with the other Mean Squares. In the present study, they are taken as the Error Mean Squares. This also means that the main effect of the holding temperature, E, and the interaction between the cooling rate and the hematocrit, AxC, are considered to be not significant. The significance tests appearing in the last column of Table 2.7 are based on the statistical F-distribution [105,107].

2.4. Conclusions and Discussion

The conclusions resulting from the analysis of the variances (Table 2.7) are as follows:

(1) The effect of cooling rate is the most significant for the cryoinjury of the human erythrocyte.

(2) The main effects of hematocrit and the glycerol concentration, the coupled interaction between the cooling rate and the warming rate, and the coupled interaction between the cooling rate and the concentration of glycerol are next most significant.

(3) The main effect of warming rate, and the interaction between the cooling rate and holding temperature are less significant for the cryoinjury of the cells.

(4) The significance of the interaction between the hematocrit and the concentration of glycerol, CxD, can not be evaluated here. Further investigation concerning the effect of this interaction on cryoinjury of the cells is required.

Table 2.7: Analysis of Variance and Significance Tests.

Factors and Interactions (k)	Sum of Squares (S_k)	Degree of Freedom (f_k)	Mean Squares ($V_k = S_k/f_k$)	F_k (V_k/V_{error})	significance
B	641.03	2	320.52	3.79	-
A	2214.20	2	1107.10	13.09	**
AxB	2192.26	4	548.01	6.48	*
C	1759.17	2	879.59	10.40	*
AxD	2510.15	4	627.54	7.42	*
D	1182.73	2	591.37	6.99	*
AxE	1630.59	4	407.65	4.82	-
AxE + CxD	810.65	2	405.33	4.79	-
Error	507.33	6	84.56 (V_{error})		

Where $S_{error} = S_E + S_{AxC} = S_7 + S_8 + S_{11}$. $F_k = V_k/V_{error}$. The significance tests are based on the statistical F-distribution. '**' means very significant with $\alpha = 0.01$, '*' means relatively significant with $\alpha = 0.05$, and '-' means less significant with α near or less than 0.05. α is so-called the significant level and defined as a probability $\alpha = P(F_k > F_\alpha)$.

(5) Holding temperatures below -75°C are relatively not significant for the cryoinjury of the red cells.

The statistical analysis shows that the cooling rate is the most significant factor; the holding temperature below -75°C is relatively insignificant. These conclusion agree well with the existing cryobiological studies [41,110,111,112,117]. The warming rate is known to be an influence factor on the cryoinjury of the cells. Using statistical analysis to investigate the interactions between two factors, we found that the effect of the interaction between the cooling rate and the warming rate on the cryoinjury of the cells is more significant (α = 0.05) than the main effect of warming rate itself (α = 0.1). This conclusion suggests that the effect of the warming process on the cryoinjury of the cells depends not only on the warming rate itself but also on the cell suspension's frozen state which was determined by the cooling rate in the cooling process taking place before the warming process.

The mechanism of cryoprotection by glycerol has not been clearly understood. In the present study, the importance of the main effect of glycerol and the coupled interaction between the cooling rate and glycerol concentration on the cryoinjury of the cells is specially indicated by the statistical analyses. This potentially indicates that the cryoprotective function of glycerol may depend on how glycerol with the cooling rate together

modifies the freezing process and the frozen state of the cell suspension.

From the experimental results, the percent hemolysis of the cells at the hematocrit of 60% is much larger than that at the hematocrit of 2%; this agrees very well with the conclusion of Mazur [115] and Pegg [52]. From the statistical analysis, the effect of the interaction between the hematocrit and the cooling rate on the cryoinjury of the cells is less significant. This agrees well with Pegg's statement [52] that the 'Packing Effect' may have a different mechanism from the 'Solution Effect' and the effect of intracellular ice-crystallization, both of which are closly related to the cooling rate.

Furthermore, the optimal combination of the five factors for the survival of the red cells can be determined. From the statistical analysis, the effect of each level of each factor on cryoinjury of the cells can be evaluated directly. In Table 2.4, the values of I_j, II_j, and III_j reflect degrees of the main effects of levels 1, 2, and 3 of the factor set in column j on the experimental results (percent hemolysis) The smallest value of I_j, II_j, and III_j corresponds to the level which induced the smallest percent hemolysis of the cells. Because the main effect of factor A (cooling rate) is the most significant factor in this experiment, it should be determined first. In column 2 of Table 2.4, the value of I_A for the factor A (cooling rate) is the smallest. Thus

level 1 of the factor A was chosen as the best for the survival of the cells. In the same way, one could find that the level 2 of factor C (hematocrit) is the best for the survival of the cells. Because the significance of the main effect of factor B (warming rate) is smaller than that of the interaction A×B (the interaction between the warming rate and the cooling rate), one should analyse Table 2.8 to determine the best level of B. Since level 1 of the cooling rate has been chosen already, one only needs to analyse the interactions between the warming rate and the first level of the cooling rate from Table 2.8. The values in Table 2.8 reflect the effects of the coupled interactions between the corresponding levels of the factors A and B on the percent hemolysis of the cells. The smallest value in Table 2.8 corresponds to the smallest effect of the coupled interaction on the percent hemolysis. Because 62.38 in Table 2.8 is the smallest, one can chose the corresponding level 1 of factor B as the best level. As for factor D (glycerol concentration), its best level can be determined either from column 9 of Table 2.4 or from Table 2.9 because the effect of factor D itself and the interaction between factors A and D are on the same significance level ($\alpha = 0.05$). The best level of the factor D is level 3. Because the factor E (holding temperature condition below $-75^{\circ}C$ within one and a half hours) is not significant for the cryoinjury of the red cells, one may chose any level of the holding temperature

Table 2.8:. Effects of interactions between the cooling rate, A, and the warming rate, B.

A / B	1	2	3
1	<u>62.38</u>	174.03	190.74
2	133.46	130.05	192.13
3	124.69	91.60	135.41

NB. The number 1, 2, and 3 in the top first row and in the left first column represent the three different levels of factors A and B respectively. The values in this Table reflect the effects of the coupled interactions between the two factors on the cryoinjury of the cells. For example, the effect of the interaction between level 2 of factor A, (cooling rate at -140°C/min) and level 3 of factor B (warming rate at +200°/min.) is represented statistically as 91.60 which is the summation of Y_i (the transformed experimental data), from test No. 22, 23, and 24 which involve level 2 of factor A and level 3 of factor B, i.e. $91.60 = Y_{22} + Y_{23} + Y_{24} = 30.00 + 26.28 + 35.32$.

Table 2.9: Effects of interactions between the cooling rate, A, and the concentration of glycerol, D. The values in the Table were determined in the similar way as the values determined in Table 8.

A / D	1	2	3
1	181.67	147.70	166.21
2	89.78	99.01	185.11
3	49.08	148.97	166.94

below -75°C. The optimal combinations of the five factors and the corresponding cryoinjuries (percent hemolysis) are shown in Table 2.10.

Finally, it should be emphasized that, statistically, the optimal combination of the five factors is the best one of the 243 possible combinations in the present study. If the selected values in the three levels of the five factors are changed, one may find another best set of the new 243 combinations for the survival of the cells. However, in each case, instead of performing 243 tests, only 27 tests will be conducted by using the Fractional Factorial Design technique.

Table 2.10: The optimal combinations of the five factors for the survival of the cells and the corresponding experimental results.

Cooling Rate (^{o}C/min.)	Warming Rate (^{o}C/min.)	Hematocrit (x)	Conc. of Glycerol (M)	Holding Temperature (^{o}C)	Result (hemolysis) (x)
-0.5	+0.5	11	4	-196	1.00±0.04
				no holding	0.88±0.11
				-75	1.11±0.31

NB. These optimal combinations of the five factors are not involved in the 27 selected combinations using Fractional Factorial Design in Table 4. They are three of the 243 combinations.

CHAPTER 3

THERMAL STRESS IN THE FROZEN CELL SUSPENSION

NOMENCLATURE

C_p	specific heat at constant pressure, kJ/kg°C
E_1	Young's modulus of the material of the tube, Pa
E_2	Young's modulus of the ice, Pa
E^*	$= E_1/E_2$
k	thermal conductivity, W/m°C
L	latent heat of water freezing, kJ/kg
r	radial coordinate, m
R_1	outside radius of tube, m
R_2	inside radius of tube, m
S	thickness of ice (R_2- X), m
t	time, sec.
T	temperature, °C
T_b	temperature at outside surface of tube, °C
T_f	freezing temperature of water, °C
ΔT	temperature difference ($T - T_f$), °C
u	displacement, m
X	interface position between ice and water, m
z	axial coordinate, m

Greek Symbols

α	thermal diffusivity, m^2/sec
α_1^*	linear thermal expansion coefficient of the

material of the tube, 1/°C

α_2^* linear thermal expansion coefficient of the ice, 1/°C

α^{**} $= \alpha_1^*/\alpha_2^*$

β initial linear strain of ice, caused by the volume expansion during water solidification.

ν poisson's ratio

ρ density, kg/m^3

σ stress, Pa

ε strain

τ thickness of the brass tube wall, m

τ^* $= \tau/R_2$

Subscripts

1 tube

2 ice

t circumferential direction

r radial direction

z axial direction

3.1. Introduction

High thermal stress in frozen cell suspension is generally belived to be one of the reasons by which the cryopreserved cells are injured during the freezing process. Many experimental evidences have been published to show the "thermal stress effect" as described in Section 1.3.4 of Chapter 1.

In this chapter, a theoretical model is established to

simulate the freezing process of the cell suspension, and to investigate generation of the thermal stress and the effects of influence factors on the thermal stress.

As a first approximation, pure water is considered as the cell suspension medium (actually, the major component of the physiological medium is water). Because the cell suspension is usually contained in a long cylindrical test tube, the freezing process of the suspension takes place mainly in the radial direction. Hence, a one-dimensional freezing pattern is assumed in the present investigation.

From the analytical model, the ice-water interface position and the temperature distributions in the ice and the tube wall were transiently determined in a computer simulation. Based on the temperature distributions determined, thermal stresses were analysed by using the polycrystalline ice model. The effects of the following four factors on the thermal stress distributions in the ice and the tube wall were investigated: (a) the cooling rate of the freezing process, which is potentially reflected by the boundary cooling temperature, T_b; (b) the ratio of the Young's modulus of the tube material to that of the ice, E^*; (c) the ratio of the linear thermal expansion coefficient of the tube material to that of the ice, α^{**}; and (d) the nondimensional thickness of the tube wall, τ^*.

Experimental tests were performed to examine the numerical results obtained from the analytical model. Experimental data, such as, the temperature distributions

in the water-ice-tube system, the thermal strains on the inside and outside surfaces of the tube wall, and the water-ice interface position were compared with the numerical results. They agreed well with each other.

3.2 Experimental Equipment and Method

An experimental equipment was specifically designed and manufactured for testing the one-dimensional water freezing process in a cylindrical brass tube as shown in Fig.3.1. A design diagram of the equipment is shown in Fig.3.2. Eight copper-constantan thermocouples were assembled inside the tube in the radial direction to measure the temperature distributions in the ice and water. Two thermocouples were fixed, respectively, on the inside and outside surfaces of the tube wall to measure the surface temperatures. The thermal strains in the axial and circumferential directions on the inside and outside surfaces of the tube wall were measured by four strain gages (CEA-13-125UW-120). The two ends of the long brass tube were sealed by two thermal insulation covers. Each cover had an elastic membrane which allowed the ice to expand freely in the axial direction. A transparent plastic plate was assembled at the central cross-section of the brass tube. The tube can be opened at the central cross-section. The morphology of the ice and the ice-water interface positions can be observed or photographed directly through the transparent plastic plate. The

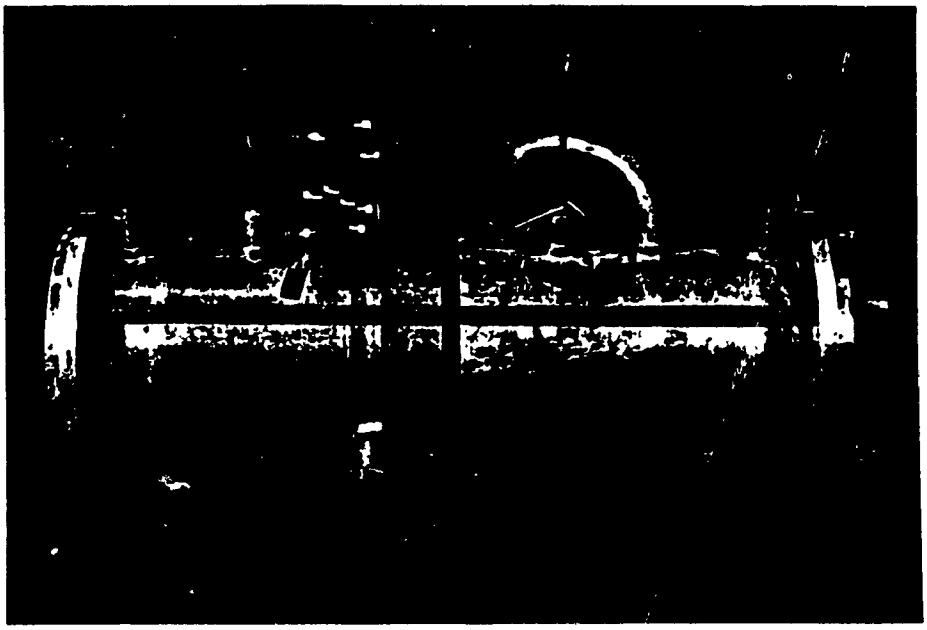

Figure 3.1: A photograph of the equipment used for the 1-D water freezing process in the brass tube.

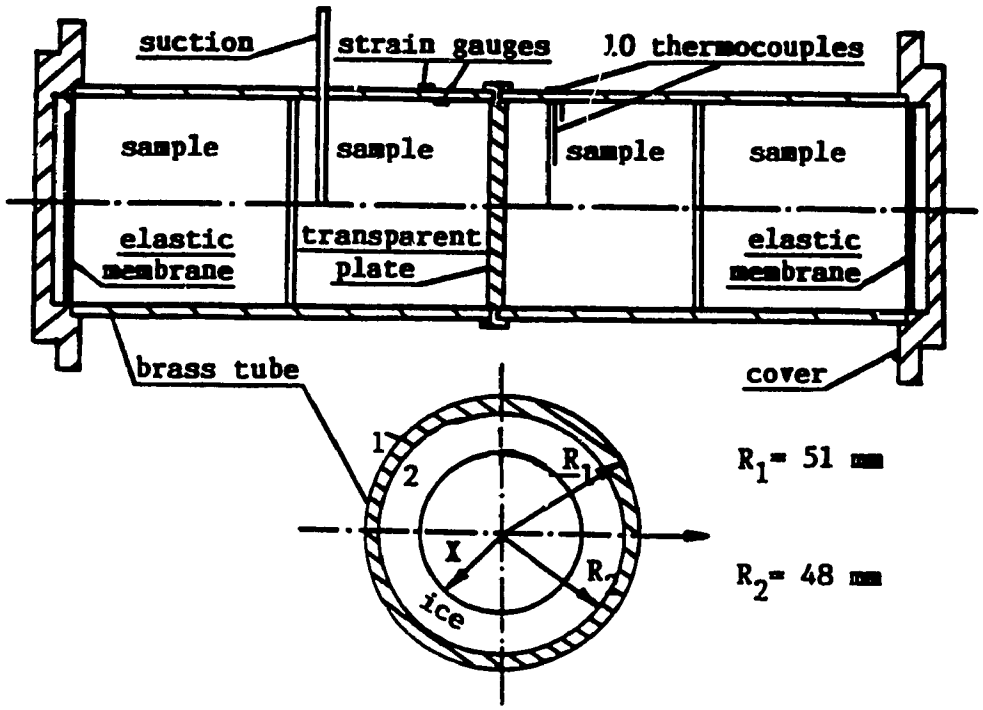

Figure 3.2: Schematic diagram of the equipment used for the 1-D water freezing process in the brass tube.

interface position can also be determined from the measured temperature distributions inside the water and ice during the freezing process.

Before starting a test, the water-filled brass tube was precooled in a tank filled with ice-water mixture, until the readings of all the thermocouples located inside the tube were 0°C. Then the tube was quickly immersed into a stirred cold ethanol bath which was placed inside a temperature controlled environmental chamber (Fig.3.3). The outside surface temperature of the brass tube was controlled at a constant value during each test. The variations of the temperatures and thermal strains measured were automatically recorded and stored in a personal computer. The absolute error for the temperature reading by using the thermocouples is ± 0.1°C. The absolute error for the strain measurement by using the strain gages is ± 0.5×10^{-6}.

3.3 Mathematical Formulation

The thermal stress analysis for the one-dimensional water freezing process inside the tube were conducted in two steps: first, solving the water freezing problem to obtain the transient water-ice interface position and the temperature distributions inside the ice and tube wall; second, determining the thermal stress/strain distributions in the ice and tube wall by using the temperature distributions obtained.

Figure 3.3: A photograph of the cooling rate control equipment.

3.3.1 Heat Transfer Process

In the following heat transfer formulation, it is assumed that the thermal properties of the tube material, the ice and water are constant; the coupling term caused by thermal stress [118] in the heat transfer governing equations may be neglected; and the water density change during the solidification may also be neglected. However, the density change is considered in the thermal stress analysis. Under these assumptions, the 1-D water freezing process taking place inside the tube, initially at the freezing temperature of water, can be formulated [119] in two time periods, separated at a specific time t^* at which the water inside the tube starts freezing.

Period 1. Before the time t^*, the heat transfer process takes place only in the tube wall:

Governing Equation:

$$\frac{\partial^2 T_1}{\partial r^2} + \frac{1}{r}\frac{\partial T_1}{\partial r} = \frac{1}{\alpha_1}\frac{\partial T_1}{\partial t} \quad \text{for } R_2 < r < R_1,\ 0 < t < t^* \qquad (2.1)$$

Boundary Conditions:

$$T_1(R_1, t) = T_b \qquad (2.2)$$

$$T_1(R_2, t) = T_f \qquad (2.3)$$

Initial Condition:

$$T_1(r, 0) = T_f \qquad (2.4)$$

Period 2. After the time t^*, the heat transfer process takes place in the tube wall and in the ice with the phase change of water.

Governing Equations:

$$\frac{\partial^2 T_1}{\partial r^2} + \frac{1}{r}\frac{\partial T_1}{\partial r} = \frac{1}{\alpha_1}\frac{\partial T_1}{\partial t} \qquad \text{for } R_2 < r < R_1,\ t > t^* \tag{2.5}$$

$$\frac{\partial^2 T_2}{\partial r^2} + \frac{1}{r}\frac{\partial T_2}{\partial r} = \frac{1}{\alpha_2}\frac{\partial T_2}{\partial t} \qquad \text{for } X < r < R_2,\ t > t^* \tag{2.6}$$

Boundary Conditions:

$$T_1(R_1,t) = T_b \tag{2.7}$$

$$T_1(R_2,t) = T_2(R_2,t) \tag{2.8}$$

$$k_1\frac{\partial T_1(R_2,t)}{\partial r} = k_2\frac{\partial T_2(R_2,t)}{\partial r} \tag{2.9}$$

$$T_2(X,t) = T_f \tag{2.10}$$

Initial Conditions:

$$T_1(r,t^*) = f(r,t^*) \qquad \text{known from Period 1.} \tag{2.11}$$

$$X(t^*) = R_2 \tag{2.12}$$

At the interface position:

$$L\rho_2\frac{dX}{dt} = k_2\frac{\partial T_2(X)}{\partial r} \tag{2.13}$$

In the above formulation, $T_f = 0^\circ C$, and T_b is a constant.

3.3.2. Thermal Stress Analysis

A theoretical thermal-stress analysis on the tube-water system in freezing faces the following two primary difficulties:

(1) The mechanical properties of the ice or the constitutive relations between the stress and strain in the ice have not been known clearly. They are greatly affected by many factors, such as, the temperature of the ice [120], the internal structure of the ice crystal [121], the

conditions of loading on the ice [122], the strain rate in the ice [123], and the impurities contained in the ice [124]. Because of the effects of these factors, there exists a wide variation of the ice mechanical properties quoted in the literature. Therefore, it is difficult to develop general constitutive relations for the ice.

(2) The initial strain of the ice caused by the volume expansion of the water during the freezing process is difficult to predict because the volume expansion is dependant on the ice internal structure which is often unknown and affected by many factors [125].

Due to these difficulties, simplifications have to be made for the thermal stress analysis. In the present model of the thermal stress analysis, it is assumed that the mechanical properties of ice are constant, and the characteristics of the isotropic polycrystalline ice may be applied to the analysis as a first approximation. For the isotropic polycrystalline ice, the brittle behaviour is characterized by the elastic deformation followed by a sudden fracture [121,126]. Therefore, the elastic theory may also be applied to the polycrystalline ice before its first fracture/crush occurs. After the crush of the ice, the strains and stresses in the ice and in the tube will be redistributed. These redistributions can not be predicted by the present model. Therefore, numerical predictions will not be valid after the time when the first crush of the ice occurs. In experimental tests, when the ice crushes inside

the tube, a sudden decrease of the strains on the tube wall can be observed from the strain gage record.

From the literature, the crush strength of ice varies in a range from 4×10^5 to 130×10^5Pa [121]. Comparing the experimental observations with the results of numerical calculation for the thermal stresses in the ice, it was found that the ice crush indeed took place when the maximum thermal stress in the ice reached this range of the ice crush strength. In the model of the thermal stress analysis, the crush of ice is therefore defined to be bound by the upper and lower limits as follows:

Upper limit: Maximum stress in ice = 130×10^5 Pa

Lower limit: Maximum stress in ice = 4×10^5 Pa

For the numerical analysis, the following additional assumptions are made: (1) the length of the brass tube is considered to be infinitely long; (2) the ice-tube system is mechanically in a quasi-equilibrium state during the freezing process; (3) the shear stress between the tube and ice may be neglected.

From the previous section, the temperature distributions in the ice and the tube wall are only function of radius r at any given time t. Based on the temperature distributions and the assumptions made, the thermal stress analysis can be simplified. For this axially symmetric plane-strain problem, only the following components of the displacement, strain, and stress of the

system are considered: u_{r1}, u_{r2}, u_{z1}, u_{z2}, ε_{rr1}, ε_{rr2}, ε_{tt1}, ε_{tt2}, ε_{zz1}, ε_{zz2}, σ_{rr1}, σ_{rr2}, σ_{zz1}, σ_{zz2}, σ_{tt1}, and σ_{tt2}.

The formulation of the thermal stress analysis is as follows:

Stress Equilibrium Equations:

$$\frac{\partial(r\sigma_{rr1})}{\partial r} - \sigma_{tt1} = 0 \tag{2.14}$$

$$\frac{\partial \sigma_{zz1}}{\partial z} = 0 \tag{2.15}$$

$$\frac{\partial(r\sigma_{rr2})}{\partial r} - \sigma_{tt2} = 0 \tag{2.16}$$

$$\frac{\partial \sigma_{zz2}}{\partial z} = 0 \tag{2.17}$$

Hooke's Law:

$$\sigma_{rr1} = \frac{E_1}{1+\nu_1}\left\{\frac{1-\nu_1}{1-2\nu_1}\varepsilon_{rr1} + \frac{\nu_1}{1-2\nu_1}(\varepsilon_{tt1}+\varepsilon_{zz1})\right\} - \frac{\alpha_1^* E_1}{1-2\nu_1}\Delta T_1 \tag{2.18}$$

$$\sigma_{tt1} = \frac{E_1}{1+\nu_1}\left\{\frac{1-\nu_1}{1-2\nu_1}\varepsilon_{tt1} + \frac{\nu_1}{1-2\nu_1}(\varepsilon_{rr1}+\varepsilon_{zz1})\right\} - \frac{\alpha_1^* E_1}{1-2\nu_1}\Delta T_1 \tag{2.19}$$

$$\sigma_{zz1} = \frac{E_1}{1+\nu_1}\left\{\frac{1-\nu_1}{1-2\nu_1}\varepsilon_{zz1} + \frac{\nu_1}{1-2\nu_1}(\varepsilon_{tt1}+\varepsilon_{rr1})\right\} - \frac{\alpha_1^* E_1}{1-2\nu_1}\Delta T_1 \tag{2.20}$$

$$\sigma_{rr2} = \frac{E_2}{1+\nu_2}\left\{\frac{1-\nu_2}{1-2\nu_2}\,\varepsilon_{rr2} + \frac{\nu_2}{1-2\nu_2}\,(\varepsilon_{tt2}+\varepsilon_{zz2})\right\} - \frac{\alpha_2^* E_2}{1-2\nu_2}\left(\Delta T_2 + \frac{\beta}{\alpha_2^*}\right) \tag{2.21}$$

$$\sigma_{tt2} = \frac{E_2}{1+\nu_2}\left\{\frac{1-\nu_2}{1-2\nu_2}\,\varepsilon_{tt2} + \frac{\nu_2}{1-2\nu_2}\,(\varepsilon_{rr2}+\varepsilon_{zz2})\right\} - \frac{\alpha_2^* E_2}{1-2\nu_2}\left(\Delta T_2 + \frac{\beta}{\alpha_2^*}\right) \tag{2.22}$$

$$\sigma_{zz2} = \frac{E_2}{1+\nu_2}\left\{\frac{1-\nu_2}{1-2\nu_2}\,\varepsilon_{zz2} + \frac{\nu_2}{1-2\nu_2}\,(\varepsilon_{tt2}+\varepsilon_{rr2})\right\} - \frac{\alpha_2^* E_2}{1-2\nu_2}\left(\Delta T_2 + \frac{\beta}{\alpha_2^*}\right) \tag{2.23}$$

Relations between Strains and Displacements:

$$\varepsilon_{rr1} = \frac{\partial u_{r1}}{\partial r} \tag{2.24}$$

$$\varepsilon_{tt1} = \frac{u_{r1}}{r} \tag{2.25}$$

$$\varepsilon_{zz1} = \frac{\partial u_{z1}}{\partial z} \tag{2.26}$$

$$\varepsilon_{rr2} = \frac{\partial u_{r2}}{\partial r} \tag{2.27}$$

$$\varepsilon_{tt2} = \frac{u_{r2}}{r} \tag{2.28}$$

$$\varepsilon_{zz2} = \frac{\partial u_{z2}}{\partial z} \tag{2.29}$$

where $\Delta T_1 = T_1 - T_f = T_1$, $\Delta T_2 = T_2 - T_f = T_2$, and β is the initial linear strain of ice, which is caused by the volume expansion of water during the phase change process.

For numerical calculations, the following six

equations are obtained from equations (2.14) to (2.29):

$$\frac{d}{dr}\left[\frac{1}{r}\frac{d(ru_{r1})}{dr}\right] = \frac{1+\nu_1}{1-\nu_1}\alpha_1^*\frac{dT_1(r)}{dr} \quad \text{for } R_2 < r < R_1 \tag{2.30}$$

$$\sigma_{rr1} = \frac{E_1}{1+\nu_1}\left[\frac{1-\nu_1}{1-2\nu_1}\frac{du_{r1}}{dr} + \frac{\nu_1}{1-2\nu_1}\left(\frac{u_{r1}}{r} + \frac{du_{z1}}{dz}\right)\right] - \frac{\alpha_1^* E_1}{1-2\nu_1}T_1(r) \tag{2.31}$$

$$\frac{d}{dr}\left[\frac{1}{r}\frac{d(ru_{r2})}{dr}\right] = \frac{1+\nu_2}{1-\nu_2}\alpha_2^*\frac{dT_2(r)}{dr} \quad \text{for } X < r < R_2 \tag{2.32}$$

$$\sigma_{rr2} = \frac{E_2}{1+\nu_2}\left[\frac{1-\nu_2}{1-2\nu_2}\frac{du_{r2}}{dr} + \frac{\nu_2}{1-2\nu_2}\left(\frac{u_{r2}}{r} + \frac{du_{z2}}{dz}\right)\right] - \frac{\alpha_2^* E_2}{1-2\nu_2}\left[T_2(r) + \frac{\beta}{\alpha_2^*}\right] \tag{2.33}$$

$$\frac{du_{z1}}{dz} = k_{z1} = \text{constant} \tag{2.34}$$

$$\frac{du_{z2}}{dz} = k_{z2} = \text{constant} \tag{2.35}$$

Equations (2.30) to (2.35) are subject to the following boundary conditions:

$$\sigma_{rr1}(R_1) = 0 \tag{2.36}$$

$$\sigma_{rr1}(R_2) = \sigma_{rr2}(R_2) \tag{2.37}$$

$$u_{r1}(R_2) = u_{r2}(R_2) \tag{2.38}$$

$$\sigma_{rr2}(X) = 0 \tag{2.39}$$

Under the assumption of no shear stress between the tube and the ice, the moment balance equations for the tube

and ice can be obtained respectively as follows:

$$2\pi \int_{R_2}^{R_1} r\sigma_{zz1}\, dr = 0 \tag{2.40}$$

$$2\pi \int_{X}^{R_2} r\sigma_{zz2}\, dr = 0 \tag{2.41}$$

Integrating equations (2.30) and (2.32) yields:

$$u_{r1} = \frac{1+\nu_1}{1-\nu_1} \frac{\alpha_1^*}{r} \int_{R_2}^{r} T_1(r) r dr + C_1 r + \frac{C_2}{r} \tag{2.42}$$

$$u_{r2} = \frac{1+\nu_2}{1-\nu_2} \frac{\alpha_2^*}{r} \int_{X}^{r} [T_2(r) + \frac{\beta}{\alpha_2^*}] r dr + C_3 r + \frac{C_4}{r} \tag{2.43}$$

Substituting equations (2.42) and (2.43) into equations (2.31) and (2.33), σ_{rr1} and σ_{rr2} can be determined. Using the boundary conditions, i.e. equations (2.36) to (2.39), and the moment balance equations (2.40) and (2.41), the six unknown constants C_1, C_2, C_3, C_4, k_{z1}, and k_{z2} can be obtained. Hence, all the strains and stresses can be determined from the Hooke's Law and the relations between strains and displacements.

3.4 Numerical Method

The Finite Difference Method was used to solve the 1-D heat transfer process taking place in the ice-tube system by using the Crank-Nicolson scheme [127] and Variable Space Grid technique [128]. Twenty-one nodes were set in the ice and 5 nodes in the tube wall along the radial direction for

the slow freezing processes (T_b>-5°C). More grids (up to 51 nodes in the ice and 15 nodes in the tube wall) were provided for quick freezing processes. The small time step was adjusted until the solution of the program was converged (small time steps, say, 10 seconds, were used for quick freezing processes, and larger ones, say, 2 minutes, for slow freezing processes). In solving the moving interface equation (2.13), the temperature gradient at the interface appearing in the equation was taken from the known value calculated through the previous time step. Using the temperature distributions calculated from the heat transfer program, a numerical integral method (Simpson's Rule) was applied to equations (2.40) to (2.43) to obtain thermal stress distributions in the ice and the tube wall.

In the computer simulation, the Young's Modulus of the ice, E_2, and the initial strain of the ice, β, were varied as control factors because they vary in certain ranges, i.e. 0.2×10^9Pa< E_2 <9.8×10^9Pa [121] and 0< β <0.03. The values of E_2 and β in Table 3.1 were determined by the computer simulation to have the best matching of the numerical results with all experimental data. After the determination of the values of E_2 and β, the freezing process and the thermal stresses in the ice-tube system were simulated by varying the values of the following four influence factors: the boundary temperature T_b, the Young's modulus ratic, $E^* = E_1/E_2$, the ratio of the linear thermal

expansion coefficient, $\alpha^{**} = \alpha_1^*/\alpha_2^*$, and the nondimensional thickness of the tube wall, τ^*. The thermal and mechanical properties of ice and brass are shown in Table 3.1.

3.5 Results and Discussion

Experimental tests were performed under three boundary temperatures (T_b): -5°C, -9°C, and -20°C. The numerical results and the experimental data are shown in Figures 3.4 to 3.14. Figure 3.4 shows the change of the thickness of the ice, $S = R_2 - X$, as a function of time, t, with the boundary temperature, T_b, as a parameter. It is expected that the lower the boundary temperature, T_b, the faster is the growth of the ice. Each curve in Figure 3.4 has an inflection point P at which the recession rate ($\frac{dS}{dt}$) is minimum. The physical reason for the existence of the inflection point can be explained as follows: During the freezing process, the recession rate is mainly dependent on two factors, i.e. the thermal resistance which increases with the growth of the ice; and the latent heat of the water solidification, which decreases due to the reduction of the internal unfrozen volume of the water in the cylindrical tube. The existence of the inflection point results from the interaction of these two factors. As a first approximation, taking the two factors into account with neglecting the sensible heat in comparison with the latent heat, the recession rate can be expressed as:

Table 3.1: The mechanical and thermal properties of the ice and the brass.

	k ($W/m^{\circ}C$)	C_p ($kJ/kg^{\circ}C$)	L (kJ/kg)	ρ (kg/m^3)
brass	52.0	0.385		8800
ice	2.0	2.18	333.84	910
	E (Pa)	ν	α^* ($1/^{\circ}C$)	β
brass	1.03×10^{11}	0.36	1.6×10^{-7}	
ice	2.50×10^{9}	0.31	5.5×10^{-7}	0.01

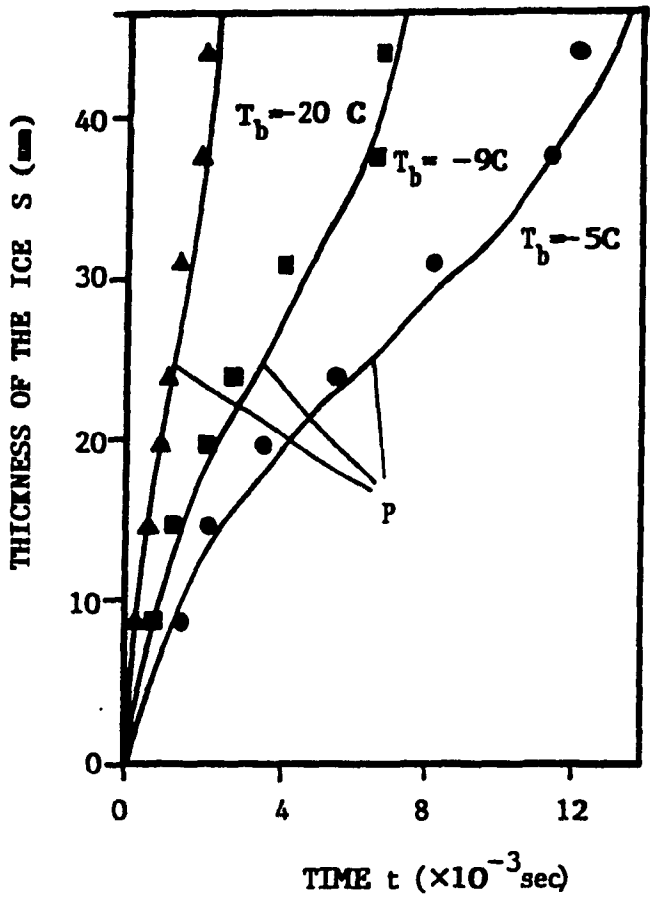

Figure 3.4: The thickness of the ice, S, as a function of time with T_b as a parameter. Point P indicates the inflection point of the recession rate ($\frac{dS}{dt}$).

● : test data for T_b=-5°C; ■ : test data for T_b=-9°C;

▲ : test data for T_b=-20°C; - : numerical results.

$$\frac{dS}{dt} = \frac{T_f - T_b}{X\left[\frac{\ln(R_2/X)}{k_2} + \frac{\ln(R_1/R_2)}{k_1}\right]\rho_2 L} \qquad (2.44)$$

From equation (2.44), it is clear that the recession rate decreases and then increases with the reduction of X from R_2 to 0. Therefore, the recession rate should reach a minimum value during the freezing process.

Figures 3.5 and 3.6 respectively show the temperature distributions and the corresponding circumferential stress distributions in the ice for T_b= -5, -9, and -20°C. They also indicate that the ice crushes at the interface positions X_1, X_2, and X_3. From Figures 3.5, and 3.6, it is found that the temperature distributions significantly affect the thermal stress distributions. The circumferential stresses, under which the ice crushes as shown in Figure 3.6, are within the range of the ice crush strength i.e. from 4×10^5Pa to 130×10^5Pa [121]. Figures 3.7 and 3.8 respectively show the distributions of the main strains and stresses inside the ice just before the ice crushes at X_2=36.0 mm with T_b = -9°C. From Fig.3.8, it is found that the circumferential compressive stresses inside the ice are much larger than the radial and axial stresses. The maximum circumferential compressive stress is located at the interface position between the ice and water. Therefore, it is expected that the compressive crush of the ice takes place first at the interface, and then propagates

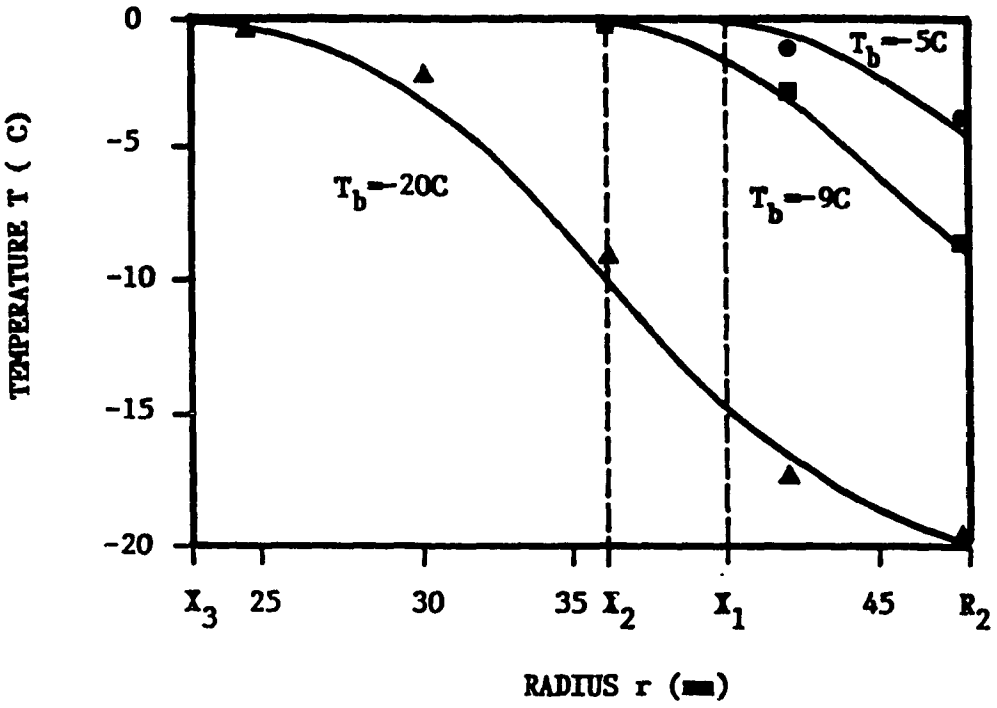

Figure 3.5: The numerical and experimental results for the temperature distributions in the ice at the time when the ice starts to crush at the interface position X_1, X_2 and X_3, respectively.

● : test data for T_b=-5°C; ■ : test data for T_b=-9°C;

▲ : test data for T_b=-20°C; - : numerical result.

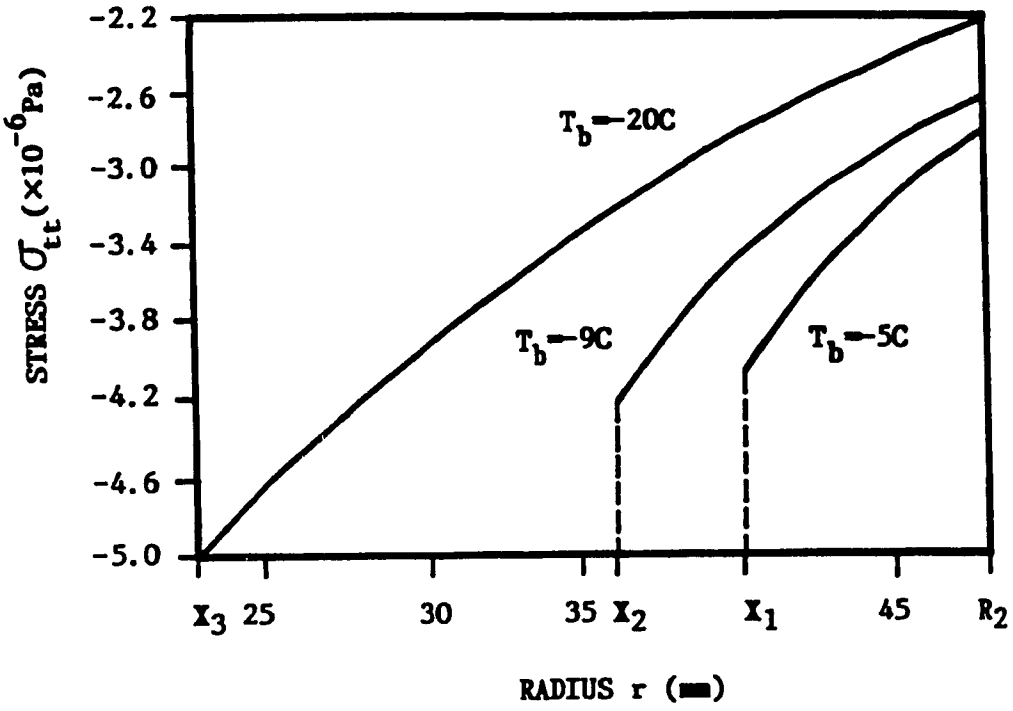

Figure 3.6: The circumferential stress distributions (numerical results) in the ice at the time when the ice starts to crush at the interface positions, X_1, X_2 and X_3, respectively.

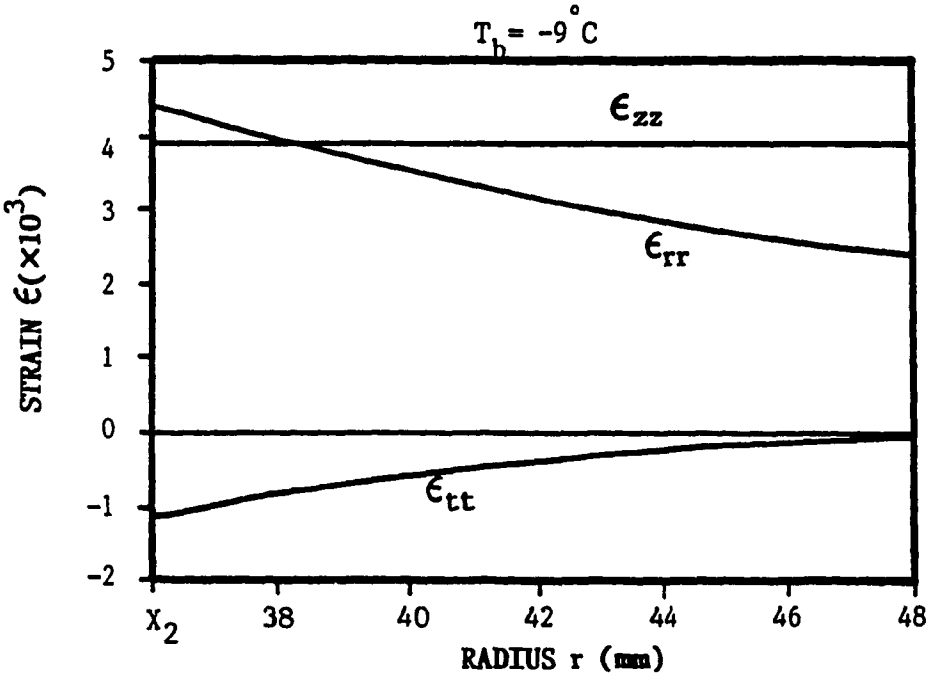

Figure 3.7: The main strain distributions (numerical results) in the ice with T_b=-9°C at the time when the ice starts to crush at X_2.

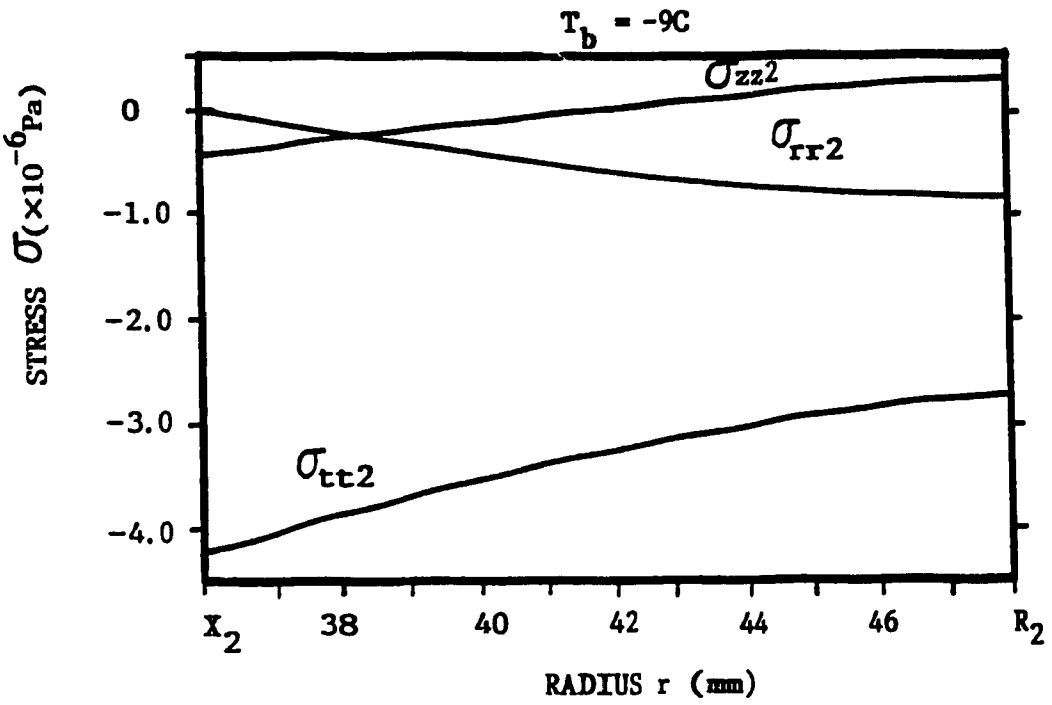

Figure 3.8: The main stress distributions (numerical results) in the ice with T_b=-9°C at the time when the ice starts to crush at X_2.

outward along the radial direction. A great number of the ice crush lines in the radial direction were observed through the transparent plastic plate when the brass tube was opened at the central cross-section after the experimental test as shown in Fig.3.9. After ice crushing, the structure and density of the ice changed. Therefore, a cylindrical interface between the crushed ice and the new-generated ice could be observed. This interface was shown as a concentric line on the cross-section of the ice. In Fig.3.9, there are two concentric lines on the cross-section of the ice, indicating that the ice has crushed twice since the freezing started. Figure 3.10 shows the transient variations of the axial and circumferential strains on the outside surface of the brass tube before the first crush of the ice. The experimental point A indicates a sudden drop of the circumferential strain, which implies the crush of the ice.

Figures 3.11 to 3.13 illustrate the numerical results for the circumferential stress distributions in the ice for different boundary temperatures T_b, different Young's modulus ratios $E^* = E_1/E_2$, and different thermal expansion coefficient ratios $\alpha^{**} = \alpha_1^*/\alpha_2^*$. Figure 3.11 indicate that for a given thickness of the ice (X=36mm), the Young's modulus ratio E^* has a great effect on the thermal stress distribution in a slow freezing process (T_b=-5°C). The larger is the value of E^*, the higher are the thermal stresses. It also can be seen that the effect of α^{**} on the

Figure 3.9: A photograph of ice and unfrozen water in the brass tube (boundary temperature T_b=-20°C, time t= 1.5hr after starting experiment). Ice-crush lines in radial direction and the interface position between the ice and water are shown in the photograph, and two cyclic lines in the ice indicate that the ice has crushed twice since the freezing started.

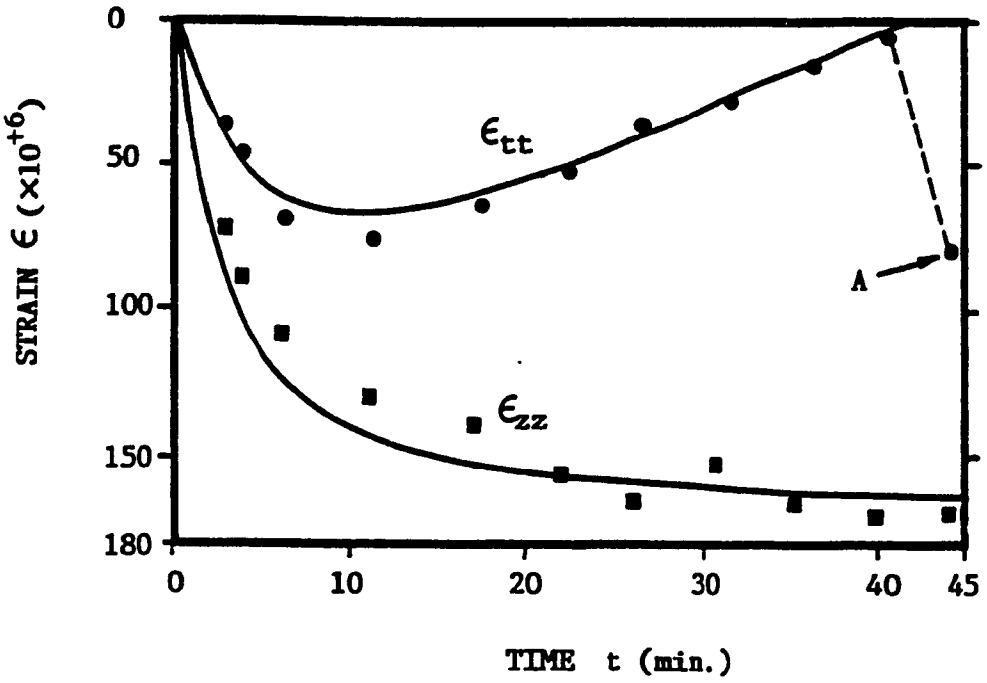

Figure 3.10: The numerical and experimental results for the variations of the axial and circumferential strains on the outside surface of the test tube during the freezing process with T_b=-9°C. Point A indicates a sudden drop of the circumferential strain, which implies the first crush of the ice inside the tube.

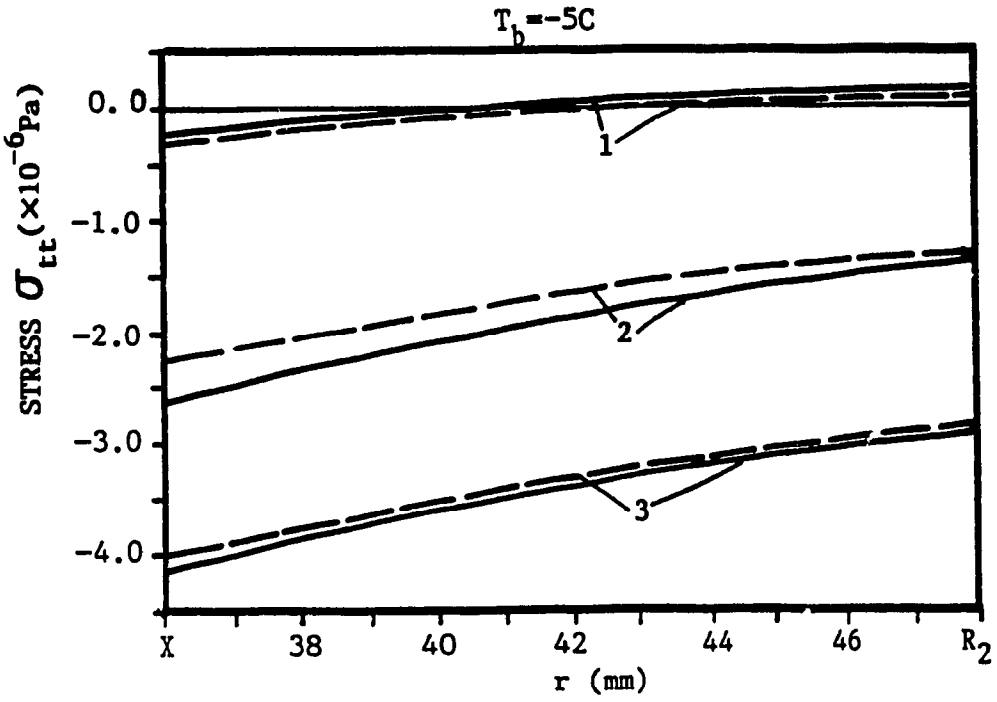

Figure 3.11: The circumferential stress distributions in the ice for T_b=-5°C, X=36mm, α^{**}=0.25 (solid lines) and α^{**}=0.001 (dotted lines) with E^* as a parameter.

Curve 1: E^*=0.001; Curve 2: E^*=2; Curve 3: E^*=100.

thermal stresses is relatively small. Figures 3.12 and 3.13 indicate that the changes of the value of E^* in the quick freezing processes (T_b=-20°C and -80°C) have less effects on the thermal stresses in the ice than that in a slow freezing process (T_b=-5°C). With an increase of the cooling rate and an increase of the value of E^*, the effect of α^{**} on the thermal stresses in the ice increases as shown in Figures 3.11 to 3.13. It is also found that the cooling rate strongly affects the thermal stress distribution in the ice. For a fixed thickness of ice, the thermal stresses in the ice generated by a quick freezing process are much larger than those generated by a slow freezing process. Figure 3.14 shows the effect of the nondimensional thickness of the tube wall, τ^*, on the thermal stress distributions in the ice. The magnitude of the thermal stress decreases with the reduction of τ^*.

From the experimental study in Chapter 2 and the previous cryobiological research, it is known that the cooling rate is a dominant factor affecting the survival of the cells in cryopreservation. First, the cooling rate strongly affects the "Solution Effect" [20,44,129], and the "Packing Effect" [52,115], which result in the cryoinjury of the preserved cells. Secondly, the cooling rate dramatically affects the degree of supercooling of the cell suspension and the morphology of ice formation (e.g. the vitrification or ice-crystallization) [62,111,112,113] which play important roles in the cryoinjury. The present

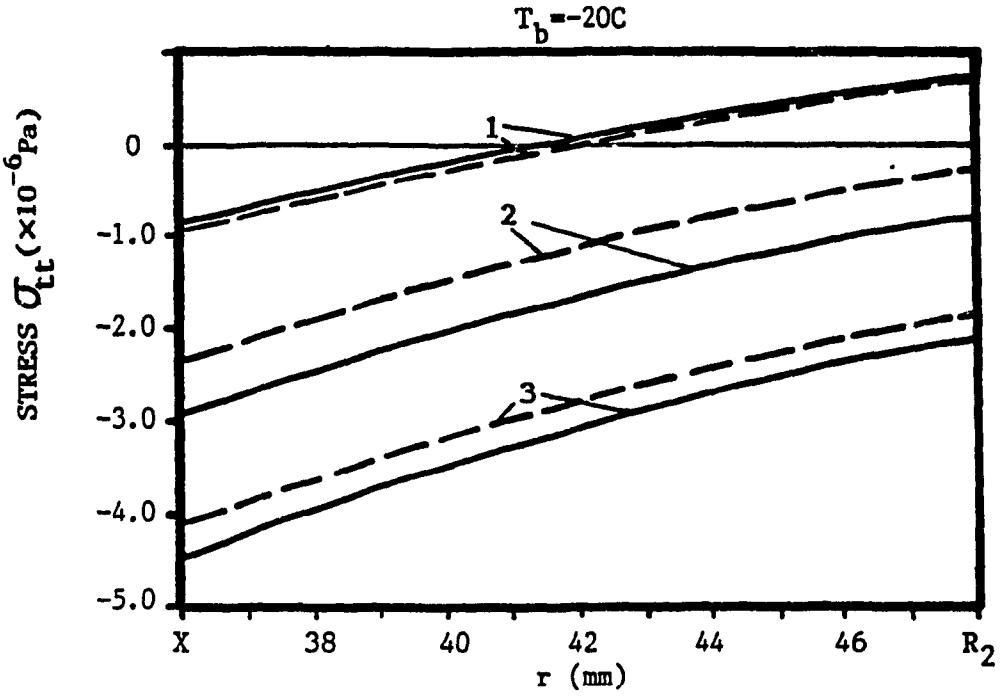

Figure 3.12: The circumferential stress distributions in the ice for T_b=-20°C, X=36mm, α^{**}=0.25 (solid lines) and α^{**}=0.001 (dotted lines) with E^* as a parameter.

Curve 1: E^*=0.001; Curve 2: E^*=2; Curve 3: E^*=100.

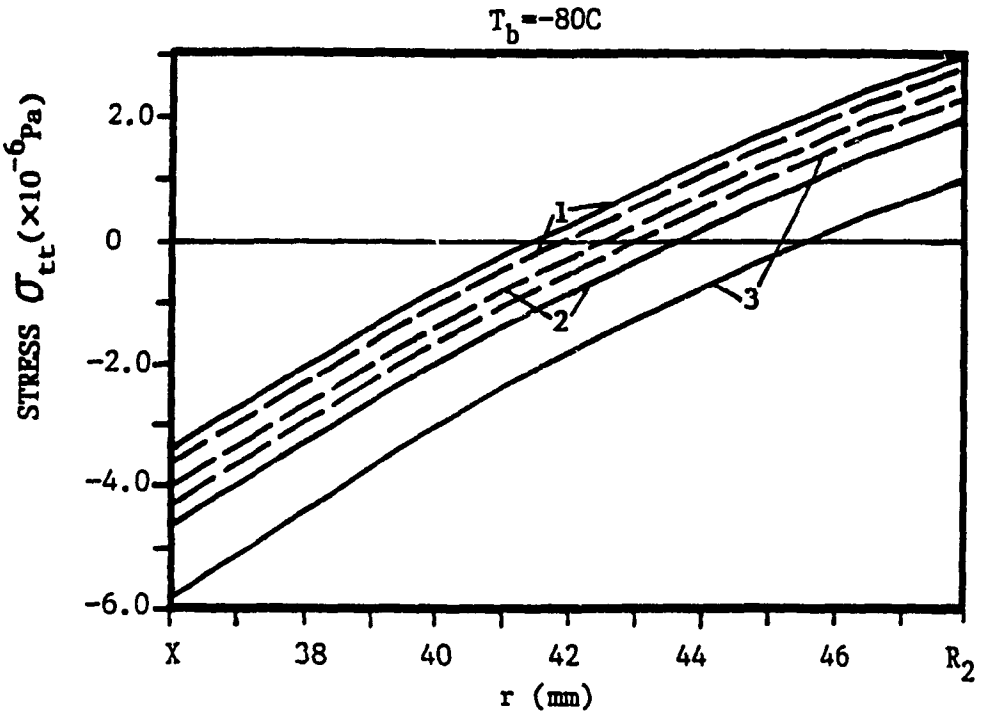

Figure 3.13: The circumferential stress distributions in the ice for T_b=-80°C, X=36mm, α^{**}=0.25 (solid lines) and α^{**}=0.001 (dotted lines) with E^* as a parameter.

Curve 1: E^*=0.001; Curve 2: E^*=2; Curve 3: E^*=100.

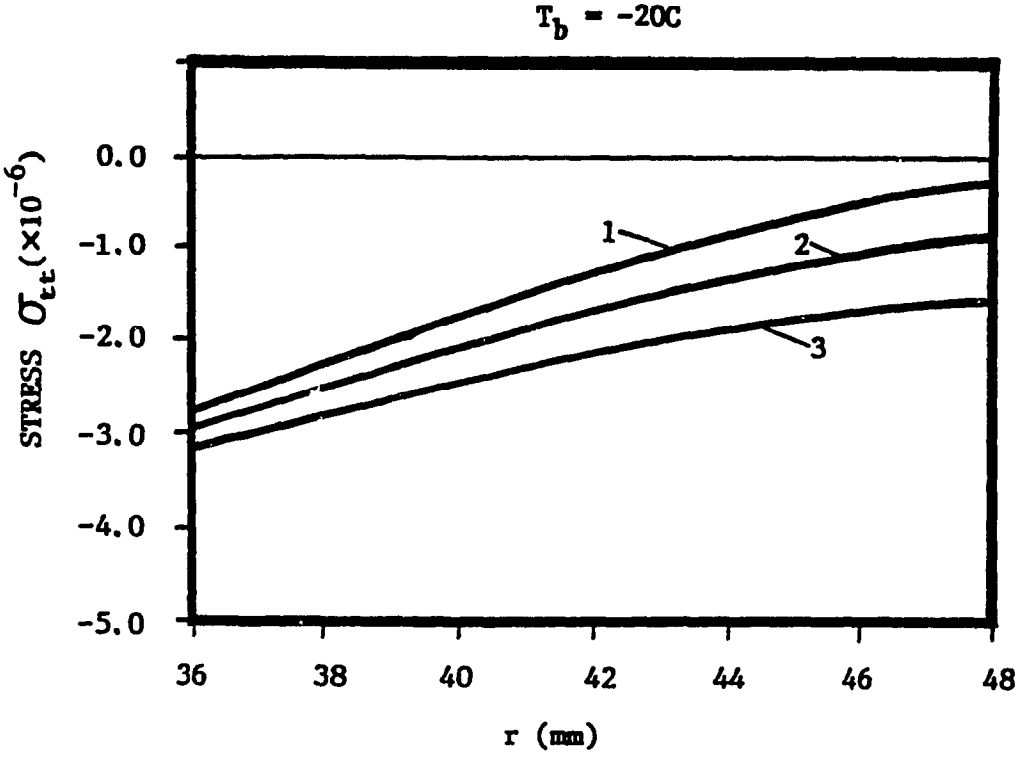

Figure 3.14: The circumferential stress distributions in the ice for T_b=-20°C, X=36mm, α^{**}=0.25 and E^{*}=2.0 with τ^{*} as a parameter.

Curve 1: τ^{*}=0.5×(τ/R2);

Curve 2: τ^{*}=1.0×(τ/R2);

Curve 3: τ^{*}=2.0×(τ/R2).

experimental and numerical investigation of the thermal stress provides an additional evidence for the importance of the cooling rate, i.e. the cooling rate greatly affects both the magnitude of the thermal stress inside the frozen cell suspension and the crush of the frozen suspension. A slow freezing process induces much smaller thermal stresses than a quick freezing process does. Therefore, a slow freezing process could benefit the cryopreservation of cells by reducing the "thermal stress effect". This prediction is consistant with the conclusion of the study on the cryopreservation of human erythrocytes in Chapter 2 [130].

3.6 Conclusions

From the numerical and experimental studies on the thermal stress distributions in the ice-tube system, the following conclusions are made:

(1) The developed research models can be used as a first approximation to predict the freezing process and the thermal stress distributions in the frozen cell suspension.

(2) The ice crush during the freezing process is caused by the circumferential compressive stresses in the ice. Because the maximum circumferential stress exists at the water-ice interface, the crush starts at the interface and then propagates outward along radial direction.

(3) The cooling rate is an important factor which strongly affects the thermal stress distributions in the

ice-tube system. The quicker is the freezing process, the higher are the thermal stresses in the ice.

(4) The ratio of the Young's moduli, E^*, the ratio of the linear thermal expansion coefficients, α^{**}, and the nondimensional thickness of the tube wall, τ^*, are also important for the thermal stress distributions. The larger the values of E^*, α^{**} and τ^*, the greater are the thermal stresses induced in the ice.

(5) In order to reduce the "thermal stress effect" on cryoinjury of cells during the freezing preservation, it is proposed that a slow freezing process and a thin-wall tube which is made of a material having small values of the Young's modulus and the thermal expansion coefficient should be used.

CHAPTER 4

EFFECT OF GLYCEROL ON CHARACTERISTICS OF THE FREEZING PROCESS OF TERNARY SOLUTION Water-NaCl-Glycerol

NOMENCLATURE

c	molarity, mole/liter
F_s	total solute mole fraction defined in eq.(4.2)
I	defined in eqs.(4.4) and (4.6)
R_1	outside radius of the tube, m
R_2	inside radius of the tube, m
T	temperature, °C
T_f	freezing point of the unfrozen solution, °C
X	interface position, m
W	mole molecular weight, g/mole

Greek Symbols

ε_{tt}	circumferential component of the strain on internal surface of the tube wall
ε_{zz}	axial component of the strain on internal surface of the tube wall
$\Delta\varepsilon$	$= \varepsilon_{tt} - \varepsilon_{zz}$

Subscripts

1	tube
2	frozen solution
3	unfrozen solution
g	glycerol
n	NaCl

o	initial condition
w	water

4.1. Introduction

Being one of the most effective penetrating-CPAs, glycerol has been employed as a typical research target to reveal the mechanism of the cryoprotection of CPAs. From previous investigations, the role of glycerol against cryoinjury of cells was generally explained by its colligative function in reducing "solution effect" [69], its low biological toxicity to the cells [95], its ability in penetrating cell membrane to prevent intracellular ice-crystallization and recrystallization [75], and its acting as a hydroxyl radical scavenger to stabilize the structure of cell membrane [88].

In this Chapter, an investigation of effect of glycerol on the characteristics of the freezing process of the cell suspension medium, Water-NaCl-Glycerol, inside a cylindrical tube is presented. The characteristics involve the movement of the interface between frozen and unfrozen solutions, the temperature distribution inside the solution -tube system, the distribution of solute concentration in the frozen solution and the crush of the frozen solution during the freezing process, etc.

4.2. Experimental Materials and Method

The main experimental equipment used for the freezing tests of the ternary solution, Water-NaCl-Glycerol, in a cylindrical test tube is the same as that described in Chapter 3, as shown in Figures 3.1 and 3.2.

The ternary solutions were prepared at room temperature. The concentration of NaCl was fixed at 0.15M which is a physiological concentration for the biological cells. The concentration of glycerol varied from 0M to 1M. Before starting each of tests, the brass tube was filled with the prepared solution and then precooled in a temperature controlled chamber until the readings of all the thermocouples located inside the tube were 1°C.

Based on the conclusions of the research in Chapters 2 and 3, it is known that a slow freezing process greatly benefits cryopreservation of cells. Therefore, in the present study, the slow freezing tests of the ternary solutions were mainly performed. The temperature at the outside surface of the tube was controlled to decrease at a slow cooling rate -0.1°C/min. The variation of the temperatures on the surfaces of the tube wall and in the solution was automatically measured by the thermocouples and recorded in a personal computer. The absolute error for the temperature measurement by using the thermocouples is ±0.1°C. The alteration of the strain on the tube surface was measured by the strain gages. The absolute error for

the strain measurement is $\pm 0.5 \times 10^{-6}$.

For each of the prepared ternary solutions, the freezing tests were repeated more than four times and stoped at the different time intervals. As soon as a test stoped, the tube was opened at the central cross-section to measure the solid-liquid interface position and to observe the morphology of the frozen solution. In each of the tests, after the ternary solution froze completely, ten samples of the frozen solution were collected from the central cross-section of the frozen solution by using a hand drill with a specifically designed hollow drilling bit (Fig.4.1). Figure 4.2 shows the cross-section of the frozen solution and the positions at which the samples were collected by drilling. After the ten frozen samples melted, the electrical conductivity of each of the samples was measured by an electrical conductivity meter (Figure 4.3a). Based on a standard curve which shows the values of NaCl concentration as a function of the electrical conductivity of NaCl solution, the NaCl concentration of each of the samples was determined. The osmolarity of each of the samples was measured by using an osmometer (Figure 4.3b). The freezing point of each of the samples was determined from a standard curve which shows the freezing point of the aqueous solution as a function of the osmolarity of the solution.

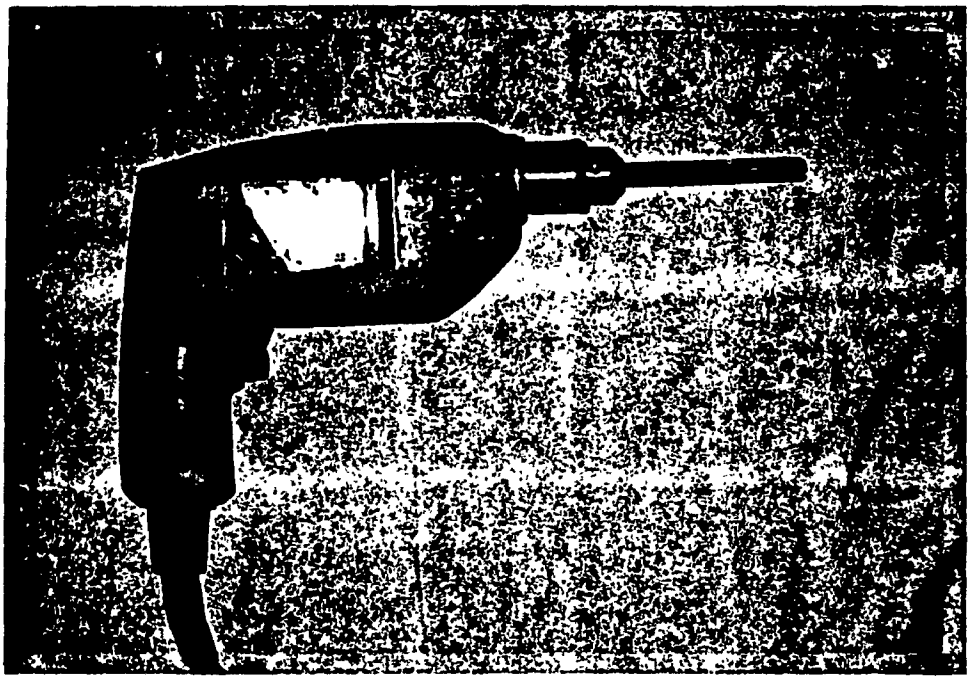

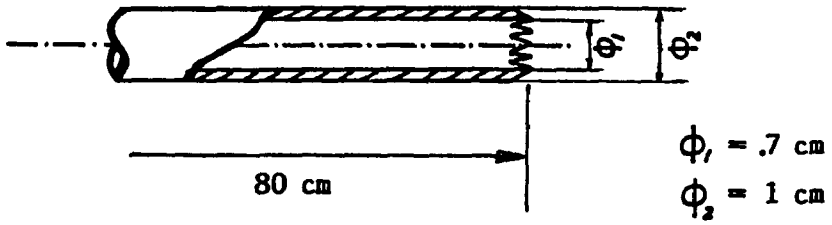

Figure 4.1: Upper: A hand drill with a hollow drilling bit which was used to collect the samples of the frozen solution at the central cross-section of the tube.

Lower: Design diagram of the drilling bit.

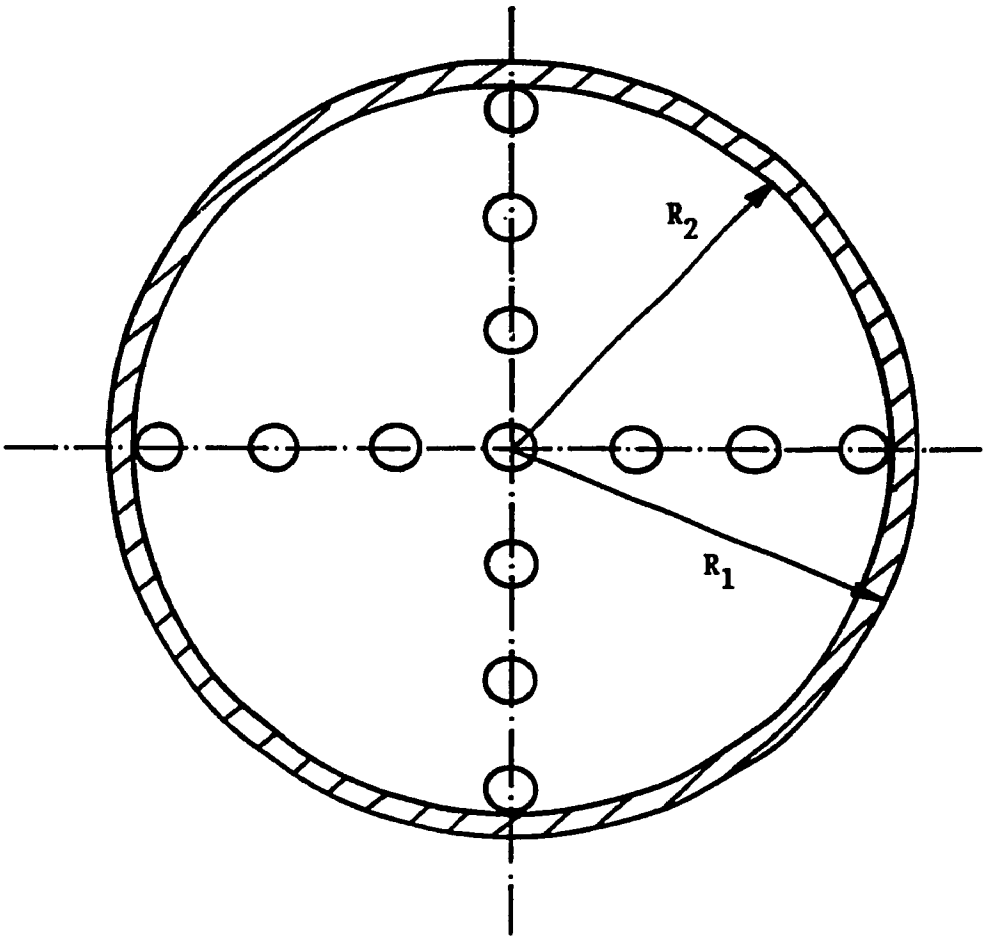

Figure 4.2: The central cross-section of the tube, and the positions at which the samples of the frozen solutions were collected by drilling.

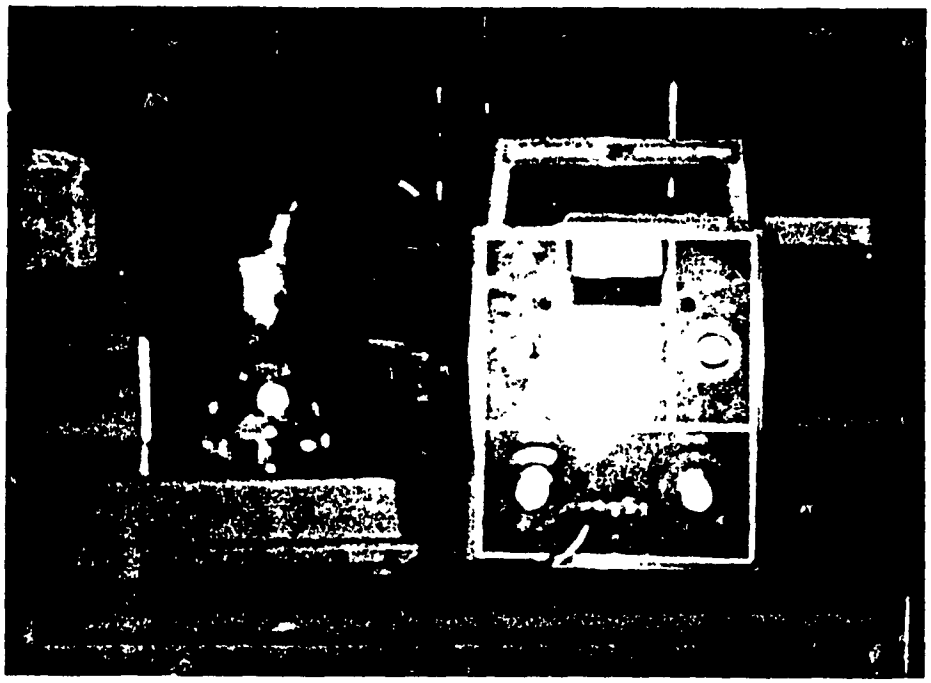

(a)

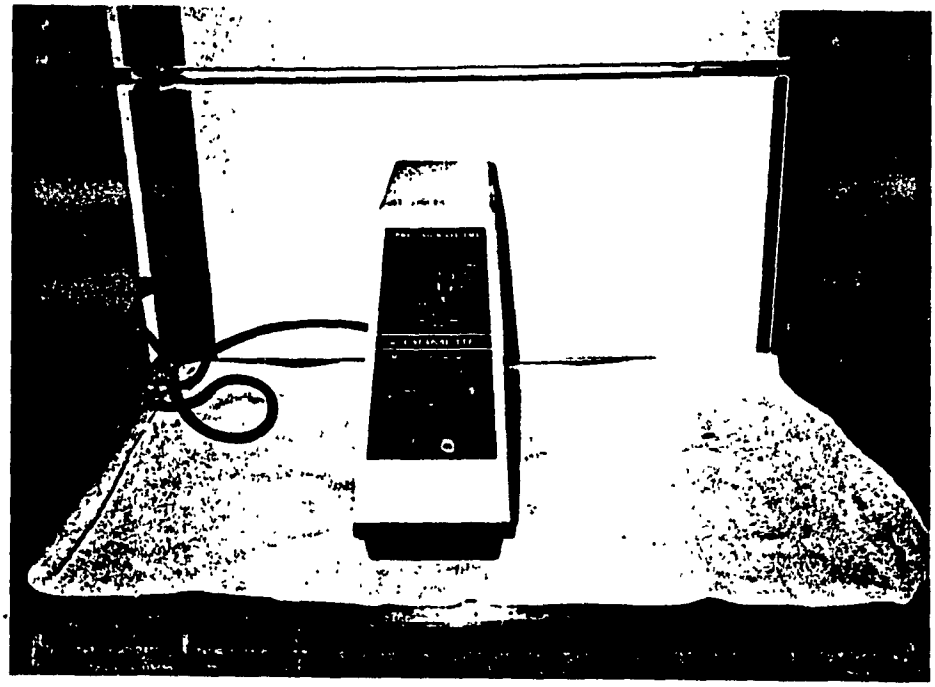

(b)

Figure 4.3: (a) A conductivity meter used to measure the concentration of NaCl in the collected frozen samples.

(b) A osmometer used to measure the freezing point of the collected frozen samples.

4.3. Results and Discussion

Experiments were conducted for the four different initial glycerol concentrations (c_{go}), 0, 0.3, 0.5, 1.0M.

The effect of glycerol on the movement of interface between the frozen and unfrozen solutions during the freezing processes is shown in Figure 4.4 with the initial glycerol concentration (c_{go}) as a parameter. It is expected that the higher the c_{go}, the slower the solidification of the solution because of the colligative property of solution. The temperature distributions in the different frozen solutions are shown in Figure 4.5 when the interface position, X, located at a distance of 0.4×R2 to the center of the tube with c_{go} as a parameter. From Figures 4.4 and 4.5, it is obvious that the initial concentration of glycerol greatly affects the thermal history of the freezing porcess of the solution even though the boundary cooling rate is kept same. This also potentially indicates that glycerol significantly changes the thermal properties of the solution.

The phase law of the ternary solution, Water-NaCl -Glycerol, has been investigated by using DTA (differential thermal analysis) and DSC (differential scanning calorimetry) techniques [131,132]. It has been known that during the freezing, water first nucleates and precipitates from the solution as ice. Therefore, the unfrozen solution becomes more and more concentrated and the freezing point

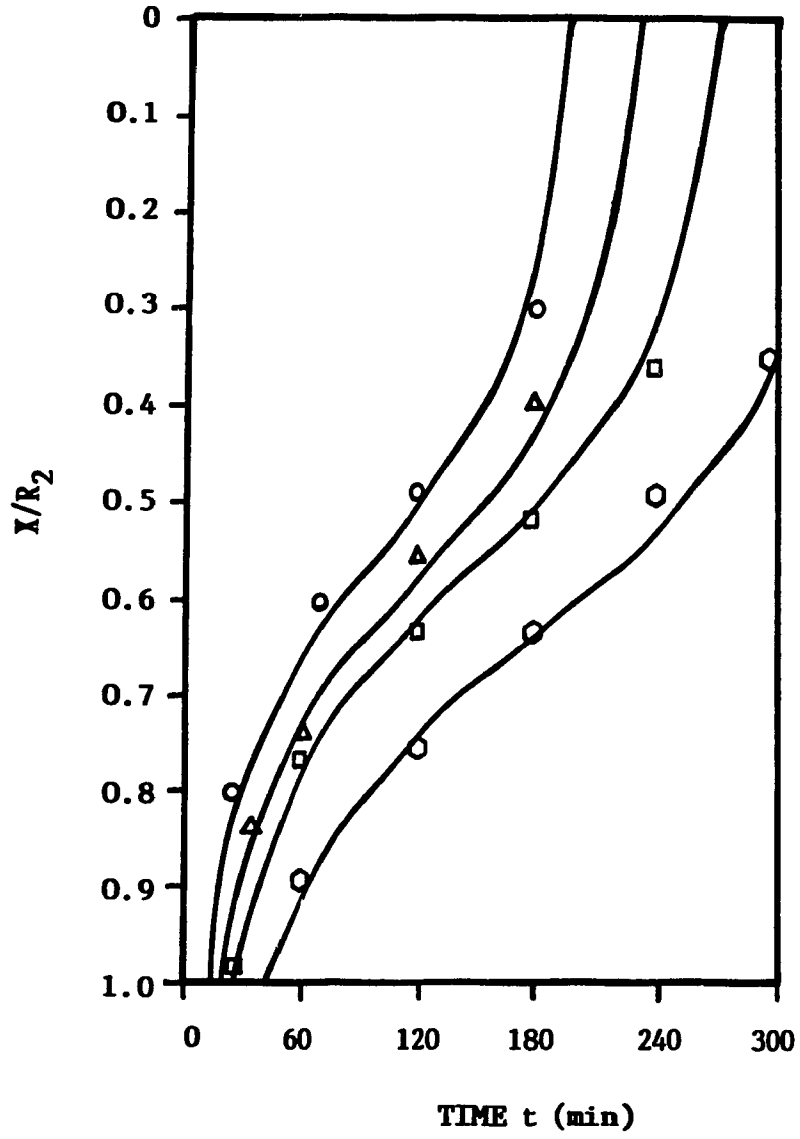

Figure 4.4: The motion of the interface between the frozen and unfrozen solutions as a function of time during the freezing process of the ternary solutions. The initial concentration of glycerol, C_{go}, varies as an experimental parameter.

○: test data for C_{go} = 0M; △: test data for C_{go} = 0.3M;

□: test data for C_{go} = 0.5M; ⬡: test data for C_{go} = 1.0M.

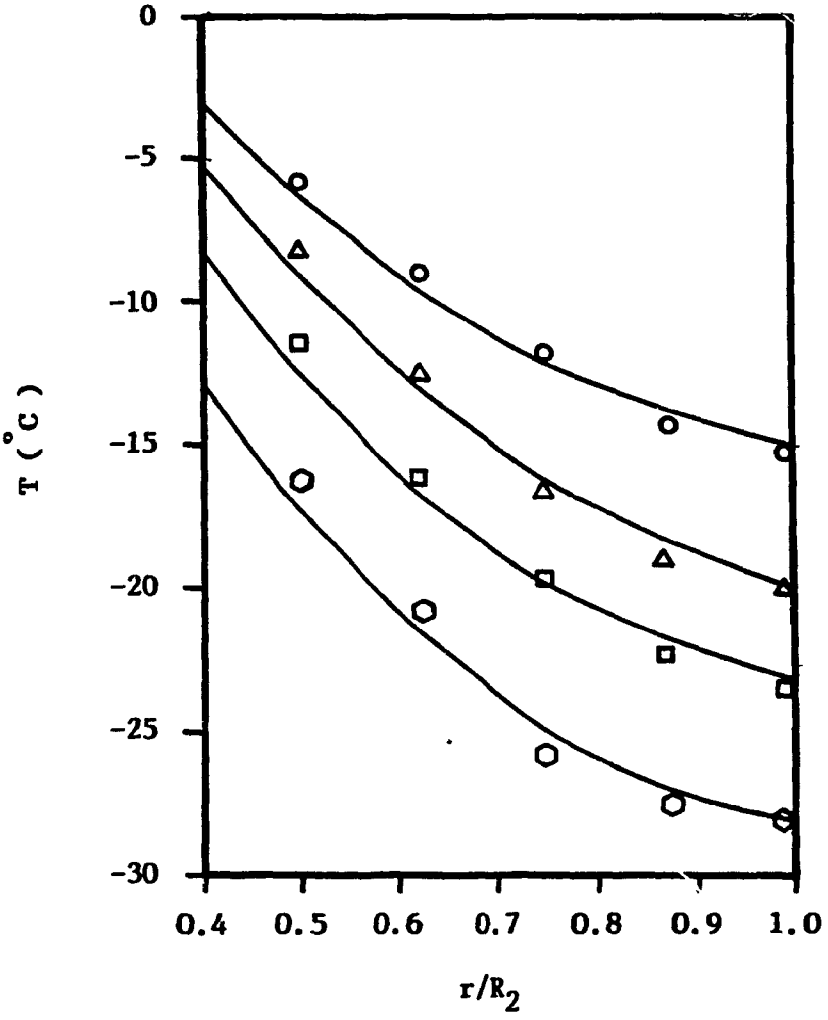

Figure 4.5: The temperature distributions in the frozen solutions with the initial glycerol concentration as a parameter.

○: test data for C_{go} = 0M; △: test data for C_{go} = 0.3M;
□: test data for C_{go} = 0.5M; ⬡: test data for C_{go} = 1.0M.

of the solution is depressed until the temperature of the concentrated solution reaches the eutectic point. At the eutectic point, the remaining unfrozen mixture solidifies.

In 1980, Fahy [36] further studied the phase diagram of the ternary system, Water-NaCl-Glycerol, and developed the following equations to calculate the freezing point of the ternary solution for the given concentrations of NaCl and glycerol respectively:

$$T_f=-\left[0.7541-\left(0.56865-S\times F_s^2-I\times F_s\right)^{0.5}\right]\times 10^3/6.405 \qquad (4.1)$$

with

$$F_s = (c_g+ 2c_n)/(c_g+ 2c_n+ c_w) \qquad (4.2)$$

where S and I are defined as follows:

(1) for a dilute solution:

$$S = 7\times|F_g-0.5|^{2.5}+0.955 \qquad (4.3)$$

$$I = 0.099F_g + 0.895 \qquad (4.4)$$

where F_g is nonaqueous mole fraction of glycerol, and

$F_g = c_g/(c_g+ 2c_n)$.

(2) for a concentrated solution:

$$S = 6.536\times(F_g-0.732)^2 + 0.08 \qquad (4.5)$$

$$I = 2.8\times(F_g-0.77)^3 +1.101 \qquad (4.6)$$

where $F_g = c_g/(c_g+ 2c_n)$

Note: Use (4.3) and (4.4) for $F_g<0.5$. If $0.5<F_g\leq 0.87$, use (4.3) and (4.4) if $f<1.12$, and (4.5) and (4.6) if $f>1.12$

(f=S×F_s+I); if $F_g \geq 0.87$, use (4.3) and (4.4) for $F_s \leq 0.083$, and (4.5) and (4.6) for $F_s \geq 0.083$.

A simple "two-layer freezing model" [133] is usually assumed in computer-simulation for the freezing process of cell suspensions in cryopreservation. As schematically shown in Fig.4.6, during the freezing process of an aqueous solution inside a cylindrical tube, the solutes are rejected towards the center of the tube by the advancing ice front. With temperature decreasing, the center part of the unfrozen solution eventually solidifies at eutectic point. The "two-layer" simply means that there are two solid layers in the final frozen solution. One layer is the pure ice and another is the solidified ternary mixture. If the "two-layer model" is true, the concentrations of the three components, c_g, c_n, and c_w in the unfrozen ternary solution, H_2O-NaCl-Glycerol, inside the cylindrical tube can be calculated by the following equations, assuming that the solute concentration in the unfrozen solution is uniform during the slowly one-dimensional freezing process.

$$c_g = c_{go}\left(\frac{R2}{X}\right)^2 \tag{4.7}$$

$$c_n = c_{no}\left(\frac{R2}{X}\right)^2 \tag{4.8}$$

$$c_w = \rho_w\left(1000 - c_g \times W_g/\rho_g - c_n \times W_n/\rho_n\right)/W_w \tag{4.9}$$

Based on the equations (4.1) to (4.9), the concentration and the freezing point of the unfrozen

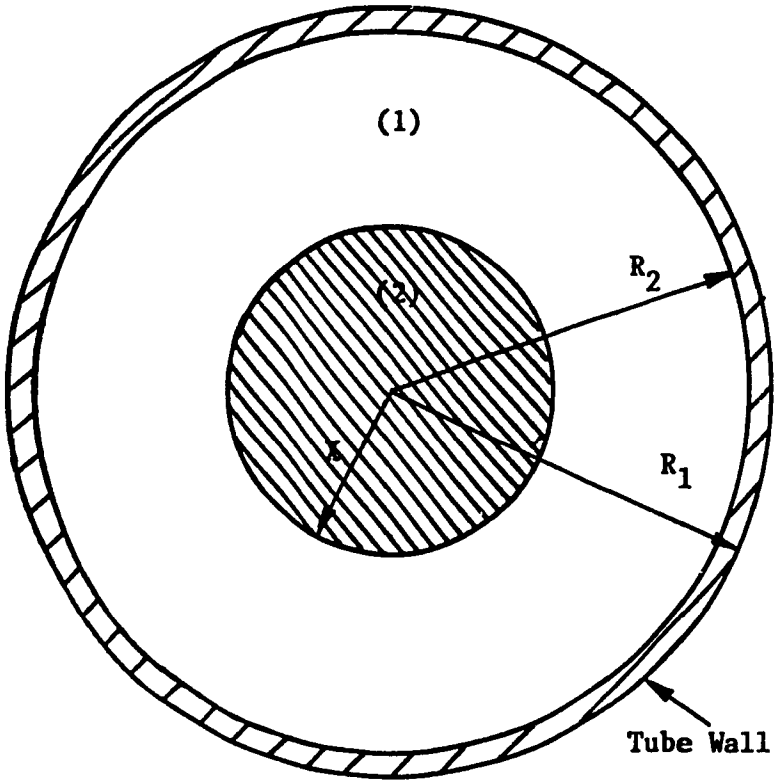

Figure 4.6: The "two-layer freezing model".

(1) ice region;

(2) ternary-mixture region.

ternary solution during the freezing process can be calculated by computer. The depression of the freezing point and the increasing of NaCl concentration in the unfrozen solution are determined thereby as functions of the interface position, X and the initial glycerol concentration, C_{go} (Fig.4.7). The eutectic point [36] of each of the unfrozen solutions with the different initial glycerol concentrations is also indicated in Fig.4.7.

Based on the theory of the "two-layer model", it is expected that the freezing point of the frozen solution and the concentration of NaCl in the frozen solution must be step-like distributed as demonstrated in Fig.4.8 and Fig.4.9 respectively. In contrast, from the experimental measurement, the real freezing points and the NaCl concentrations of the ten frozen solution samples collected from the central cross-section of the frozen solution by drilling are those which are also shown in Fig.4.8 and Fig.4.9 respectively. It is obvious that the distributions of the measured freezing point and NaCl concentration are totally different from those predicted from the "two-layer model". Actually, NaCl distributes everywhere inside the frozen solution instead of the step-like distribution. This indicates that the traditional "two-layer freezing model" does not fit well with the real freezing process of the ternary solution.

From the previous research on the solidification processing of alloys, it has been found that the solid-

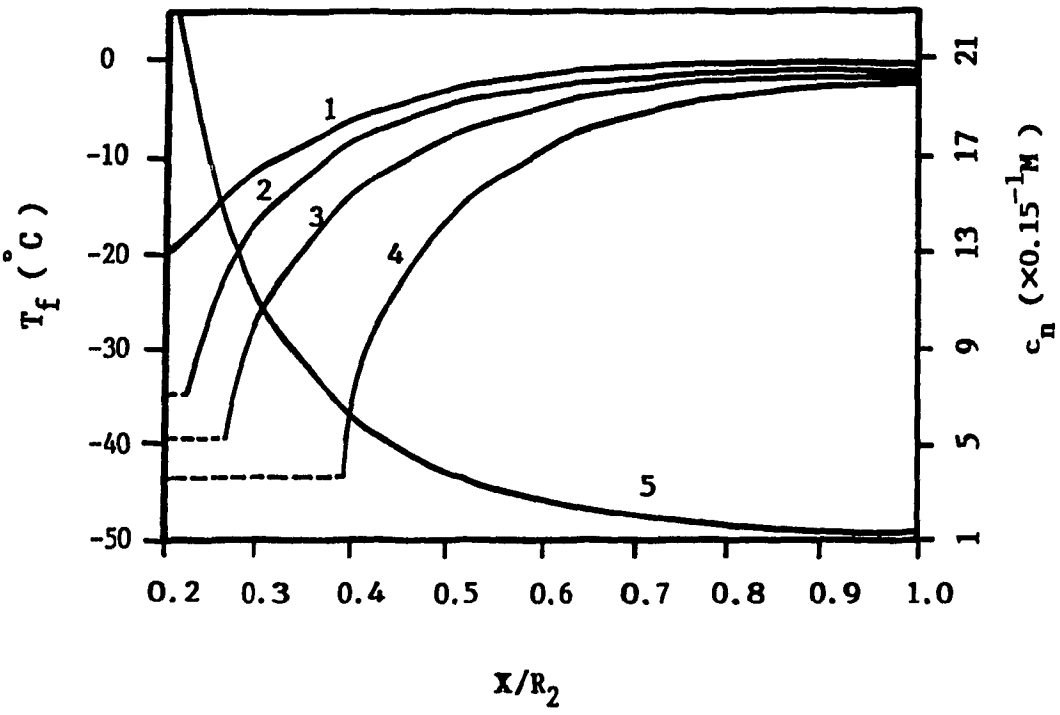

Figure 4.7: The alterations of the freezing point of the unfrozen ternary solution and the NaCl concentration in the solution as a function of the interface position, X, under the assumption of the "two-layer freezing model". The initial glycerol concentration, C_{go}, varies as a parameter for the different freezing processes.

Curve 1, 2, 3, and 4 express the alterations of the freezing point of the unfrozen solutions with C_{go} = 0M, 0.3M, 0.5, an 1.0M respectively. The eutectic point for each of the freezing processes is marked with a dotted line.

Curve 5 expresses the alteration of the NaCl concentration.

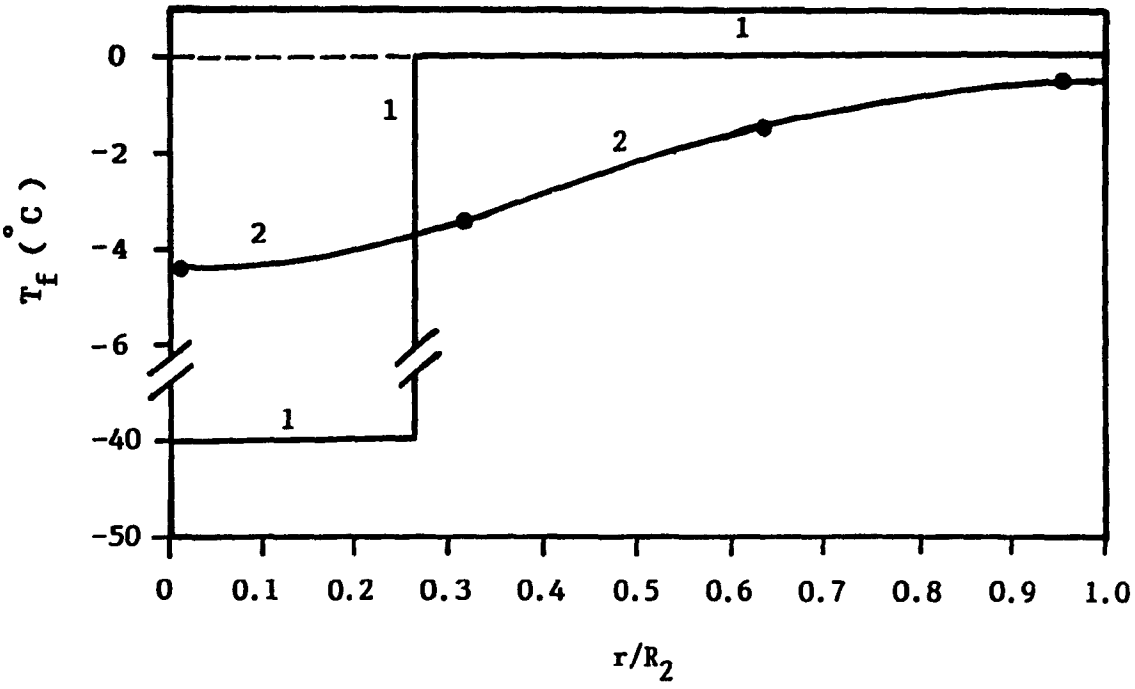

Figure 4.8: The distribution of the freezing point T_f in the frozen ternary solution with C_{go} = 0.5M.

Curve 1: Theoretical distribution of T_f calculated from the "two-layer freezing model".

Curve 2: The distribution of T_f measured from the present experiments.

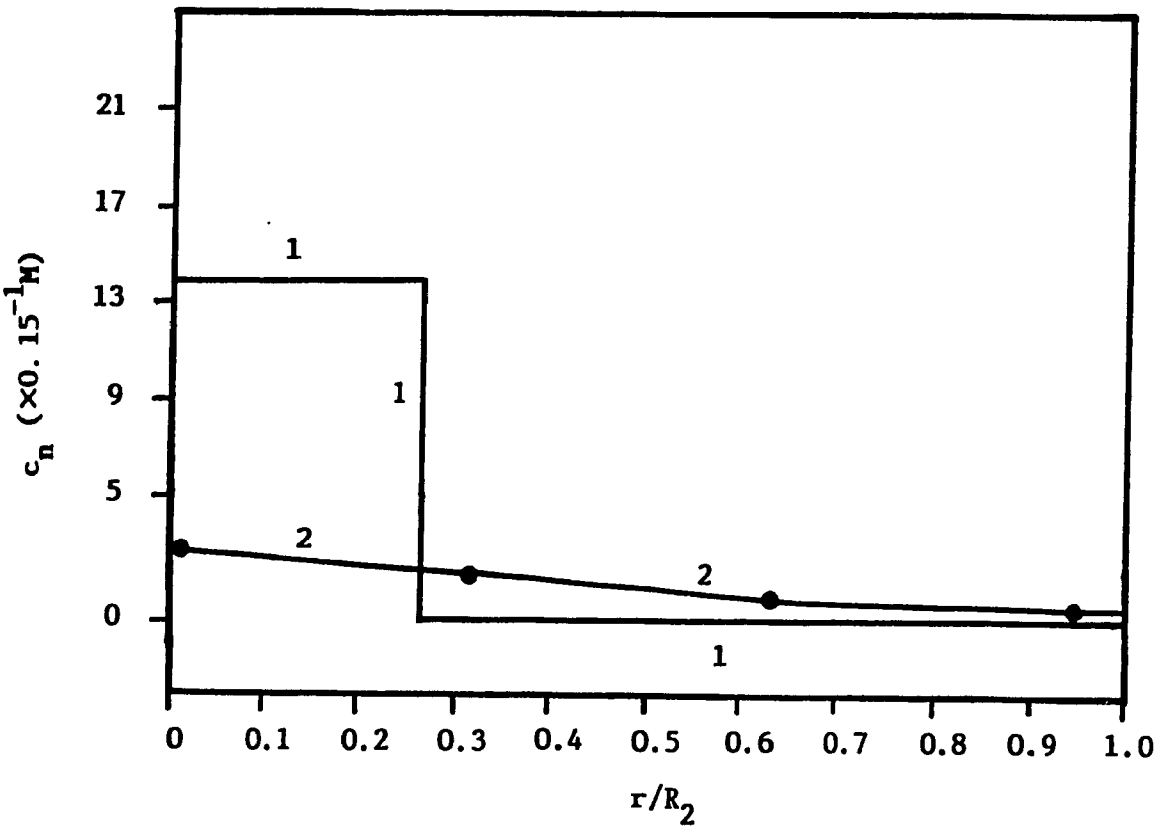

Figure 4.9: The distribution of NaCl concentration C_n in the frozen ternary solution with C_{go} = 0.5M.

Curve 1: Theoretical distribution of C_n calculated from the "two-layer freezing model".

Curve 2: The distribution of C_n measured from the present experiments.

liquid interface of an alloy during the solidificaiton was not a planar shape unless the liquid alloy was never supercooled [134,135]. Because the supercooling of the liquid alloys usually existed together with the solute redistribution [135,136], the shape of the solid-liquid interface was usually dendritic or finger-like during the solidificaiton as shown in Fig.4.10(a). A fully developed, dendritic solid front of a solidifying alloy [136] is shown in Fig.4.10(b).

Analogizing the freezing process of the ternary solution (Water-NaCl-Glycerol) to the solidification of the alloys, a freezing pattern of the ternary solution was hypothesized as follows:

As shown in Fig.4.11(a), at beginning of the cooling process, the solution which contacts the tube wall is first cooled, and water randomly nucleates and precipitates from the solution as initial ice crystals which form a thin layer on the internal surface of the tube. Since solutes are rejected by the ice, the solutes become concentrated in the liquid region close to the ice front. The initial ice layer is unstable and won't grow uniformly in the further freezing process because of the non-uniform redistribution of the solutes inside the unfrozen solution and the supercooling of the solution. Some of ice crystals grow faster and some slower. Therefore, the ice front becomes a finger-like or dendritic shape (Fig.4.11 (b)).

In freezing, the solutes in liquid region 1 i.e. the

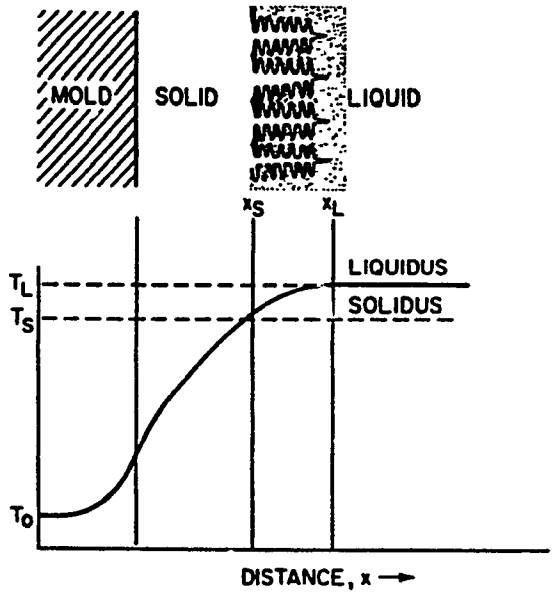

(a)

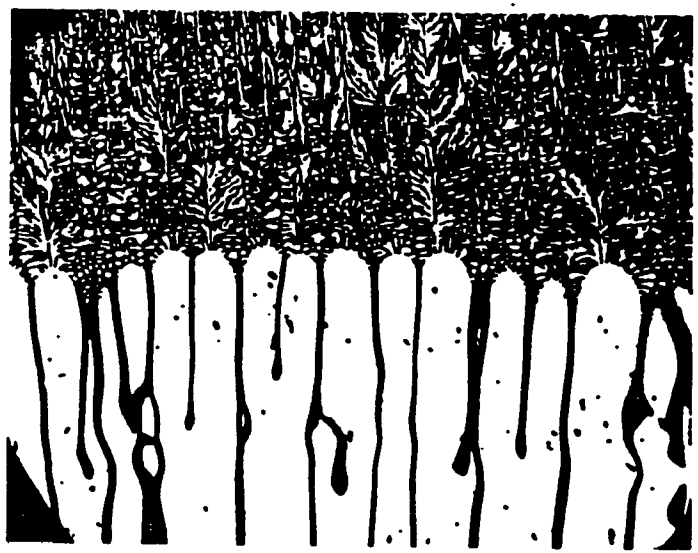

(b)

Figure 4.10: (a) Diagram illustrating the solidification of an alloy against a flat mold wall.

(b) Microscopic picture (magnification, ×150) of a fully developed, dendritic solid front of a solidifying Al-Cu alloy. (From Sharp and Hellawell [135,136])

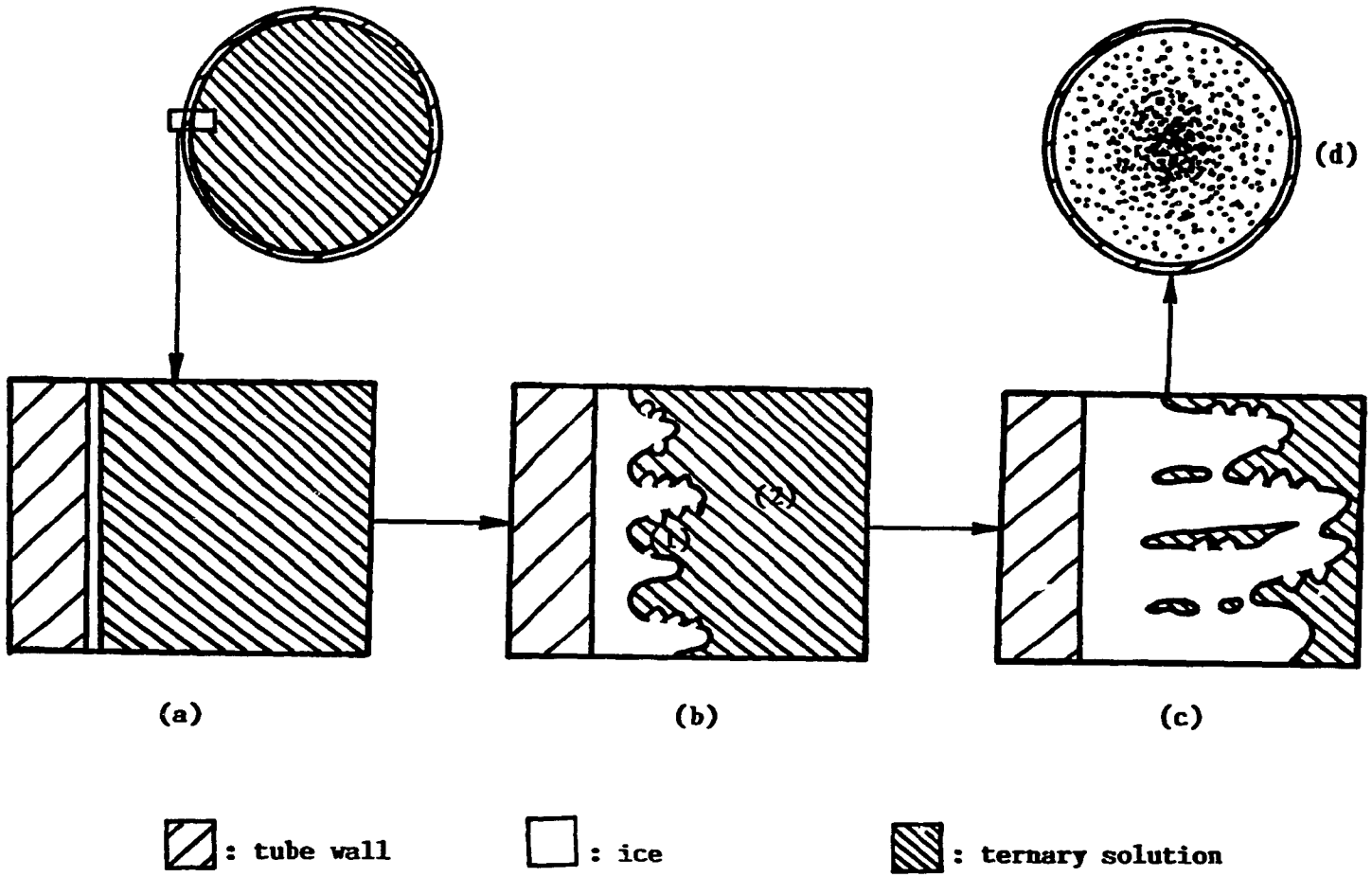

Figure 4.11: Digrams illustrating the hypothesized freezing model of the ternary solution, i.e. "water melon model".

unfrozen solution in the grooves among the "fingers" (Fig.4.11(b)) becomes more and more concentrated. In contrast, liquid region 2 is a relative water-rich region. Colligatively, the freezing point of the solution in region 1 is lower than that in region 2. Therefore, the "finger tips" grow faster than the other parts of the "finger". With the growth of the "fingers", the ice grooves become narrower and narrower. And meanwhile the connection (Fig.4.11(c)) among the "fingers" takes place due to (1) the new ice nuleation and ice growth in the supercooled solution in the grooves; (2) the cross-contact of the "finger tips"; and (3) vitrification or eutectic solidification of the solution in the grooves, etc.

Consequently, the concentrated solution is "entrapped" into many ice compartments just like seeds in a water melon. They eventually either solidify at the eutectic points or vitrify at the temperature of glass transition. It can be imagined that the cross-section of the final frozen solution should be like that of a water melon (Fig.4.11(d)). This freezing model may be called as "water melon model". It is apparent that the "water melon model" can be applied to explain the present experimental finding that the solutes distribute "everywhere" inside the frozen solution.

Based on the morphological observation of the frozen solution after each experimental test, it was found that the frozen solutions without glycerol had crushed several

times during the freezing process. In contrast, no crush was observed in the frozen solutions with glycerol (0.3M, 0.5M or 1M). These observations agree very well with the experimental record of the variation of the strain on the internal surface of the tube wall during the freezing process. Figure 4.12 demenstrates the strain change on the internal surface of the tube wall as a function of time for the freezing process without glycerol. The sudden drops (marked with arrows) of the circumferential component of the strain (ε_{tt}) indicate the crushing of the frozen solution inside the tube. Figure 4.13 shows the strain change during the freezing process with different concentrations of glycerol. There was no sudden drop of the strain during the freezing processes, which implied that the crushing of the frozen solution did not occur.

During the cooling process of the solution-tube system, the variation of the strain on the internal surface of the tube wall are generated by (1) cooling contraction of the tube, and (2) interactive force between the tube wall and the frozen solution inside the tube. As described in the section 3.2 of Chapter 3, the brass-tube equipment was so designed and made that the tube wall and the frozen solution can contract or expand freely in the axial direction during the freezing process. Therefore, the axial component (ε_{zz}) of the strain on the surface of the tube wall is primarily induced by the cooling contraction, and hence it reduces smoothly during each of the cooling

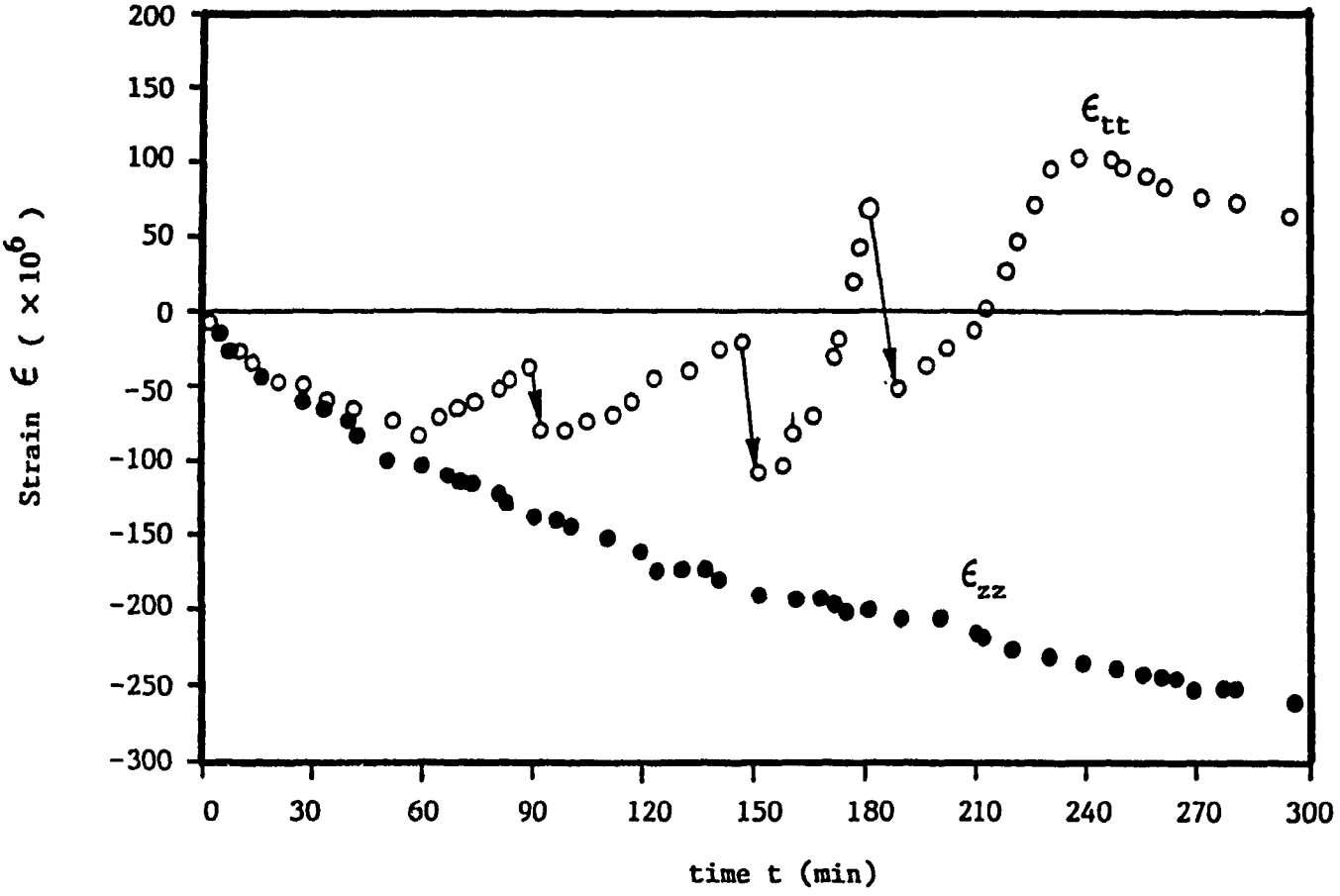

Figure 4.12. Variation of the strain on the inside surface of the tube wall during the freezing process of the solution without glycerol.

○: experimental data for circumferential component of the strain

●: experimental data for axial component of the strain.

(Note: Arrows indicate the crush of the frozen solution inside the tube during the process)

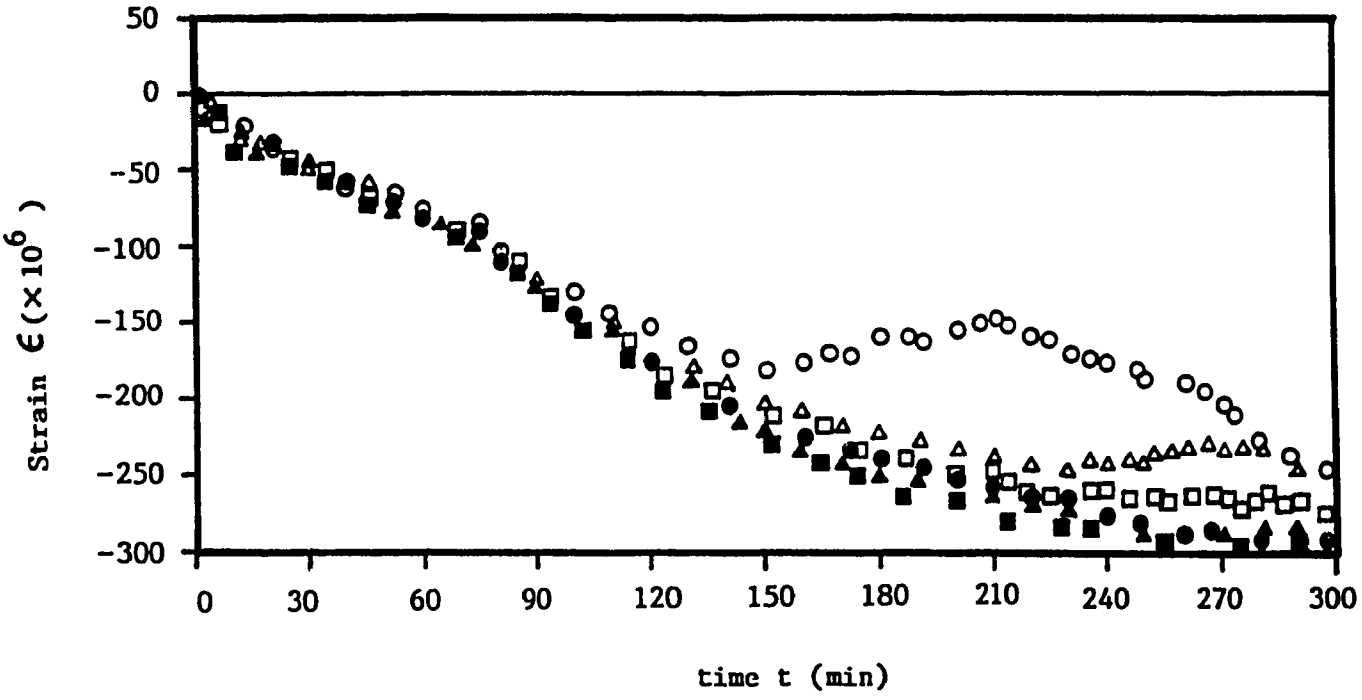

Figure 4.13. Variation of the strain on the inside surface of the tube wall during the freezing process of the solution with glycerol.

○ : data of ϵ_{tt} for the freezing process with c_g = 0.3 M

● : data of ϵ_{zz} for the freezing process with c_g = 0.3 M

△ : data of ϵ_{tt} for the freezing process with c_g = 0.5 M

▲ : data of ϵ_{zz} for the freezing process with c_g = 0.5 M

□ : data of ϵ_{tt} for the freezing process with c_g = 1.0 M

■ : data of ϵ_{zz} for the freezing process with c_g = 1.0 M.

processes as shown in Figure 4.12 and 4.13. It can also be seen that the difference between the ε_{tt} and ε_{zz} for the freezing process without glycerol is much larger than that for the freezing process with glycerol, indicating that thermal stresses induced in the frozen solution without glycerol are much larger than those in the frozen solution with glycerol.

From the research work of Jones and Glen [137], it was known that some substances in water (e.g. HF and NH_3) had a considerable softening or hardening effect on mechanical properties of the frozen solution. It is known that the mechanical properties of the frozen solution greatly affect the thermal stress induced in the frozen solution [54]. Therefore, based on the present investigation and the "water melon model", it is expected that glycerol may significantly change the internal structure and the mechanical properties of the frozen solution, resulting in the reduction of the thermal stress. Besides, it has been known from Chapter 3 that the volume expansion of the water solidification greatly contribute to generate high thermal stress in the frozen solution. Because the presence of glycerol in the ternary solution reduces the percentage amount of water in the solution, the volume expansion of the frozen solution should be reduced. This could be another reason by which the glycerol reduces the thermal stress and thereby eliminates the crushing of the frozen solution. Both the high thermal stress and the crush of the

frozen cell suspension are related to the cryoinjury of cells in cryopreservation. It is therefore proposed that glycerol contributes to reduce cell's cryoinjury caused by the "thermal stress effect" during the cryopreservation of cells.

4.4 Conclusions

Based on the experimental results for the freezing process of the ternary solution, water-NaCl-glycerol, the following conclusions can be made:

(1) Glycerol greatly affects the performance of the transient freezing process of the ternary solution. The higher the initial glycerol concentration, the slower the freezing process.

(2) There is a continuous distribution of solute concentration in the frozen solution, which is in contradiction to the traditional "two-layer freezing model". A "water melon model" for the freezing process of the ternary solution is invoked and agrees well with the experimental results.

(3) Glycerol concentrations over 0.3M are sufficient to reduce the high thermal stress in the frozen solution and to prevent the frozen solution from crushing.

(4) It is hypothesized that glycerol significantly reduces the thermal stresses inside the frozen solution by at least following two factors: (1) alternating the internal structure and physical properties of the frozen

solution; and (2) reducing the percentage of water in the solution and hence reducing the volume expansion of the frozen solution caused by water solidification.

(5) It is proposed that glycerol contributes to reduce the cryoinjury of cells caused by "Thermal Stress Effect" during the freezing preservation of cells.

CHAPTER 5

OSMOTIC INJURY OF THE HUMAN ERYTHROCYTES IN CRYOPRESERVATION AND ITS PROTECTION

NOMENCLATURE

C	concentration of tracers, g/cm^3
D	mass diffusion coefficient, cm^2/sec
D^*	nondimensional mass diffusion coefficient
erfc	complementary error function
Exp	exponential function
M	molarity, mole/liter
M′	initial osmolarity, osmole/liter
M″	final osmolarity, osmole/liter
r	radial coodinate, cm
R	radius of spherical cell, cm
t	time, sec
t^*	nondimensional time
V	aqueous volume inside cell, cm^3
ΔV	change of V, cm^3
W	total mass of tracers, g

Subscripts

g	glycerol
i	inside cell
o	outside cell
s	nonpermeable solute for cell membrane
w	water

5.1. Introduction

As surveyed in Chapter 1, the osmotic injury of cells has been generally believed to be one mode of cryoinjury, which is caused by osmotic alteration in the extracellular solution during slow cooling and quick warming processes. Before cooling, cells are usually suspended in an isoosmotic solution. During cooling, extracellular solution becomes hyperosmotic because of the precipitation of water as ice. A slow cooling process provides enough time for cells to dehydrate, which may induce serious shrinkage of the cell and abnormal cross-linking of the cell membrane structure [20,24]. During a quick warming process, the extracullar ice melts so rapidly that the shrunk cells suddenly experience a hypoosmotic environment which causes a fast water penetration into the cells, inducing cell rupture [38,47].

Using an inhibitor of water transportation through cell membrane, the importance of the osmotic injury to the human erythrocyte is evaluated, and the function of glycerol in preventing osmotic injury is examined in this chapter. Furthermore, the mechanisms of glycerol opposing osmotic injury are analysed, and physiochemical properties which a CPA candidate should have in order to prevent the osmotic injury are recommended.

5.2. Importance of Osmotic Injury of Human Erythrocyte in Cryopreservation

Two general mechanisms for the permeation of water through erythrocyte membrane have been proposed [138]. One model is based on the concept that the molecular motion of the hydrocarbon chains of membrane lipids generates structural defects through which water permeates [139]. The second model indicates that there are aqueous membrane channels or "pores" assembled from membrane integral proteins which span the cell membrane [138]. A majority (90%) of the total water flux penetrates cells by the membrane channels or "pores" [138]. It has been found that some mercurials, such as, PCMBS (*p-(chloromercuri) benzene-sulfonic acid)* and FMA *(fluorescein mercuric acetate)*, can react with amino-acid SH (sulfhydryl) groups on the proteins, thereby blocking the protein channels [140,141]. It was reported that PCMBS inhibited 80-90% of the osmotic water permeability of the erythrocyte membrane [141,142].

Since the osmotic injury of the frozen-thawed cells is a direct consequence of water permeation into or out of the cells, the osmotic injury should be limited to a certain extent if the water permeation is inhibited. In the following experiment, the water transportation through the cell membrane is inhibited by using PCMBS in order to evaluate the significance of the osmotic injury in the human erythrocytes after freezing-thawing treatments.

5.2.1. Experimental Method and Material

According to the published protocols [141,143], human erythrocytes were washed three times by centrifugation at 2000 g with a buffer solution containing 0.15M NaCl, 5mM sodium phosphate and pH 7.5. The washed erythrocytes were then suspended into six different media as indicated in Fig.5.1. The main components of the media are 0.15M NaCl, 5mM Hepes (N-2hydroxy-ethylpiperazine-N'-2-ethane sulfonic acid), 5.5 mM glucose, and 0.5% bovine serum albumin. The difference among the media is that Media 1, 3 and 5 contain 2mM PCMBS, and Media 2, 4 and 6 do not contain PCMBS. Besides, Media 1 and 2 contain 0.5M glycerol; Media 3 and 4 contain 1M glycerol; and Media 5 and 6 contain 2M glycerol. The final hematocrit of the cell suspensions is 10%.

The cell suspensions were kept at 37°C for 24 hours before the freezing test. Each of the six cell suspensions was divided into seven aliquots. Each of the aliquots contains 0.8ml of the cell suspension. Three of the seven aliquots were used for the freezing-warming tests and four of them were kept for the unfrozen controls. Using the similar techniques and methods as described in Chapter 2, a slow cooling rate, -0.5°C/min, and a rapid warming rate, +200°C/min, were obtained and used to treat the prepared cell suspensions. The percentage hemolysis of the frozen-thawed cells were determined by spectrophotometry.

The original purpose of using glycerol in the present experiment was to prevent the intracellular ice crystalli-

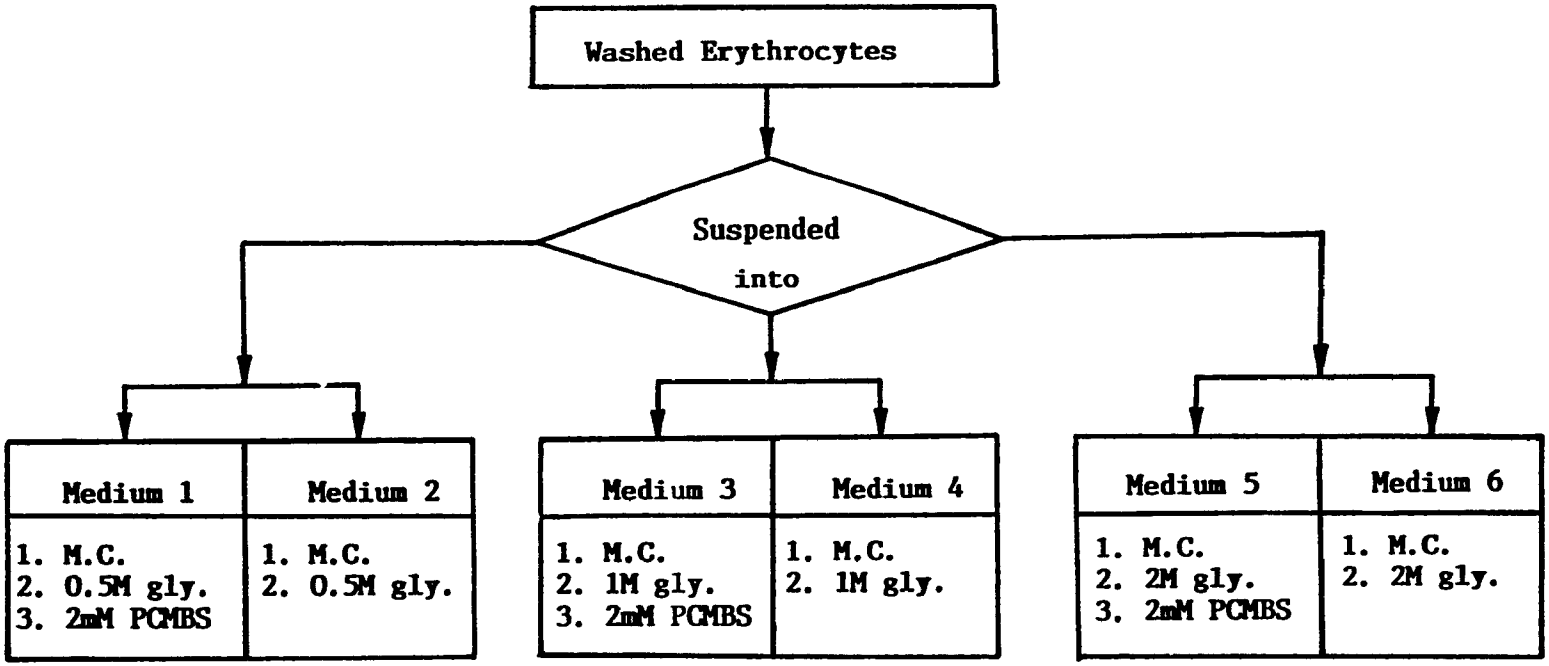

Figure 5.1: The composition of the prepared six different cell suspension media.

M.C. stands for Main Components of each of the media, i.e. 0.15M NaCl, 5mM Hepes (N-2hydro-xyethylpiperazine-N-2-ethane sulfonic acid), 5.5 mM glucose, and 0.5% bovine serum albumin.

zation as recommended by Pegg [52], and to prevent the "thermal stress effect" on the cells as suggested in Chapter 4 of this thesis. Besides, the hematocrit, 10%, is optimal for minimizing the "packing effect" as shown in Chapter 2.

5.2.2. Results and Discussion

Figure 5.2 shows the percent hemolysis of the frozen-thawed human erythrocytes with or without the treatment of PCMBS. The concentration of glycerol was a parameter in the tests. The difference between the percentage hemolysis of PCMBS-treated and untreated cells showed the least osmotic injury of the cells in the presence of PCMBS. The osmotic injury in the frozen-thawed cells was very significant as indicated in Fig.5.2. Besides, the osmotic injury of the cells decreased with an increase of the glycerol concentration, indicating that glycerol contributed to prevent the osmotic injury.

5.3. Effect of Glycerol on Transient Process of Osmotic Lysis of the Human Erythrocytes

The function of glycerol in preventing the osmotic injury to human erythrocytes and the importance of osmotic injury caused by both freezing (hyperosmotic) and thawing (hypoosmotic) treatments have been revealed. As an extension of the investigation in the last section (5.2), the following two experiments were designed to investigate (1) separate effects of hypo- and hyperosmotic environments on the osmotic-lysis of human erythrocytes (Experiment 1);

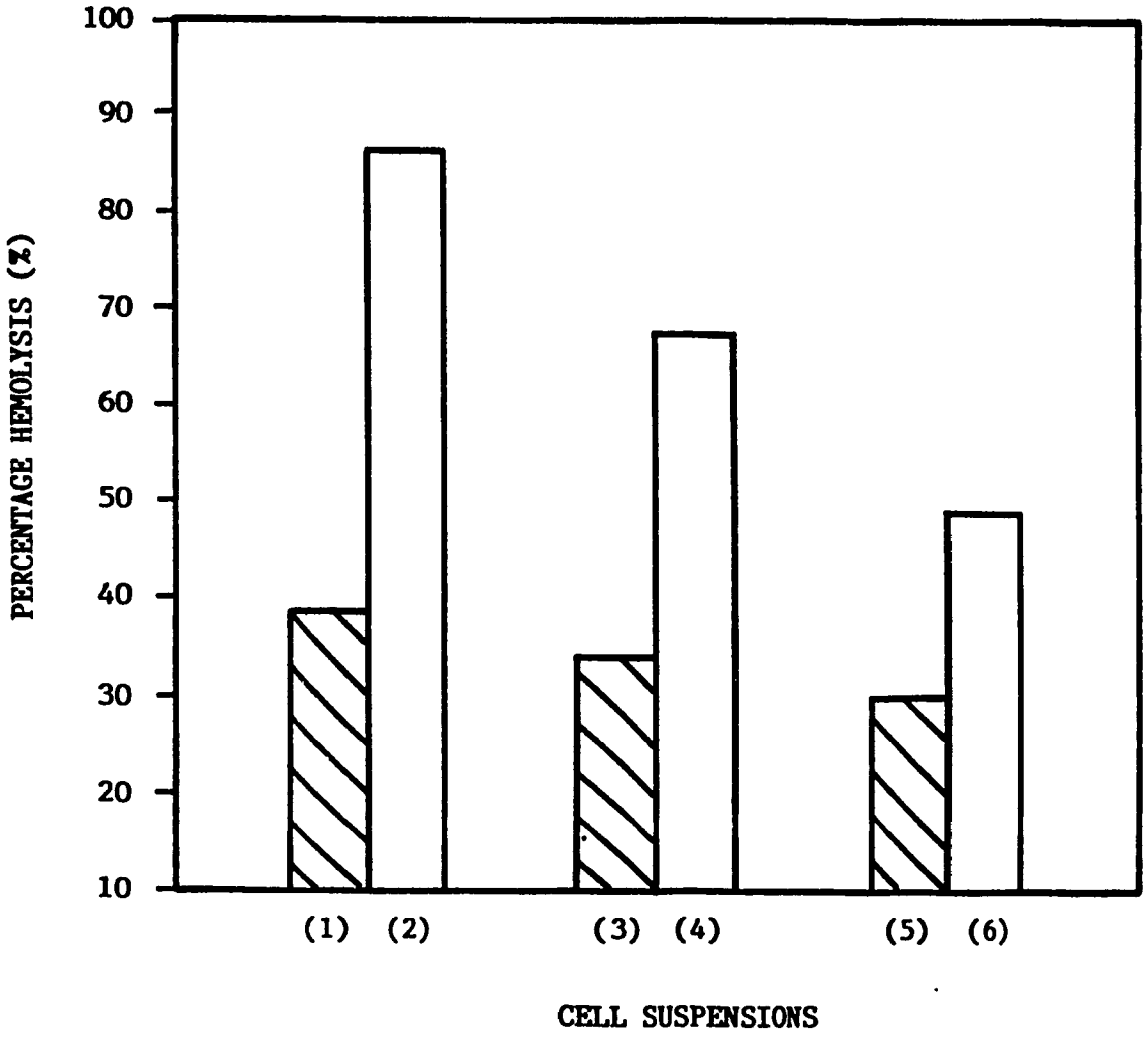

Figure 5.2: The cryoinjury (percent hymolysis) of the frozen-thawed human erythrocytes suspended in the six different media as shown in Figure 5.1.

Numbers (1) to (6) stand for the frozen-thawed cells suspended in the media 1 to 6, respectively. Media 1, 3 and 5 contain 2mM PCMBS, and Media 2, 4 and 6 don't contain PCMBS. Besides, Media 1 and 2 contain 0.5M glycerol; Media 3 and 4 contain 1M glycerol; and Media 5 and 6 contain 2M glycerol.

and (2) effect of glycerol concentration on the transient process of the osmotic-lysis (Experiment 2). These experiments were conducted at room temperature without freezing the cell suspensions in order to ensure that the hemolysis of the cells is caused only from hypo- or hyperosmotic injury.

5.3.1. Experimental Method and Materials

Experiment 1:

The erythrocytes were washed twice by 0.15M NaCl solution. The washed cell suspensions (30μl) with a hematocrit of 2% was then quickly diluted with the hypo- and hyperosmotic solutions (3ml) with NaCl concentrations varying from 0M to 20×0.15M.

Experiment 2:

The washed erythrocytes were first equilibrated against 0.15M NaCl solutions containing glycerol from 0M to 2M. Then the suspensions (30μl) with a hematocrit of 2% were diluted quickly into hypoosmotic solutions (3ml) containing the same concentration of glycerol but the different concentration of NaCl (0.06M), i.e. the initial osmolarity difference between the extra- and intra-cellular solutions was fixed at 180 mOsm for all tests.

The transient process of osmotic lysis of the human erythrocyte was investigated by measuring the variation of the transmitting light absorbance of the diluted cell suspensions. The transmitting light absorbance is proportional to the cell density i.e. the number of intact cells

per unit volume in cell suspension. The greater the light absorbance, the greater the number of intact cells in the diluted suspension. In order to avoid the effect of hemoglobins released from the lysed erythrocytes on the light absorbance, a specific monochromatic light with a wavelength of 800nm was selected by spectrophotometry. Hemoglobins do not absorb this monochromatic light, and hence the transmitting light absorbance of the diluted cell suspension is only affected by the cell density. The light absorbance of the diluted cell suspensions in Experiments 1 and 2 were continuously measured and plotted by a computer controlled spectrophotometer (Fig.5.3) at the wave length of 800nm.

5.3.2. Results and Discussion

Figure 5.4 shows the transient changes of the light absorbance of the diluted cell suspensions in Experiment 1 with the concentration of NaCl as a parameter. The osmotic lysis of the erythrocytes under the hypoosmotic conditions was very rapid, especially if the concentration of NaCl was lower than 0.1 M. In contrast, the hyperosmotic lysis was much slower and less serious than the hypoosmotic lysis although the hemolysis under hyperosmotic conditions also increased with the increase of NaCl concentration. Therefore, it is expected that the osmotic lysis of the human erythrocytes in cryopreservation may primarily take place during the warming process in which cells experience hypoosmotic environment.

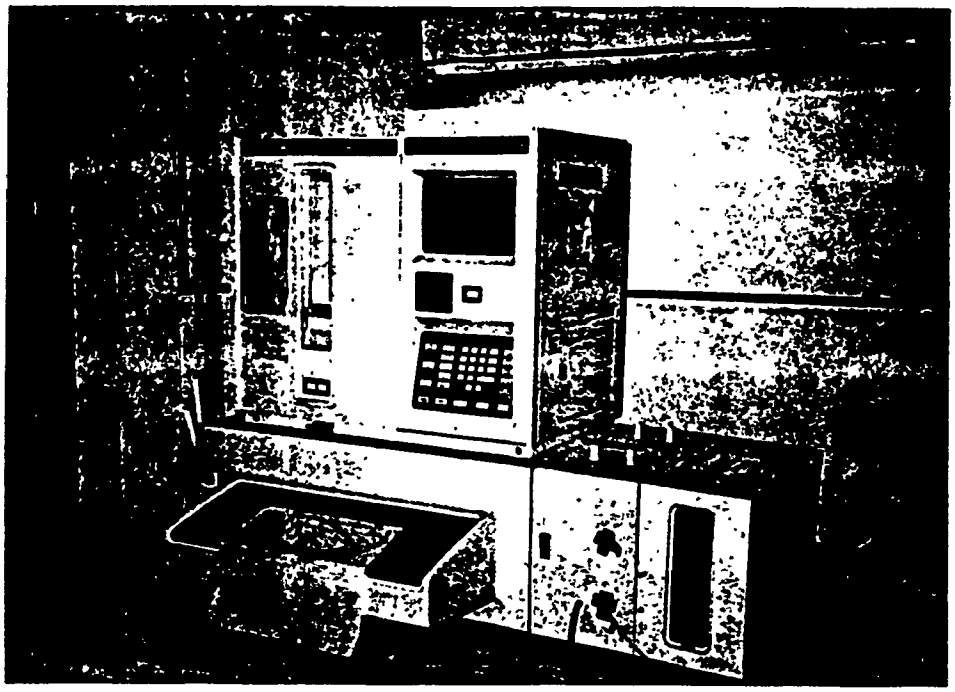

Figure 5.3: A computer controlled spectrophotometer used to measure the alteration of the transmitting light absorbance of the diluted cell suspensions at the wave length of 800nm.

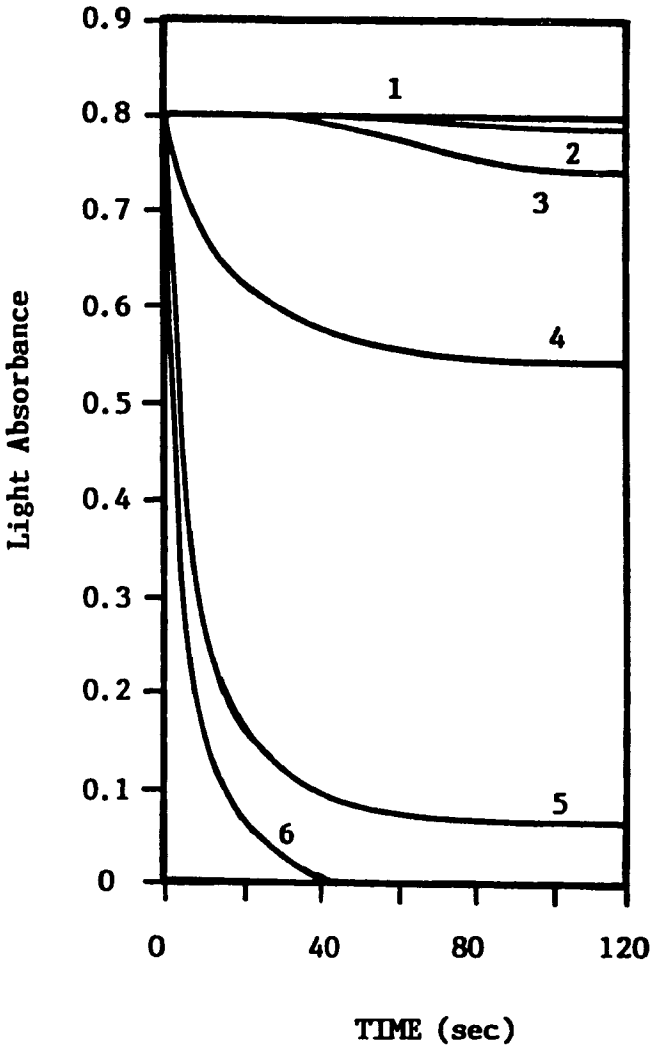

Figure 5.4: The transient alteration of light absorbance of the cell suspensions diluted in the different hypo- and hyper-osmotic solutions with the NaCl concentration, C_n, as a parameter.

Curve 1: $C_n = 1 \times 0.15M$; Curve 4: $C_n = 0.6 \times 0.15M$;

Curve 2: $C_n = 10 \times 0.15M$; Curve 5: $C_n = 0.4 \times 0.15M$;

Curve 3: $C_n = 20 \times 0.15M$; Curve 6: $C_n = 0 \times 0.15M$;

It should be noted that any rapid change of the light absorbance, which may occur within the first few milliseconds after the dilution of the cell suspension, cannot be measured by the spectrophotometer because of its limited sensitivity. Therefore, data of the light absorbance measured within the first few miliseconds of each test is not valid.

The effect of glycerol on the transient process of hypoosmotic lysis of the cells is shown in Fig.5.5. The rate of hemolysis quickly decreased with an increase of the glycerol concentration in the cell suspension although the initial osmolarity difference between the extra- and intracellular solutions is fixed at a same value (180mOsm) in all tests. This finding suggests that glycerol contributes at least to reduce the rate of water transportation through the cell membrane under the present experimental conditions because the osmotic lysis of cells is a direct consequence of water transportation through cell membrane.

The function of glycerol in retarding the water permeation through the cell membrane is very significant for prevention of the osmotic injury of the cells in cryopreservation. It is proposed that, because of the retarding of the water permeation by glycerol, the time which is required for the osmotic lysis of the cells is extended. Therefore, in the presence of glycerol, the cells would experience relatively less shrinkage during cooling process before they are frozen and relatively less

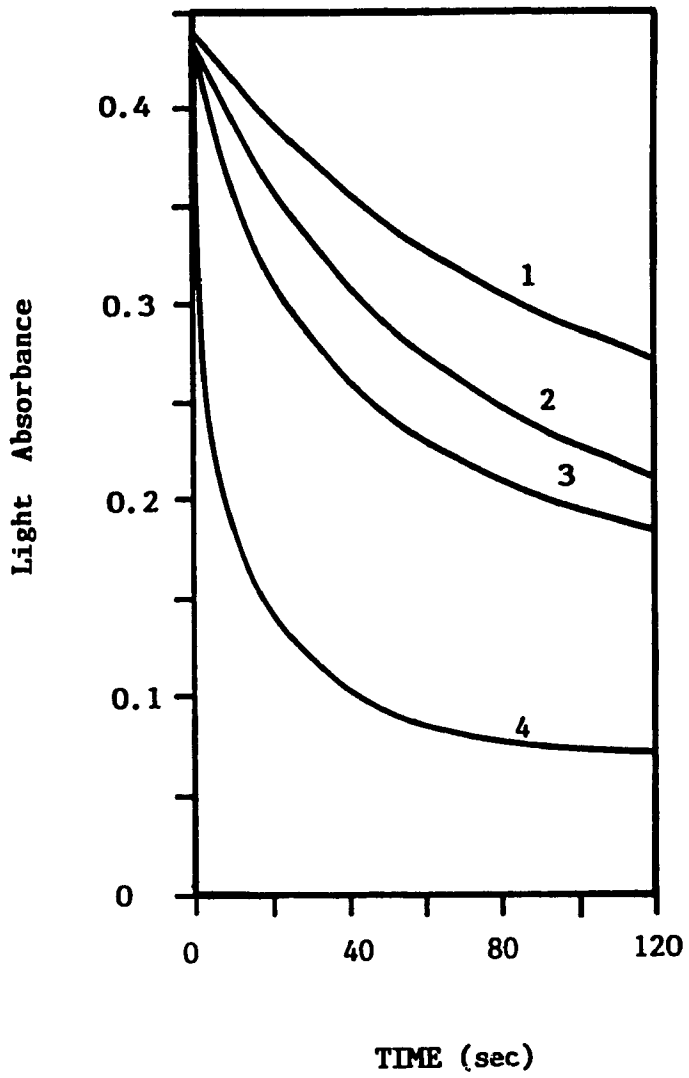

Figure 5.5: The transient alteration of the light absorbance of the cell suspensions diluted in hypo-osmotic solutions (C_n=0.6×0.15M) with the glycerol concentration, C_g, as a parameter.

Curve 1: C_g = 2M; Curve 3: C_g = 0.5M;
Curve 2: C_g = 1M; Curve 4: C_g = 0 M;

expansion during warming process before the osmotic equilibrium between the intra- and extra- cellular solutions is achieved.

5.4. Possible Mechanisms of Glycerol In Retarding Water Permeation through Cell Membrane

Several possible mechanisms by which glycerol retards water permeation through cell membrane are invoked and analysed as follows:

5.4.1. Hydration Effect

It is known that glycerol can dissolve in water at any proportion. In aqueous solution, glycerol molecules bind with a part of water molecules by hydrogen bonds to form hydrates [144]. Therefore, the number of water molecules which can freely move in solution is reduced because of the glycerol-water binding. Based on the Boltzmann energy distribution, the percentage (N^*) of the number of the bound glycerol molecules over the total number of the glycerol molecules can be calculated as follows:

$$N^* = \frac{N_b}{N} = \frac{Exp(-\Delta E/RT)}{1 + Exp(-\Delta E/RT)} \qquad (5.1)$$

where N_b is number of the bound glycerol molecules, N is the total number of glycerol molecules in solution, ΔE is the bond energy, R is the universal gas constant, and T is temperature (K).

For example, assuming that one glycerol molecule can bind with only one water molecule by a hydrogen bond, taking a typical hydrogen bond energy, $\Delta E = -2$ kcal/mole,

R = 1.98 cal/K·mole, and temperature at 198K (25°C), one can get:

$$N^* = 97\% \tag{5.2}$$

Therefore, percentage (P1) of the number of free water molecules over the total number of water molecules can be calculated as follows:

$$P1 = \frac{M_w - M_g \times N^*}{M_w} = 1 - \frac{N^*}{55.6/M_g - 4.1} \tag{5.3}$$

where M_w and M_g are molarities of water and glycerol respectively.

Figure 5.6 shows the variation of P1 as a function of molarity of glycerol. It is found that the number of free water molecules decreases with an increase of the glycerol concentration in cell suspension.

5.4.2. Dimension Effect

Based on the mechanisms of water permeating across the cell membrane [138,139], it is known that the free water molecules have to contact the membrane in order to penetrate cell membrane through the "pores". However, in the presence of glycerol, a part of membrane surface is covered or bound by glycerol molecules through hydrogen bonds. Therefore, the percentage (P2) of the membrane surface area available for the water penetration out of the total membrane surface area is reduced. P2 can be calculated as follows:

$$P2 = 1 - \frac{M_g \times W_g}{\rho_g \times 1000} \tag{5.4}$$

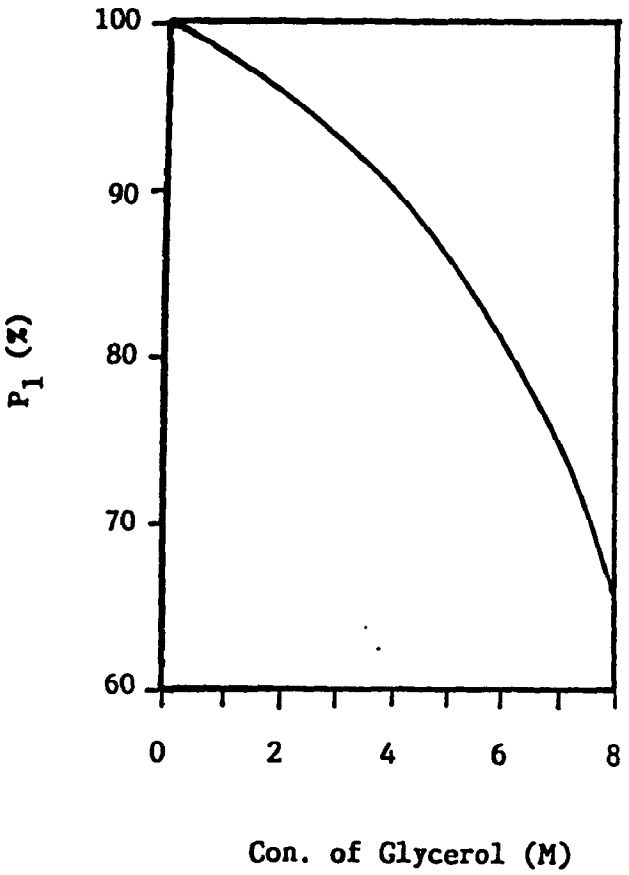

Figure 5.6: Effect of glycerol concentration on the percentage (P1) of the number of free water molecules over the total number of water molecules in the solution.

where W_g is mole molecular weight of glycerol, and ρ_g is density of glycerol.

The change of P2 as a function of the concentration of glycerol is shown in Figure 5.7. It is obvious that the effective membrane surface area for the water permeation decreases with an increase of glycerol concentration.

5.4.3. Drag Effect

The continuing collision or interaction between the free water molecules and the solute molecules retards the diffusion of free water molecules in a solution [145], which may slow down the motion of free water molecules towards cells. This drag effect can be quantitatively shown by a simplfied model as follows:

Figure 5.8 shows a spherical cell suspended inside an aqueous solution with a solute "G" (e.g. glycerol). Assuming that some of free water molecules are labeled as tracers, and the tracers penetrate the cell as soon as they contact the cell membrane [145]. The diffusion process of the tracers, initially r_o distance away from the center of the cell, can be mathematically formulated as follows:

Governing Equation:

$$\frac{\partial C}{\partial t} = \frac{D_{wg}}{r} \frac{\partial^2 (rC)}{\partial r^2} \qquad (5.5)$$

Boundary Condition:

$$C(R,t) = 0 \qquad (5.6)$$

$$C(\infty,t) = 0 \qquad (5.7)$$

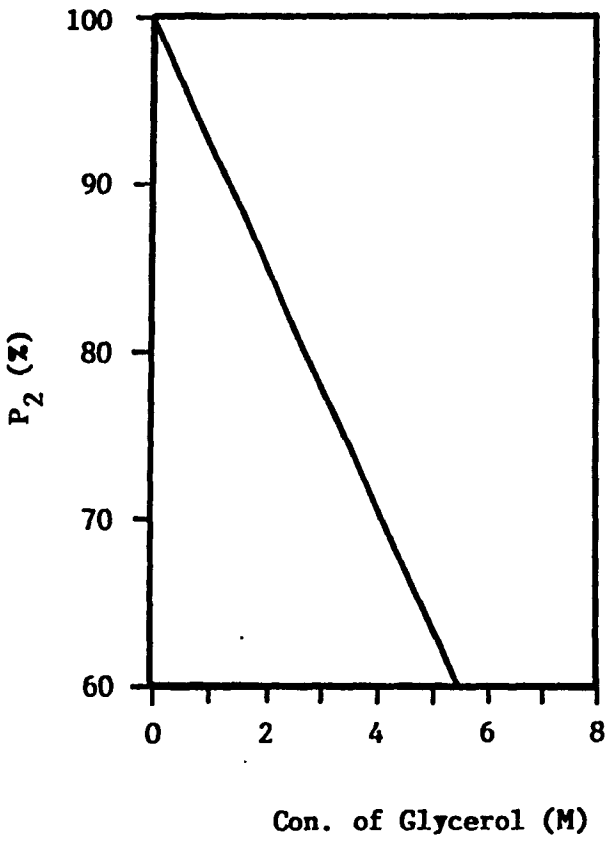

Figure 5.7: Effect of glycerol concentration on the percentage (P2) of the membrane surface area available for the water permeation over the total membrane surface area.

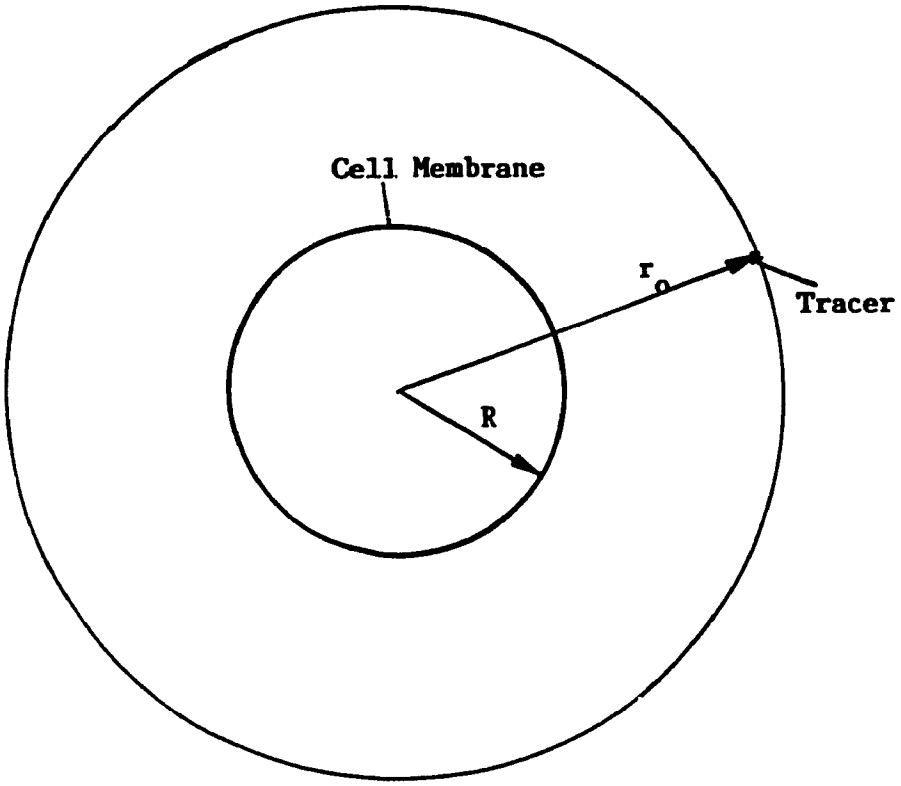

Figure 5.8: A research model to study the "Drag Effect":

A spherical cell suspended inside an aqueous solution with a solute "G" (e.g. glycerol). Assuming that some of free water molecules are labeled as tracers, and the tracers penetrate the cell as soon as they contact the cell membrane. The number of the tracers, which are initially r_o distance away from the center of the cell and penetrate into the cells within the time period of t_o, can be determined by the model.

Initial Condition: $$C(r,0) = \frac{W}{4\pi r_o^2}\,\delta(r-r_o) \qquad (5.8)$$

where C is concentration of the tracers, D_{wg} is diffusion coefficient of water in the solution with solute "G", t is time, r is radial coordinate, W is the total weight of the tracers, and δ expresses δ function.

Solving equations (5.5) to (5.8), one can get:

$$C(r,t) = \frac{W}{8\pi r_o\ \pi D_{wg} t}\,\frac{1}{r}\left\{\mathrm{Exp}\left(\frac{-(r-r_o)^2}{4D_{wg}t}\right) - \mathrm{Exp}\left(\frac{-(r+r_o-2R)^2}{4D_{wg}t}\right)\right\} \qquad (5.9)$$

where Exp expresses the exponential function.

The percentage (P3) of the tracers which contact the cell membrane within a time period of t_o can be calculated:

$$P3 = \frac{D_{wg}}{W}\int_0^{t_o}\frac{\partial C(R,t)}{\partial r}\,4\pi R^2\,dt$$

$$= \frac{1}{r^*}\,\mathrm{erfc}\left[\frac{r^*-1}{t^*\times D^*}\right] \qquad (5.10)$$

where $r^* = r_o/R$, $D^* = D_{wg}/D_w$, $t^* = 2\sqrt{D_w t_o}/R$, erfc expresses the complementary-error function, and D_w is the water self-diffusion coefficient in pure water.

Figure 5.9 shows the variation of P3 as a function of nondimensional water diffusion cofficient D^*. The percentage of the water-tracers which contact cell membrane within a time period (nondimensional time $t^*=20$) decreases quickly with a decrease of D^* (D_{wg}/D_w). Because D_w is a constant at a fixed temperature, value of D^* mainly depends

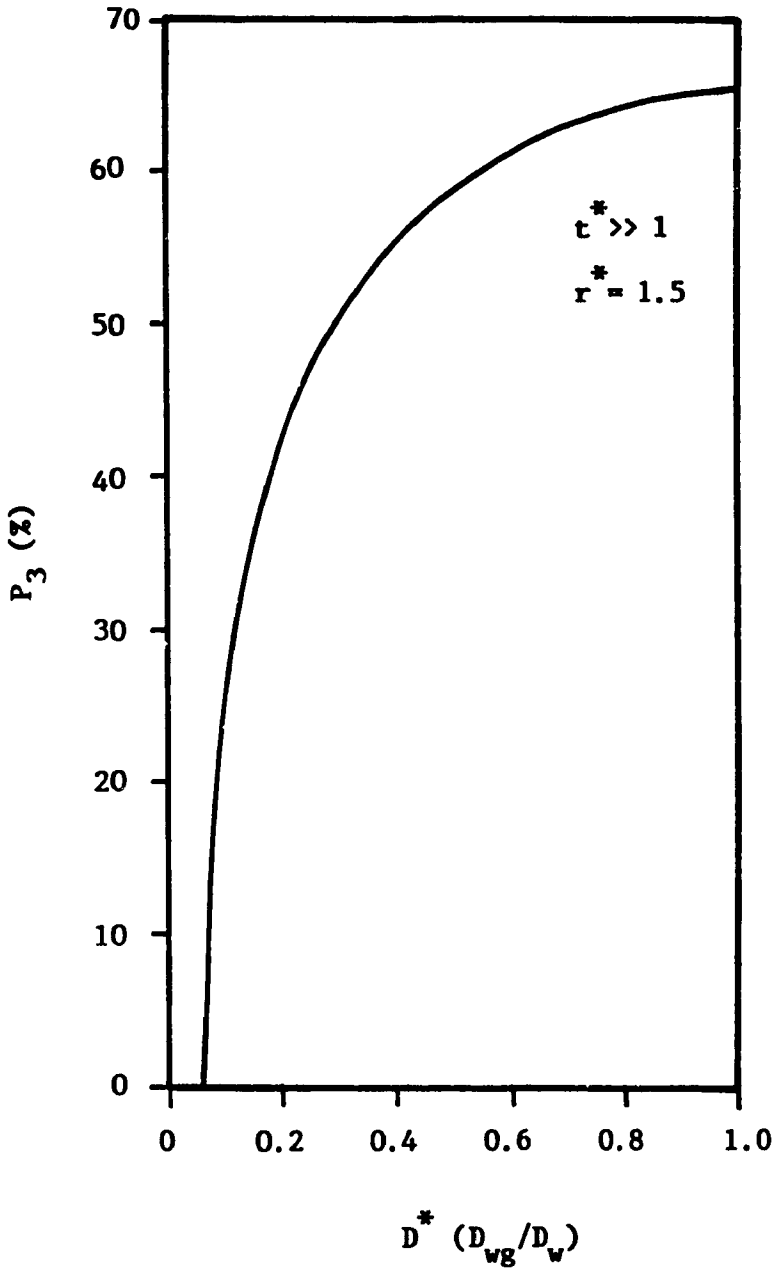

Figure 5.9: The percentage (P3) of the tracers, which are initially r^* (r_o/R = 1.5) distance away from the center of the cell and penetrate into the cells within the time period of t^* ($2\sqrt{D_w t_o}/R$ = 20), as a function of nondimensional diffusior coefficient D^* (D_{wg}/D_w).

on the value of D_{wg}. Therefore, the smaller the value of D_{wg}, the smaller the P3. In order to retard the movement of the free water molecules towards the cell, a small value of D_{wg} is required.

The D_{wg} can be empirically calculated by the following equation [146]:

$$D_{wg} = 1.28\times10^{-8}\times \left[(\phi\ W_g)^{0.5}\ \frac{T}{\mu_g} \right] \qquad (5.11)$$

where W_g= molecular weight of solute, T = temperature (K), μ_g= viscosity of solution with solute "G", and ϕ is a empirical constant.

Equation (5.11) indicates that a small value of D_{wg} can be reached in a high-vicosity (μ_g) solution with a small molecular-weight (W_g) solute at low temperature (T). It has been known that glycerol generates high viscosity in aqueous solution, particularly at low temperatures [144] as shown in Fig.5.10. The molecular weight of glycerol, 92, is one of the smallest among all CPAs used. Therefore, it is expected that at low temperatures, glycerol slows down the diffusion of free water molecules towards the cells.

5.4.4. Effect of Glycerol on Total Amount of Water Required by cells to Equilibrate the Hypoosmotic Environment

Figure 5.11 demonstrates a model of human erythrocyte suspended in a hypoosmotic solution. The extra- or intra-cellular osmotic environment is similar to those prepared in Experiment 2 of the Section 5.3.1: Initially,

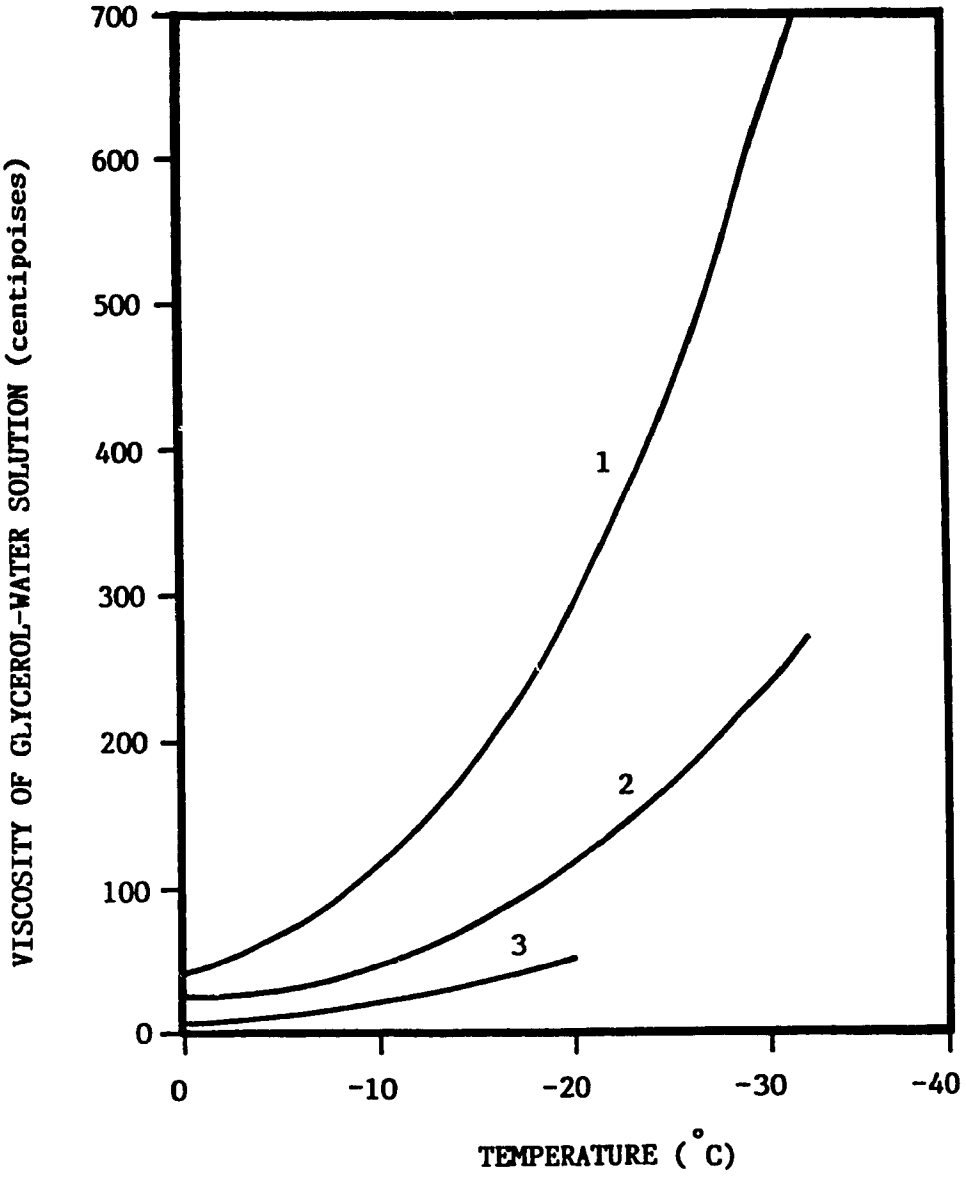

Figure 5.10: Viscosity of glycerol-water solution as a function of low temperature with the glycerol concentration C_g as a parameter.

Curve 1: C_g = 66.7% wt;

Curve 2: C_g = 60% wt;

Curve 3: C_g = 50% wt;

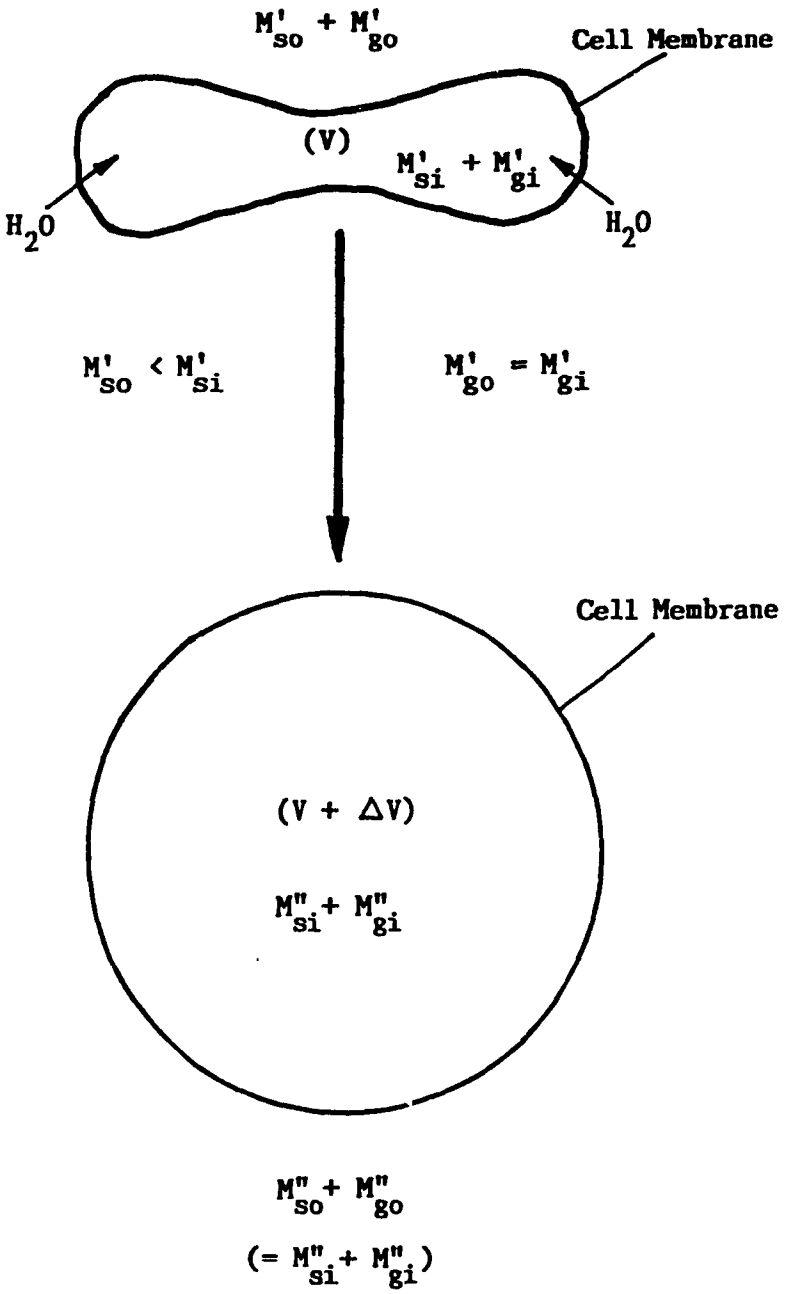

Figure 5.11: Top: A human erythrocyte initially suspended in the hypoosmotic solution.

Bottom: A expanded human erythrocyte at a osmotically quasi-equilibrium state.

the osmolarity of glycerol (M'_{go}) in extracellular solution is the same as that (M'_{gi}) in intracellular solution, but the osmolarity (M'_{so}) of nonpermeable solutes in the extracellular solution is lower than that (M'_{si}) in the intracellular solution.

Before theoretical analysis, the following assumptions are made:

(a) The hemotocrit of the cells is so small that the penetration of water into the cell does not affect the concentration of extracellular solution;

(b) Because the permeability of the cell membrane to glycerol is much smaller than to water, glycerol may be assumed as a nonpermeable agent during a short period of time.

Under these assumptions, the total volume of water (ΔV) required for the cell to equilibrate the hypoosmotic environment can be determined by the following equations:

Initially,

$$M'_{gi} = M'_{go} \tag{5.12}$$

$$M'_{si} > M'_{so} \tag{5.13}$$

At the osmotic quasi-equilibrium state:

$$M''_{gi} + M''_{si} = M''_{go} + M''_{so} \tag{5.14}$$

$$(\Delta V+V)\times(M''_{si}+ M''_{gi}) = V\times(M'_{si}+M'_{gi}) \tag{5.15}$$

From assumption (a):

$$M''_{go} + M''_{so} = M'_{go} + M'_{so} \tag{5.16}$$

where prime ' means the initial state, and double prime " means the osmotic quasi-equilibrium state.

From equations (5.11) to (5.16), one can get:

$$\Delta V = \frac{(M'_{si} - M'_{so}) \times V}{(M'_{go} + M'_{so})} \tag{5.17}$$

$$= \frac{1}{(M'_{go}/M'_{so}+1)} \times \Delta V^* \tag{5.18}$$

$$\text{where} \quad \Delta V^* = \frac{(M'_{si} - M'_{so}) \times V}{M'_{so}} = \text{constant} \tag{5.19}$$

If $M'_{go} = 0$, i.e. there is no glycerol, from eq.(5.18), one can get:

$$\Delta V = \Delta V^*$$

Therefore, ΔV^* is the volume of water required for the cell to equilibrate the hypoosmotic environment without glycerol.

If $M'_{go} > 0$, i.e. there is glycerol, from eq.(5.18), one can get:

$$\Delta V < \Delta V^*$$

From equation (5.17), it is found that for a given initial osmolarity difference between the extra- and intracellular solutions (M'_{si}-M'_{so}), the volume (ΔV) of water penetrating into the cell to equilibrate the hypoosmotic environment is reduced with an increase of the initial glycerol concentration (M'_{go}). Figure 5.12 demonstrates the variation of $\Delta V/\Delta V^*$ as a function of M'_{go}/M'_{so}. From

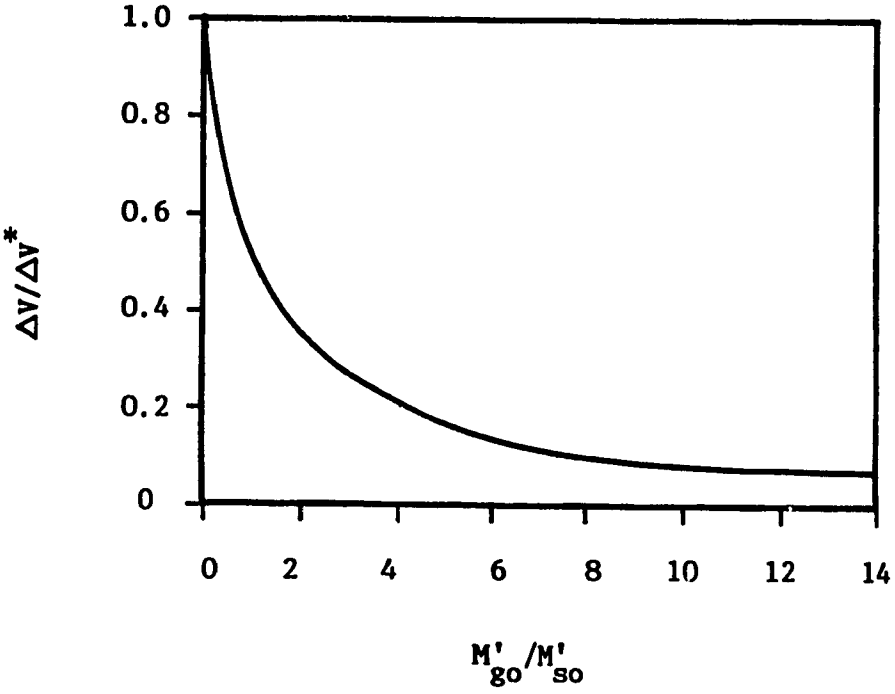

Figure 5.12: Effect of the glycerol concentration on the volume amount of water required for the cells to equilibrate the hypoosmotic environment.

eq.(5.18), for example, if M'_{so} = 0.15M and M'_{go} = 1.5M, ΔV is only 1/11 of ΔV^*. In other words, in the presence of glycerol, only a small amount of water penetrates into the cell in order to equalize intra- and extra-cellular osmotic pressures, and hence the osmotic lysis of the cell is depressed.

5.5. Conclusion

From the experimental and theoretical studies above, the conclusion are made as follows:

(1) The osmotic lysis of the human erythrocytes experienced the slow cooling and rapid warming treatments is very significant;

(2) Glycerol significantly prevents the osmotic lysis of the cells. The higher the glycerol concentration, the less the osmotic lysis.

(3) Inhibition of water transportation through cell membrane by PCMBS significantly improves the cryoprotection afforded by glycerol.

(4) The mechanisms of glycerol opposing the osmotic injury of the cells may be explained by its "hydration effect" which reduces the number of free water molecules, the "dimension effect" which reduces the effective membrane area for water transportation, the "drag effect" which retards the diffusion of the free water molecules towards cell membrane, and the function of glycerol in reducing the amount of water required to penetrate into the cell to

equalize intra- and extra-cellular osmotic pressures.

(5) It is proposed that a compound which has the following properties or abilities is a good CPA candidate to prevent the osmotic injury of cells in cryopreservation:

(a) binding water molecules to make more hydrates;

(b) penetrating cell membrane;

(c) having a small molecular weight;

(d) generating high viscosity in the aqueous solution particularly at low temperature;

CHAPTER 6

EFFECT OF MECHANICAL INTERACTION BETWEEN ICE AND CELLS ON CRYOINJURY OF THE CELLS IN FREEZING PRESERVATION

NOMENCLATURE

E	Young's modulus of the membrane, dyn/cm^2
L	diameter of the membrane, cm
ΔL	elongation of the membrane, cm
N_θ	membrane stress resultant in θ direction, dyn/cm
N_ϕ	membrane stress resultant in ϕ direction, dyn/cm
$N_{\theta\phi}$	membrane shear stress resultant, dyn/cm
p_θ	θ component of the total loading force on surface of the infinitesimal element of the membrane, dyn/cm^2
p_ϕ	ϕ component of the total loading force on surface of the infinitesimal element of the membrane, dyn/cm^2
p_n	normal component of the total loading force on surface of the infinitesimal element of the membrane, dyn/cm^2
u_θ	membrane displacement in θ direction, cm
u_ϕ	membrane displacement in ϕ direction, cm
u_n	membrane displacement in direction normal to the membrane surface, cm
ε_θ	membrane strain in θ direction
ε_ϕ	membrane strain in ϕ direction
$\varepsilon_{\theta\phi}$	membrane shear strain
τ	thickness of the membrane, cm
ν	poisson ratio

6.1. Introduction

In the process of cooling cell suspensions, extracellular water first precipitates as ice. it has been observed by using a cryomicroscope [48,55] that at below but approaching zero temperatures, some of the cells remaining inside the unfrozen suspension were packed by the surrounding ice walls, and their membranes were damaged during the packing process before the whole solution was frozen.

The mechanical interaction between the packed cells and the ice walls has been proposed as one of the reasons causing the cryo-lysis of the cell membranes [50,57]. However, a detailed investigation of the effect of mechanical interaction on membrane damage has not been conducted because of the following difficulties:

(1) Due to the lack of instrumentation and the complexity of the extracellular environment during the freezing process, it is very difficult to measure experimentally the mechanical stress and strain in the membrane of the packed cells.

(2) A theoretical analysis of the membrane stresses and strains cannot be carried out because of the unknown mechanical properties of the membrane at low temperatures.

Recently, Thom [147] designed a new piece of equipment to investigate the deformation of the human erythrocytes at subzero temperatures (from 0°C to -20°C). In his experiments [147,148], the cells were suspended in

solutions with low freezing points. High-frequency electric fields (0.1<frequency<5MHz) were generated by the equipment to polarize the cell membrane, and the force of the electric field was applied to stretch the polarized membrane. From the known force of the electric field and the measured elongation of the cell membrane, the Young's modulus of the membrane at each different low temperature was estimated. The cell membrane was shown to be a linear elastic material at the subzero temperatures. The deformability of the membrane was significantly reduced with decreasing temperature.

Based on Thom's experimental data [148], a simplified packing model of the human erythrocyte between the ice walls is studied numerically in this chapter by using the finite element method. The effects of the ice-cell interaction on membrane stress and membrane lysis are analysed.

6.2. Mathematical Formulation

6.2.1. Research Model

A typical case of the ice-cell interaction during the packing process is shown in Fig.6.1(a), i.e. a cell is packed by two parallel ice walls which are approaching face to face [48,55]. As a first approximation, the research model for this typical ice-cell interaction is shown in Fig.6.1(b). In the model, the axis-symmetrical distributive force p_o acting on the upper and lower surfaces of the cell

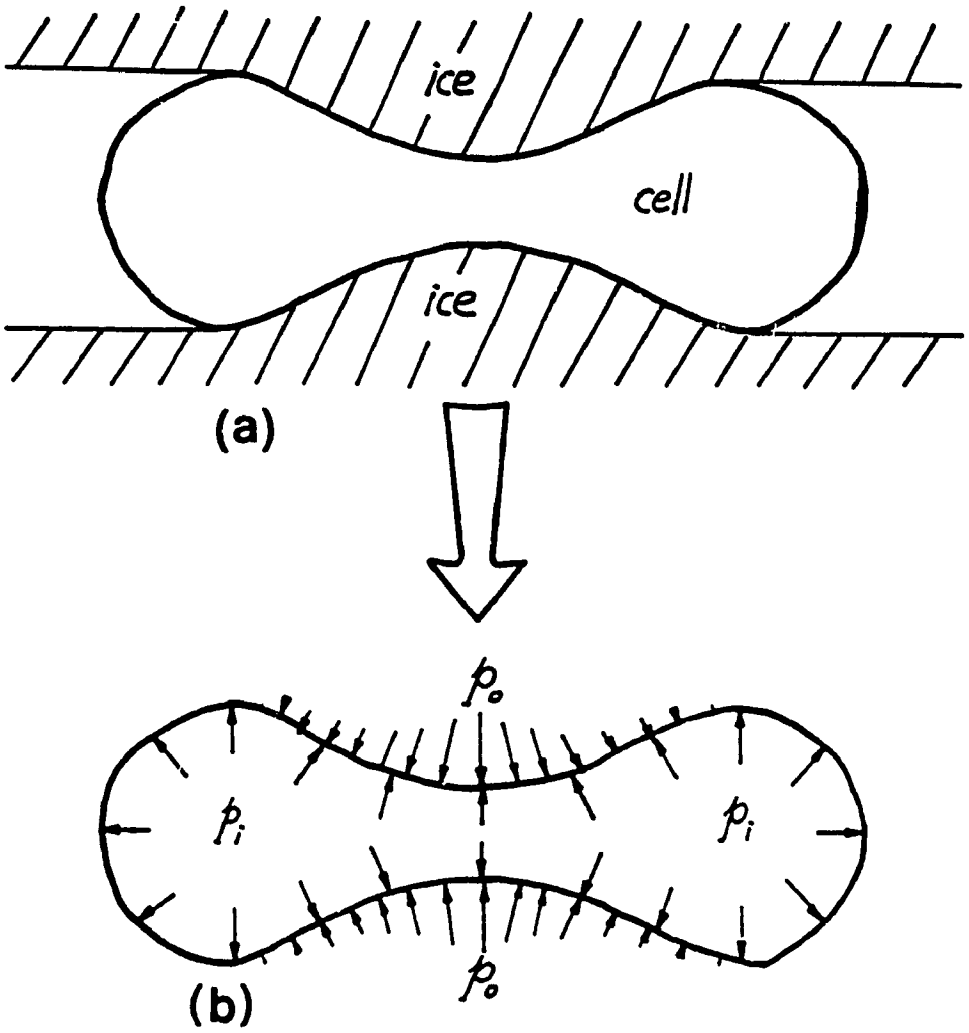

Fig. 6.1.(a) A typical case of the ice-cell interaction during the cooling process.

(b)The simplified research model for the typical case of the ice-cell interaction. p_o is the distributive packing force generated by the ice. p_i is the distributive force generated by cytoplasm.

membrane is assumed to be the packing force generated by the moving ice walls. The membrane of the human erythrocyte is, as usual, simplified as an isotropic, homogeneous and elastic shell filled with incompressible cytoplasm [96,98,101]. p_i expresses the distributive force acting uniformly on the internal surface of the cell membrane. p_i is generated by the cytoplasm during the packing process because of the incompressibility of the cytoplasma. Under the distributive forces, intracellular water may move out of the cell through the membrane. However, it is assumed in the present study that there is no water penetration across the membrane during the rapid packing process, i.e. the cell volume is always constant. The p_o is assumed to have the following linear form:

$$p_o = \begin{cases} A\times(r-r_o) & 0<r\le r_o \\ 0 & r>r_o \end{cases} \qquad (6.1)$$

where A is a constant, r is distance from any point on the membrane to the symmetric axis of the membrane (Fig.6.2), and r_o= 2.737 μm [97] which is distance from the top point of the membrane to the symmetric axis (Z axis).

6.2.2. Coordinate System

The membrane of the human erythrocyte is a surface of revolution by rotating a biconcave plane curve about the symmetric axis as shown in Fig.6.2. The meridians and the latitude circles on the surface of rotation are lines of principal curvature and form an orthogonal family of parameter lines [149]. The meridian curve on the cell

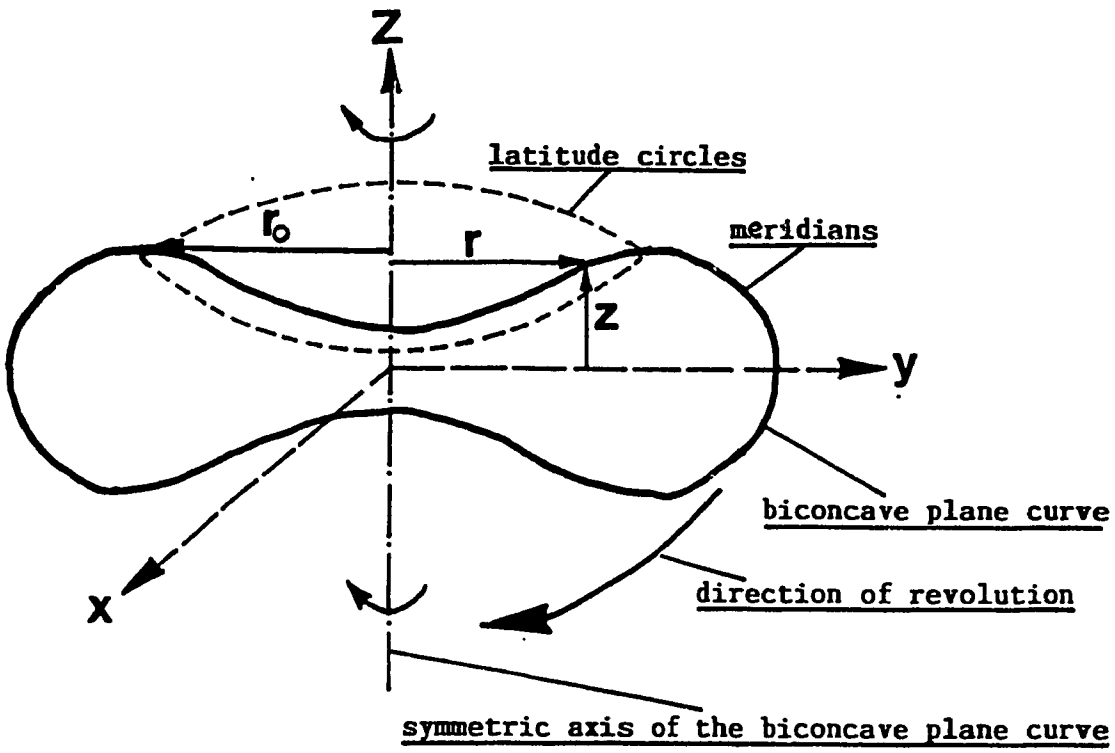

Fig. 6.2. Geometry of the membrane of the human erythrocyte.

membrane is described as follows [97]:

$$z(r)= \pm 0.5\left[1-\left(\frac{r}{R_o}\right)^2\right]^{0.5}\left[C_o+C_2\left(\frac{r}{R_o}\right)^2+C_4\left(\frac{r}{R_o}\right)^4\right] \qquad (6.2)$$

where R_o is the radius of the cell membrane and equal to 3.91μm, C_o=0.81μm, C_2=7.83μm and C_4=-4.39μm.

There are two principal radii at any point P on the membrane surface as shown in Fig.6.3. R_ϕ is the radius of curvature of the meridian at point P and also is one of the principal radii at this point. Another principal radius is R_θ which is the distance along the line normal to the surface drawn from point P to the axis of revolution of the surface. R_θ and R_ϕ can be determined by the following equations [150]:

$$R_\phi = - \left[1 + (r')^2\right]^{1.5}/r'' \qquad (6.3)$$

$$R_\theta = r \left[1 + (r')^2\right]^{0.5} \qquad (6.4)$$

where $r'= \frac{dr(z)}{dz}$, and $r''= \frac{d^2r(z)}{dr^2}$.

The position of any point P on the membrane can be determined by angles θ and ϕ. As shown in Fig.6.3, θ is the angle between plane Y=0 and any plane which passes through the Z axis, and ϕ is the angle between the Z axis and the normal to the membrane surface. Angles θ and ϕ are taken as curvilinear coordinates of the membrane surface.

6.2.3. Basic Assumptions

Mathematical formulation for the stress analysis of

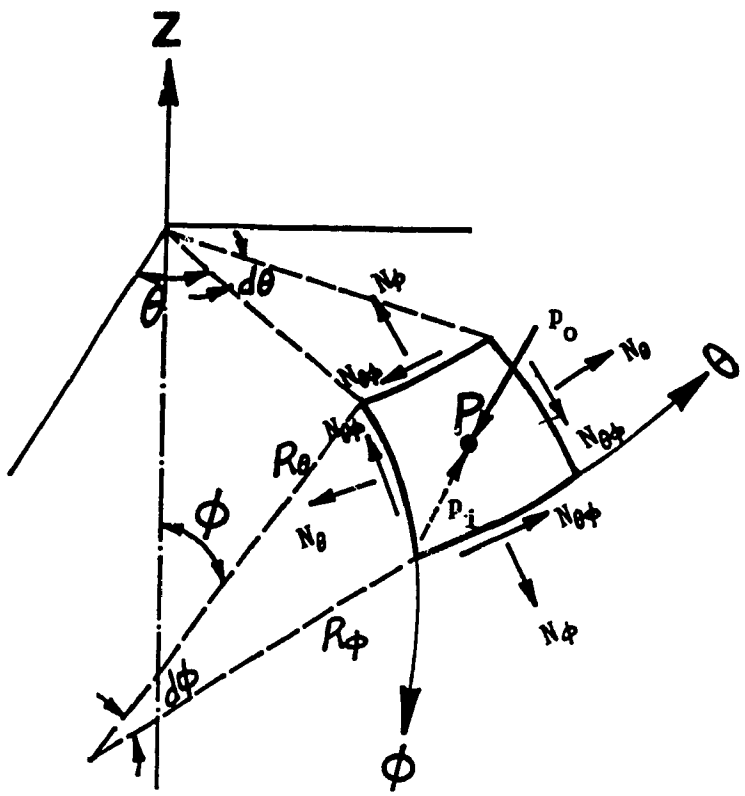

Fig. 6.3. The coordinates (θ,ϕ) on the membrane surface and forces acting on a infinitesimal element at point P on the membrane surface.

the cell membrane is based on Love's theory [149] of a thin elastic shell under the following assumptions:

(1) The shell is thin.

(2) The deflections of the shell are small.

(3) The transverse normal stresses are small and may be neglected.

(4) The normal to the reference surface (usually, the middle surface) of the shell remains normal to it and undergoes no change in length during deformation.

(5) The membrane material is incompressible.

From Love's theory, it has been shown [149] that a thin elastic shell supports arbitrary loading by means of internal stress resultants and stress couples (resulting bending moments) on the cross-section of the shell. Under appropriate loading conditions, however, the bending moments are either zero or so small that they may be neglected. Such a state of stress is referred to as the membrane state of stress because of the analogy to membranes which cannot support bending moments [149]. In the stress analysis of the cell membrane, the membrane state of stress is generally assumed, i.e. all bending moments are neglected. Therefore, only the stress resultants exit as indicated in Fig.6.3.

6.2.4. Governing Equations:

Under the assumptions and analyses above, the general equations for the stress analysis of the cell membrane model are set out below:

Equilibrium Equations:

$$\frac{\partial\left(N_{\phi}r\right)}{\partial\phi} + R_{\phi}\frac{\partial\left(N_{\phi\theta}\right)}{\partial\theta} - N_{\theta}R_{\phi}\cos\phi + p_{\phi}^{*}rR_{\phi} = 0 \tag{6.5}$$

$$\frac{\partial\left(N_{\phi\theta}r\right)}{\partial\phi} + R_{\phi}\frac{\partial\left(N_{\theta}\right)}{\partial\theta} + N_{\phi\theta}R_{\phi}\cos\phi + p_{\theta}^{*}rR_{\phi} = 0 \tag{6.6}$$

$$\frac{N_{\phi}}{R_{\phi}} + \frac{N_{\theta}}{R_{\theta}} + p_{n}^{*} = 0 \tag{6.7}$$

Stress Resultants:

$$N_{\phi} = \frac{E\,\tau}{1-\nu^{2}}\left(\varepsilon_{\phi} + \nu\varepsilon_{\theta}\right) \tag{6.8}$$

$$N_{\theta} = \frac{E\,\tau}{1-\nu^{2}}\left(\varepsilon_{\theta} + \nu\varepsilon_{\phi}\right) \tag{6.9}$$

$$N_{\phi\theta} = \frac{E\,\tau}{2(1+\nu)}\varepsilon_{\phi\theta} \tag{6.10}$$

Strain-Displacement Relations:

$$\varepsilon_{\phi} = \frac{1}{R_{\phi}}\left[\frac{\partial\left(u_{\phi}\right)}{\partial\phi} + u_{n}\right] \tag{6.11}$$

$$\varepsilon_{\theta} = \frac{1}{r}\left[\frac{\partial\left(u_{\theta}\right)}{\partial\theta} + u_{\phi}\cos\phi + u_{n}\sin\phi\right] \tag{6.12}$$

$$\varepsilon_{\phi\theta} = \frac{1}{R_{\phi}}\frac{\partial\left(u_{\theta}\right)}{\partial\phi} - \frac{1}{r}\left[u_{\theta}\cos\phi - \frac{\partial\left(u_{\theta}\right)}{\partial\theta}\right] \tag{6.13}$$

Periodical Conditions:

$$N_{\phi}(\theta,\phi) = N_{\phi}(\theta,\phi+2\pi) \tag{6.14}$$

$$N_{\phi}(\theta,\phi) = N_{\phi}(\theta+2\pi,\phi) \tag{6.15}$$

$$\varepsilon_{\phi}(\theta,\phi) = \varepsilon_{\phi}(\theta,\phi+2\pi) \tag{6.16}$$

$$\varepsilon_{\phi}(\theta,\phi) = \varepsilon_{\phi}(\theta+2\pi,\phi) \tag{6.17}$$

$$u_{\phi}(\theta,\phi) = u_{\phi}(\theta,\phi+2\pi) \tag{6.18}$$

$$u_{\phi}(\theta,\phi) = u_{\phi}(\theta+2\pi,\phi) \tag{6.19}$$

The similar periodical condition is also satisfied for N_{θ}, $N_{\theta\phi}$, ε_{θ}, $\varepsilon_{\theta\phi}$, u_{θ}, and u_n respectively.

6.3. Numerical Method

The stress analysis of the cell membrane is conducted numerically by using a finite element method. The numbering of the finite elements and nodes on the membrane surface is shown in Fig.6.4. The finite element frame of the membrane is shown in Fig.6.5. The computer simulation of the ice-cell interaction is performed by using the software code, ABAQUS (Hibbitt, Karlsson, Sorensen Inc.).

In order to determine whether the ABAQUS is applicable and accurate for the analysis, the Thom's experiments [147,148] for the stretch of the cell membrane at -10°C under the distributive forces of the electric field were first simulated in the computer using the ABAQUS. As shown in Fig.6.6, the distributive force of electric field, p_o, acts uniformly on the outside surface of the membrane, and the cell membrane is stretched. Membrane elongations under four different values of p_o were numerically determined by the ABAQUS and compared with Thom's experimental data

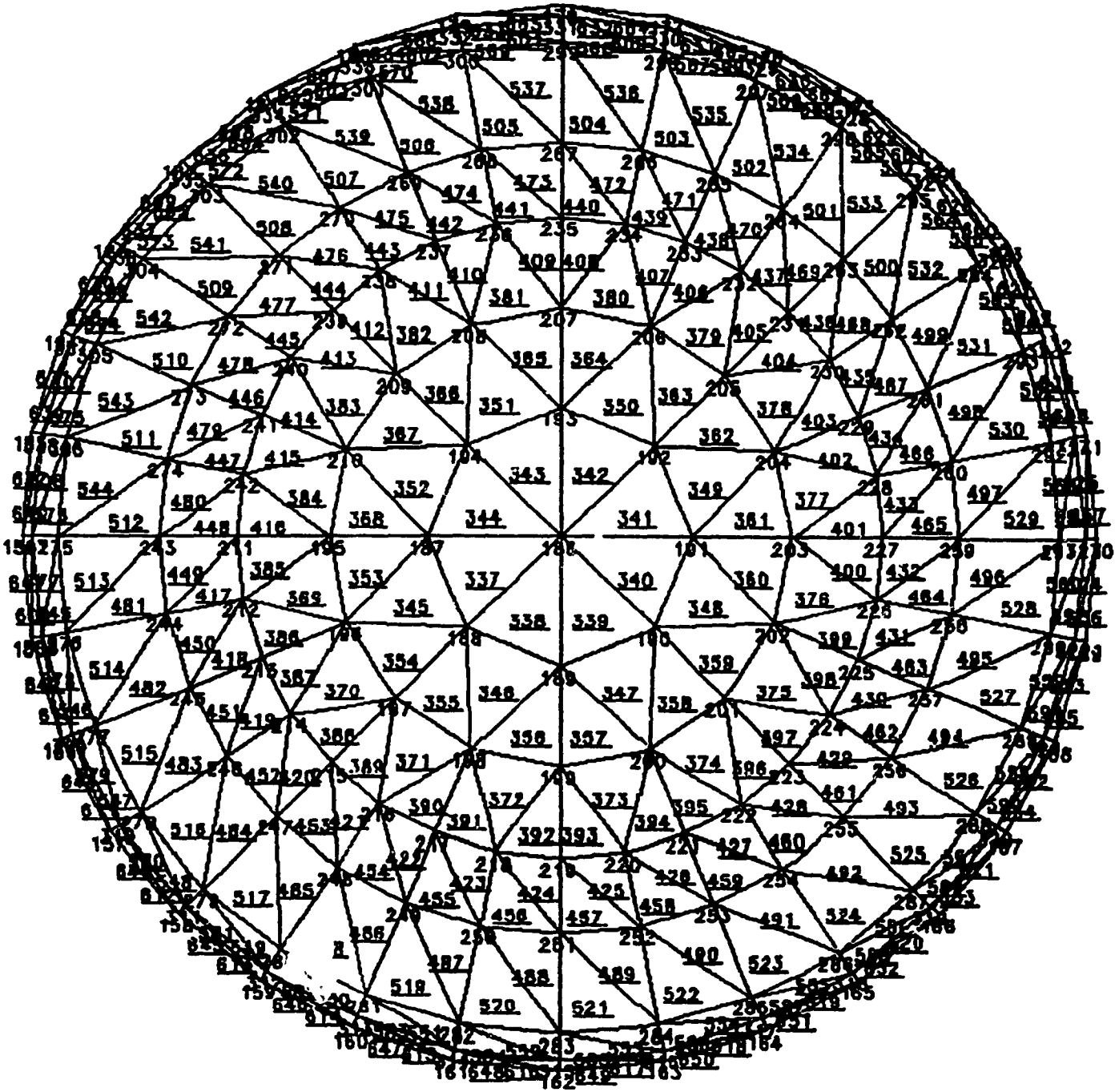

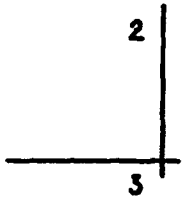

Fig. 6.4. The numbering of finite elements and nodes on the cell membrane.

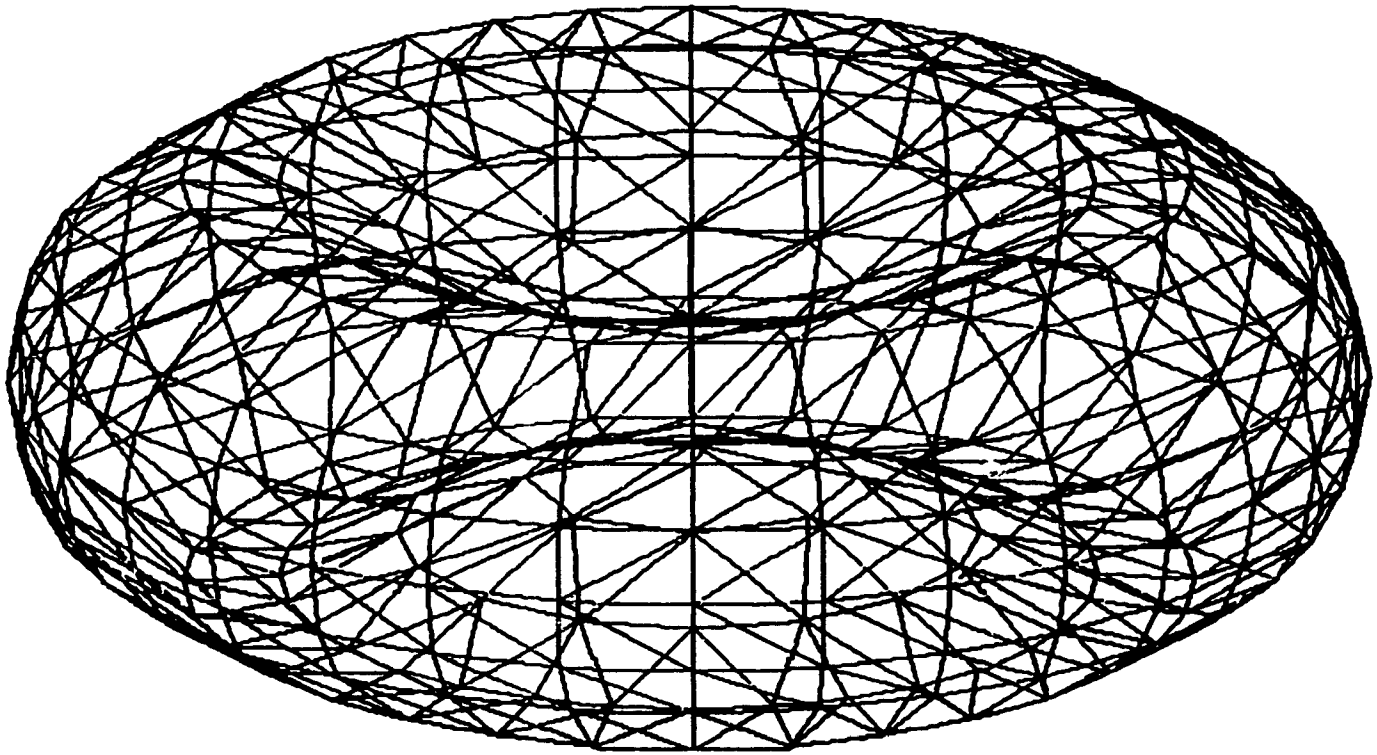

Fig. 6.5. Three dimensional view of the finite element frame of the membrane.

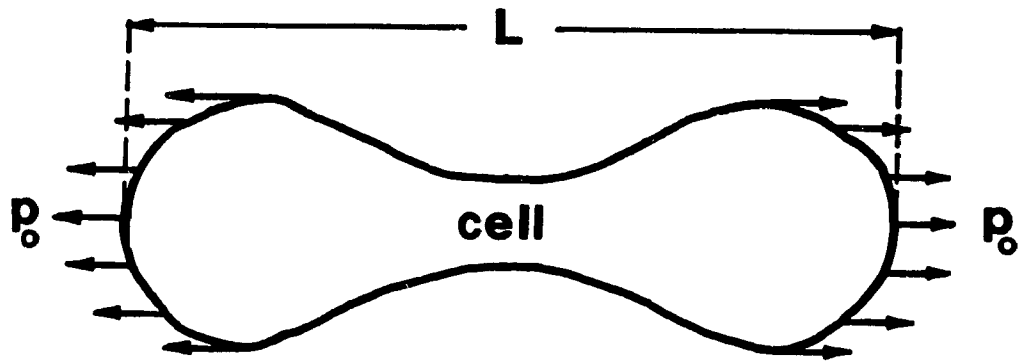

Fig. 6.6. The human erythrocyte stretched by the distributive force, p_o.

[148]. The numerical results agreed with the experimental data. A comparison between these results is shown in the next section.

The stress analysis for the research model of the cell packing process between the two ice walls was conducted under the following procedure:

(1) Input all required data into computer, including the numbering of the elements and nodes on the membrane surface, the mechanical properties of the membrane at -10°C, and the initial volume of the cell, etc. Some of the constants used are listed in Table 6.1 [97,100,102,148].

(2) For a given distributive force p_o on the external surface of the membrane, assume a corresponding force p_i on the internal surface of the membrane.

(3) Calculate the membrane stresses, strains and the volume change of the cell by using the ABAQUS software.

(4) Compare the volume of the deformed cell, V', with the initial cell volume, V. Because of the incompressibility of the cytoplasm, theoretically V must be equal to V'.

(5) If $V > V'$, increase p_i by a small amount of Δp_i.

If $V < V'$, decrease p_i by a small amount of Δp_i.

(6) Repeat step (2) to (5) until $V' = V$.

(7) Seek the maximum strain, ε_{max}, in the membrane. ε_{max} is compared with ε_{cri} which is the criterion of the strain at which the membrane will breakdown. At -10°C, ε_{cri} is equal to 0.05 [147,148].

If $\varepsilon_{max} < \varepsilon_{cri}$, increase p_o by Δp_o.

Table 6.1. Some constants used in the computer simulation of the cell packing process [97,100,102,148].

τ (μm)	ν	E (dyn/cm^2)	L (μm)	V (μm^3)
0.01	0.498	10^{10}	7.82	90

If $\varepsilon_{max} > \varepsilon_{cri}$, decrease p_o by Δp_o.

(8) Repeat step (2) to (7) until $\varepsilon_{max}=\varepsilon_{cri}$.

6.3. Results and Discussion

The elongation of the membrane of the human erythrocyte under the different distributive forces of the electric field, p_o, are shown in Fig.6.7. It is indicated that if p_o was smaller than 4.86×10^6 dyn/cm^2, the numerical results agreed well with the experimental data, but if p_o was equal to or greater than 9×10^6 dyn/cm^2, the error between the numerical and experimental data was large. From Thom's data [148], it is clear that the relative elongation stays almost constant when it reaches 0.05, indicating that 0.05 is the value of the membrane strain at which the membrane loses its elasticity and will break.

The critical strain and stress resultant distributions in the membrane just before the membrane break are shown in Fig.6.8 and Fig.6.9 respectively. $N_{\theta\phi}$ and $\varepsilon_{\theta\phi}$ are both zero because of the axis-symmetric loading forces. They are not shown in the figures. As indicated in Fig.6.8, the maximum strain is located at the center of the concavity of the membrane and has reached the value of ε_{cri} (0.05). Accordingly, as shown in Fig.6.9, the maximum stress resultant is the stretch stress resultant and located at the same place as the maximum strain is. Therefore, it is anticipated that the membrane would rupture first at the center of the concavity of the membrane. The next possible

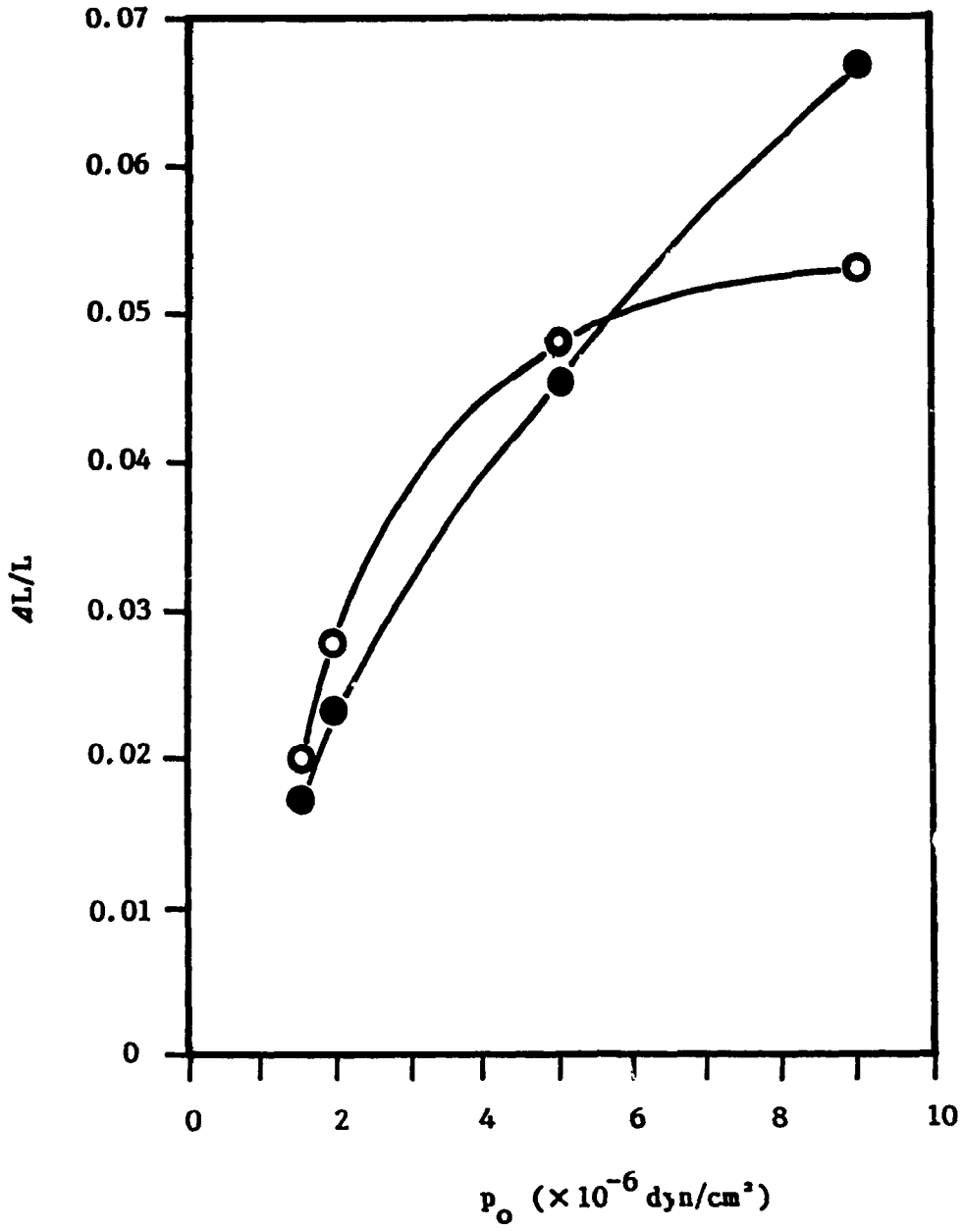

Fig. 6.7. Numerical and experimental data of the elongation of the cell membrane under different values of the stretch-distributive force, p_o.

O : experimetnal data.

● : numerical data.

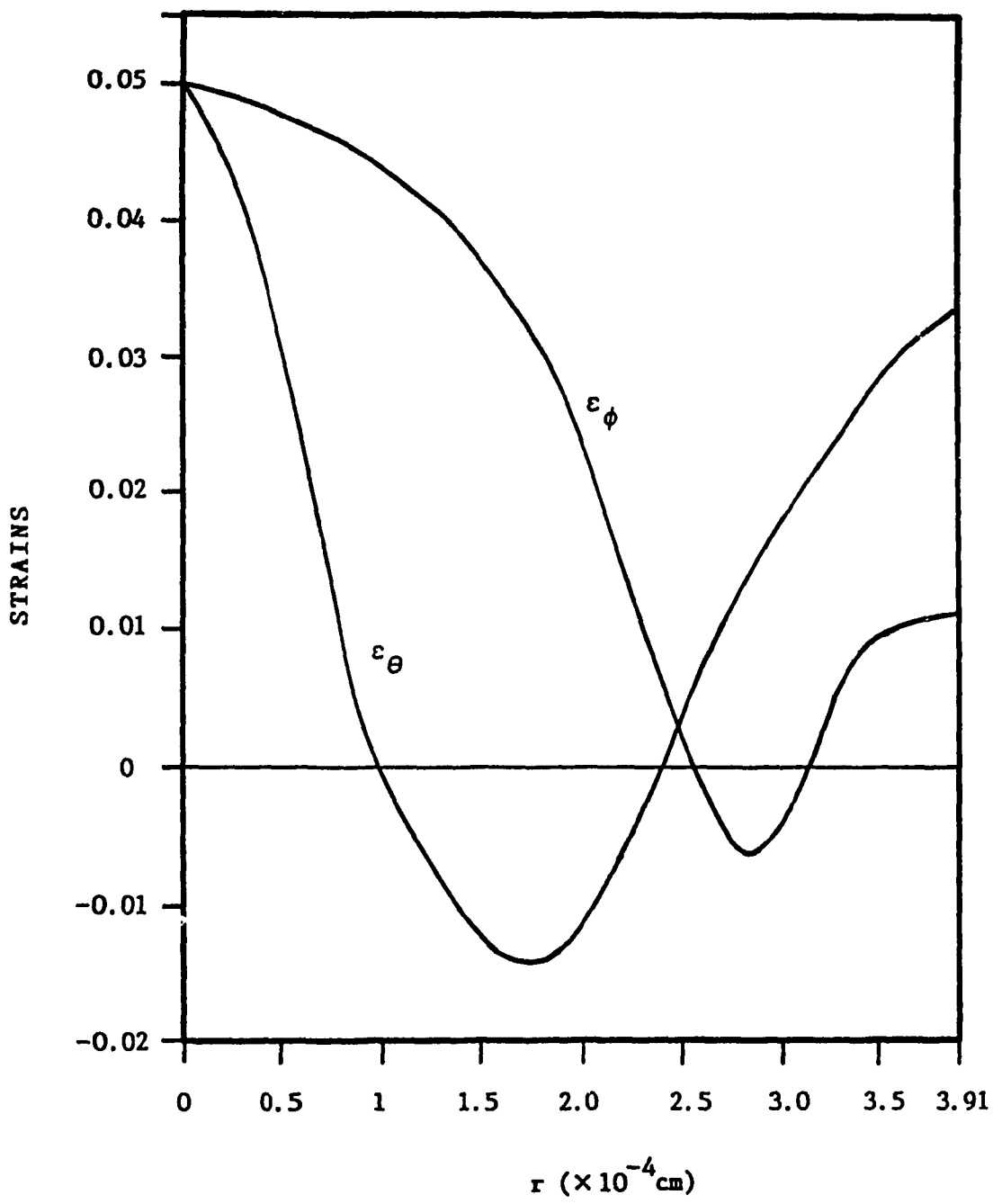

Fig. 6.8. Critical strain distribution in the cell membrane just before the lysis of the membrane.

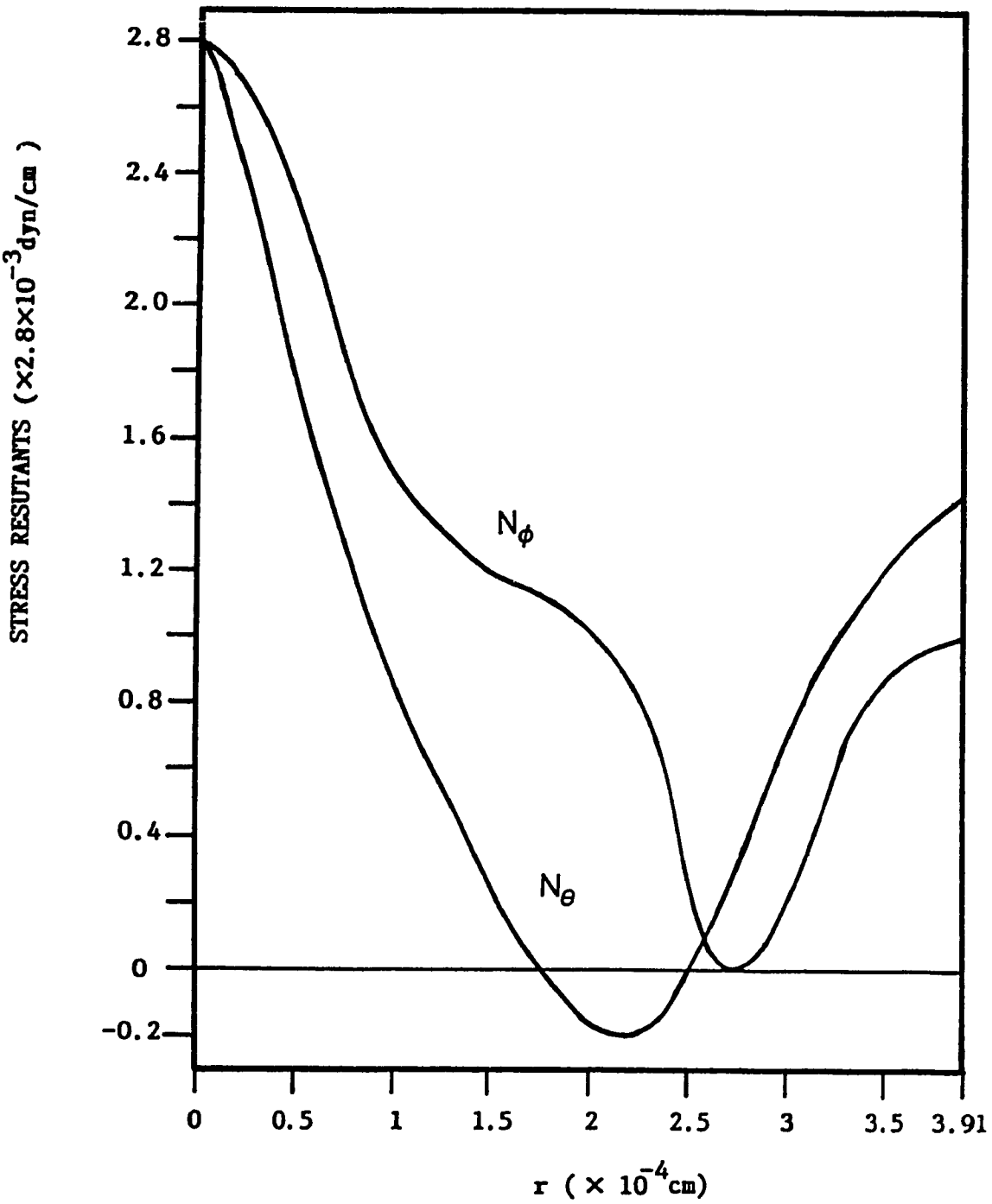

Fig. 6.9. Critical stress-resultant distribution in the cell membrane just before the lysis of the membrane.

place for the membrane to rupture is the outer edge ($r=3.91\mu m$) of the membrane at which the membrane strain is also relative large. The computer simulation has shown that at this critical state, the intracellular pressure, p_i, is equal to $3.6\times10^2 dyn/cm^2$, and the extra-cellular packing force p_o is:

$$p_o = -3.95\times10^8\times(r - 2.737\times10^{-6})\ dyn/cm^2.$$

Fig.6.8 and 6.9 also show that some parts of the membrane are compressed. Even though the compressive stress resultants are much smaller than the stretch stress resultants, the membrane under these compressive stresses may be unstable because the strength of the membrane to support compressive stresses is much lower than that to support the stretch stresses [150,151]. Therefore, buckling of the membrane may occur under the compressive stresses. (The buckling of the membrane is not considered further in this study).

6.4. Conclusion

This model study of the packing process of the cell between advancing ice walls provided some primary answers to the initial hypothesis that the mechanical interaction between the ice and cell may cause the cryo-lysis of the cells:

(1) The ice-cell interaction could generate a high enough strain and stress in the cell membrane to cause rupture of the cell.

(2) Under the conditions of the present research model, the maximum stretch stresses and strains were located at the center of the concavity of the membrane. Therefore, it is anticipated that the membrane would rupture first at this place. It is also predicted that buckling of the membrane may occur during the packing process because of compressive stresses in the membrane.

CHAPTER 7

SUMMARY AND RECOMMENDATIONS

7.1. Summary

This thesis presents a study of the mechanisms of cryoinjury in cells during freezing preservation and its prevention, taking the human erythrocyte as a research model. The main research work and conclusions are summarized as follows:

The separate effect of each of the five influence factors and their coupled interactions on cryoinjury in the human erythrocyte was evaluated quantitatively in Chapter 2. These factors are the cooling rate, the warming rate, the hematocrit, the concentration of glycerol and the holding temperature at which the frozen cell suspensions are kept. From the experimental results and statistical analysis, the following conclusions are drawn:

(1) The cooling rate is the most significant factor affecting cryoinjury of the cells.

(2) The effects of the hematocrit, the glycerol concentration, and the coupled interaction between the cooling rate and warming rate are also significant.

(3) Holding temperatures below $-75^{\circ}C$ are not significant for the cryoinjury of human erythrocytes.

The optimization technique, Fractional Factorial Design, was used for the first time and developed to

determine optimal conditions for the cryopreservation of the cells. This technique has been shown to be very powerful in both designing experiments and analyzing experimental data. The main advantages of the Fractional Factorial Design are:

(1) To reduce the number of experimental tests and thus saving time and effort.

(2) To evaluate statistically the significance of the separate effect of each of experimental factors and their coupled interactions on cryoinjury of the cells.

(3) To determine the optimal combination of the influence factors for the cryosurvival of the cells.

(4) To facilitate the design of experiments and the analysis of experimental data in a straightforward manner by means of special design tables. (The assumptions underlying the use of the Fractional Factorial Design are the same as those underlying the use of the Analysis of Variance.)

Based on the present study, general procedures or methodology to optimize influence factors for the cryopreservation of biological cells and tissues are as follows:

(1) Select factors which may affect the cryosurvival of the cells/tissues;

(2) Select variation-ranges of the factors;

(3) Choose the different levels for each of the factors in their variation-ranges;

(4) Design the experimental tests using the Fractional

Factorial Design technique;

(5) Perform experiments and measure the cryoinjury of the frozen-thawed cells/tissues by bioassays;

(6) Analyse the aliasing of the factors and their coupled interactions.

(7) Evaluate statistically the relative significance of each of the main effects of the factors and their coupled interactions on the cryoinjury;

(8) Determine the optimal combination of the levels of the influence factors for the cryosurvival of the cells;

(9) Modify or refine the levels of the significant factors in the light of the results of the statistical analysis if the optimal combination of the factors is not good enough for the cryosurvival of the cells/tissues. The modification can be repeated until acceptable conditions are determined.

From the present investigation, the optimal conditions for the cryopreservation of the human erythrocytes were:

(a) Slow cooling rate at -0.5°C/min;

(b) Slow warming rate at +0.5°C/min;

(c) Hematocrit of cells of 11%;

(d) Glycerol concentration of 4M (molarity);

(e) Holding temperatures below -75°C.

In Chapter 3, taking pure water as a first approximation of a cell suspension, the freezing process of water inside the cylindrical test tube and the generation

of thermal stress in the ice was investigated. The equipment was specifically designed and manufactured for the experimental tests. The analytical model and mathematical formulation for the freezing process were established and developed. The theoretical results generated by the computer simulation agreed well with the experimental data. In the computer simulation, the effects of the following four factors on the thermal stresses in the frozen cell suspension were investigated:

(1) the cooling rate;

(2) the ratio of the Young's modulus of the tube material to that of the ice, E^*;

(3) the ratio of the linear thermal expansion coefficient of the tube material to that of the ice, α^{**};

(4) the nondimensional thickness of the tube well, τ^*.

From the experimental and theoretical studies, it was found that:

(1) The cooling rate strongly affects the thermal stress distributions in the frozen cell suspension. The quicker the freezing process, the higher the thermal stresses.

(2) The crush of the cell suspension is caused by the circumferential compressive stresses in the ice. Because the maximum circumferential stress exists at the interface between the frozen and unfrozen solutions, the crush starts at the interface and then propagates radially.

(3) The influence factors, E^*, α^{**}, and τ^* also

greatly affect the magnitude of the thermal stress. The larger their values, the greater are the thermal stresses.

(4) In order to reduce "thermal stress effect" on the cryoinjury of cells during the freezing process, a slow cooling rate must be used. This is consistent with the conclusion in Chapter 1. Moreover, a thin-walled tube which is made of a material having low values of Young's modulus and thermal expansion coefficient should be used.

The important function of glycerol in preventing the "thermal stress effect" was experimentally demonstrated in Chapter 4. It was found that glycerol significantly reduced the thermal stresses in the frozen ternary physiological solution (Water-NaCl-Glycerol), and the concentration of glycerol over 0.3M is sufficient to prevent the crush of the frozen solution.

Based on the results of the experimental measurements for freezing point distribution and NaCl-concentration distribution in the frozen ternary solution, a "water melon model" for the freezing process of the solution was invoked rather than the traditional "two-layer" freezing model.

The "water melon model" indicates:

(1) During the freezing process, water precipitates as ice, and the remaining unfrozen solution becomes more and more concentrated;

(2) Under the pertubation of the concentrated solutes, the ice front becomes "finger-like" in shape;

(3) The highly concentrated solution in the grooves among the ice "fingers" is gradually trapped in the ice during the freezing process and eventually solidified at the eutectic point, or vitrified. Therefore, the solutes distribute throughtout the frozen solution like seeds in a water melon.

In Chapter 5, osmotic injury to human erythrocytes during cryopreservation was evaluated using PCMBS, an inhibitor for water transportation through the cell membrane. The experimental results revealed that (1) the osmotic injury to the cells is, indeed, very significant for the cryosurvival of the cells, and (2) the modulation of water transportation through cell membrane can effectively diminish the osmotic injury, or at least improve the cryoprotection afforded by glycerol.

The function of glycerol in preventing and retarding the osmotic lysis of the cells was disclosed from the designed experiments. Based on the theoretical analysis, the possible mechanisms of glycerol in preventing osmotic injury were as follows:

(1) "Hydration Effect": The binding of glycerol with water molecules reduces the number of free water molecules in the solution;

(2) "Dimension Effect": The presence of glycerol in the cell suspension reduces the effective surface area of the cell membrane for water permeation.

(3) "Drag Effect": The high viscosity of glycerol at low temperature retards the motion of the free water molecules in the solution.

(4) Glycerol significantly reduces the amount of water required to penetrate cells in order to equalize the intra- and extra-cellular environments.

Based on the model studies, in order to reduce the osmotic injury to cells, a good CPA candidate should have at least the following important abilities or properties:

(1) penetrate the cell membrane;

(2) have a small molecular weight;

(3) bind water molecules to make more hydrates;

(4) generate high viscosity in the aqueous solution at low temperature.

The mechanical packing process of the human erythrocyte between the two advancing ice walls was analysed using a theoretical model and the finite element technique in Chapter 6. The cell membrane stresses and strains caused by the ice-cell interaction were calculated by computer.

From the computer simulation, it was revealed that:

(1) The ice-cell interaction induces high membrane stresses and strains, which can fracture or burst the membrane;

(2) Under the conditions in the present model, the maximum stretch stress and strain are located at the center

of the concavity of the membrane. Therefore, the membrane ruptures first at the center of the concavity of the membrane during the packing process. It is predicted that buckling of the membrane may occur because compressive stresses exist in the membrane.

7.2. Some Recommendations for the Future Research

Arising out of the present investigation, the following recommendations are offered for further development of some of the problems considered in this thesis.

(1) To Study the Effect of CAPs on Mechanical Properties of Frozen Cell Suspensions and Tissues

The function of glycerol in preventing the generation of the high thermal stress and the crush in the frozen ternary solution (Water-NaCl-Glycerol) has been revealed in Chapter 4. However, the general theoretical analysis of thermal stress in frozen cell suspensions or tissues still cannot be conducted because of the lack of the information of their mechanical properties. A further study on the mechanical properties is recommended as follows:

(a) Designing and manufacturing a specific freeze-loading machine by which the frozen biomaterials (solutions or tissues) can be loaded at different forces and strain-rates. During the loading, the cooling rate, the warming rate, and the temperature of the frozen materials must be controlled.

(b) Using the machine, important mechanical

characteristics of the frozen solutions/tissues will be investigated, including the creeping process, the strain-rate related stress-strain relations, and the evolution of crack in the loaded frozen materials. Experimental parameters include the temperature, the cooling rate, the warming rate, kinds of CPAs in the frozen materials, and the concentration of CPAs.

(c) Based on the experimental data, a new constitutive law of frozen materials can be established.

Using the constitutive law, thermal stress analysis for the freezing biomaterials can be conducted, and the crush in the frozen materials during the cooling process can be predicted numerically. From computer simulation, the optimal conditions, including the cooling rate, the warming rate, the material properties of the container, the kinds of CPAs and the optimal CPA concentration can be determined to minimize the thermal stress and the crush in the frozen biomaterials during cryopreservation.

(2) To Study the Interaction between the Cooling and Warming Processes on the Cryoinjury in Cells.

As indicated in Chapter 1, the interaction between the cooling and the warming rates is a very important factor affecting the cryoinjury of the cells. This fact indicates that, potentially, an optimal survival of the cryopreserved cells can be achieved only if a good match of the cooling and warming processes is reached.

In cryopreservation, the cell suspension is commonly placed in a cylindrical tube. Cooling or warming rate on the tube wall can be controlled. Heat is exchanged mainly through the tube wall during the cooling and warming processes. In cooling, many alterations in the cell suspension, including the ice formation, the concentration of the solution, etc. are the direct result of physical laws. The cell suspension is gradually frozen from the tube wall towards the center of the tube, and the cells in the unfrozen solution experience a hyper-osmotic environment. In warming, the frozen solution melts from the tube wall to the center of the tube, and the thawed cells experience a hypo-osmotic environment. It is apparent that the variation of the extracellular environment which the frozen cells experience during the warming process is totally different from what the cells have experienced during the cooling process. Variations of the extracellular environment include the movement of interface between the frozen and unfrozen solutions, the variation of temperature distribution in the solution-tube system, and the alteration of solute concentration in the solution, etc.

It is hypothesized that the cell cryoinjury caused by the interaction between the cooling and warming processes will be reduced if the difference between the extracellular environment during cooling process and that during warming process is reduced. In other words, for a given cooling process, the corresponding optimal warming process for the

survival of the cells is one which can repeat in reverse the variations of the extracellular environment which have taken place during the cooling process. In order to examine the hypothesis, the following research plan is recommended:

(a) A concentric double-tube apparatus is designed as schematically shown in Fig.7.1. The cell suspension in the apparatus can be cooled or heated by cooling or warming both inner and outer tube walls. Experimental data on the variation of the extracellular environment during the cooling process can be detected and recorded in a personal computer.

(b) A theoretical model and mathematical formulations for the freezing and thawing processes of the cell suspension will be developed for computer simulation. Taking the experimental data of the extracellular environment during the cooling process as a reference, the warming process of the frozen solution will be simulated by controlling the warming rates at both the inner and the outter tube walls until the optimal warming rates is predicted. At the optimal warming rates, the warming process will repeat in reverse the variation of the extracellular environment which the cells have experienced during the cooling process.

(c) Using the designed apparatus, cooling and warming tests of the cell suspension will be performed to examine the optimal warming rates predicted by computer simulation. The theoretical model will be modified until the numerical

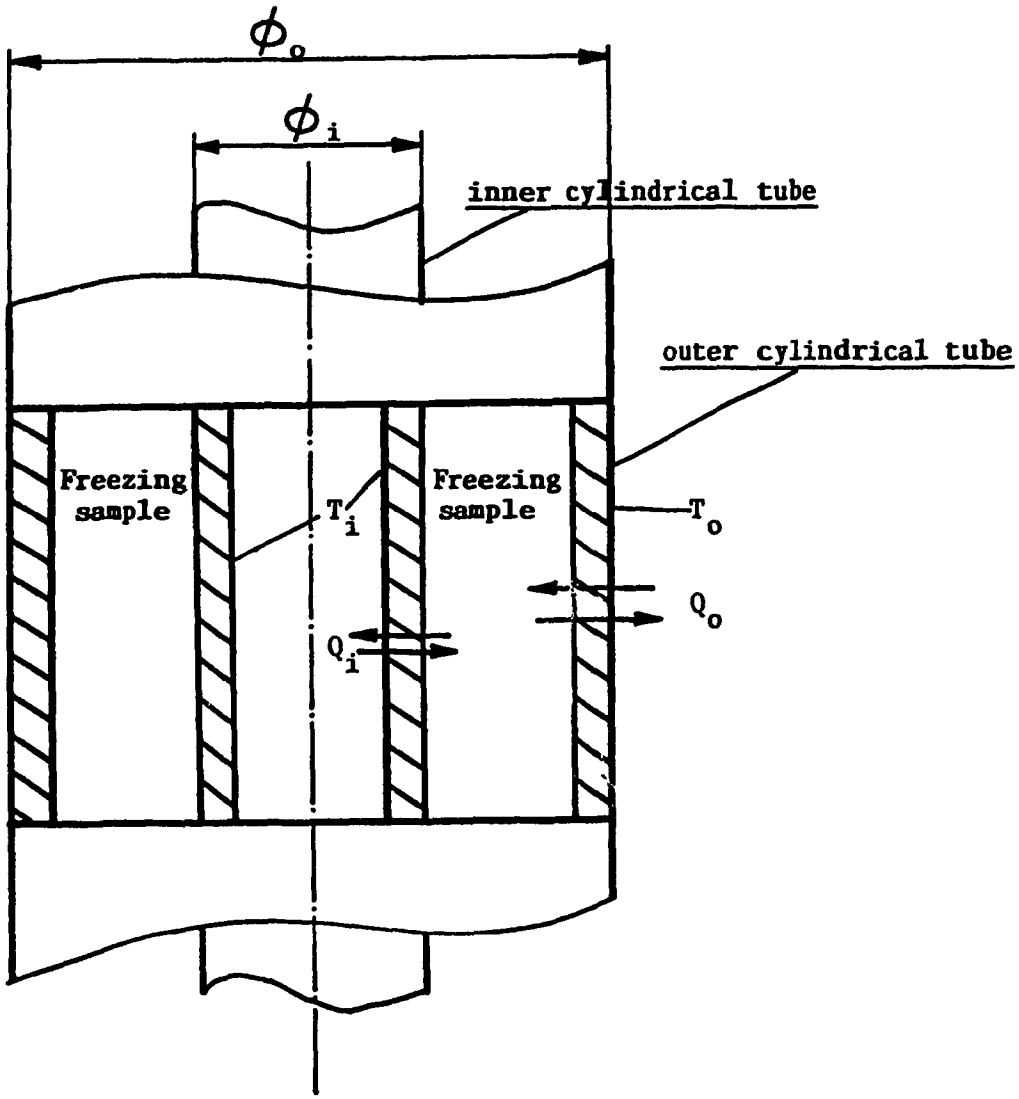

Fig. 7.1. Schematic drawing of a new apparatus used for the freeze-preservation of biological samples. The cooling and warming rates at the inner and outer cylindrical tubes can be controlled. T_i and T_o are temperatures at the surfaces of the inner and outer tube walls. Q_i and Q_o express the heat transfer through the inner and outer tube walls during cooling or warming processes.

result agree well with the experimental results and the real optimal warming rate is reached.

(d) The cell suspensions will be cooled by a fixed cooling process, but different warming processes. The cell cryoinjury will be evaluated by biological assays.

(e) The original hypothesis will be examined by the results from (d). If the cryoinjury in cells warmed by the optimal warming rate is the lowest in comparison with that in cells warmed by any other warming rates, the original hypothesis is proved. If not so, the modification of the hypothesis will be made in the light of (b), (c) and (d).

The results and conclusion to be generated from this study will be significant not only for the cryopreservation of cells but also for the cryopreservation of tissues and organs.

REFERENCES

1. Polge, C., Smith, A.U., and Parks,A.S., "Revival of spermatozoa after vitrification and dehydration at low temperatures". Nature (London) 164, p.666-672, 1949.
2. Doebbler, G.F., "Cryoprotective compounds: review and discussion of structure and function". Cryobiology 3, p.2-11, 1967.
3. McGrath, J.J., "Thermodynamic modeling of membrane damage" in 'Effects of low temperatures on biological membranes', Morris, G.J. and Clarke, A. Eds. p.335-377, Academic Press Inc., New York, 1981.
4. Farrant, J., "Mechanisms of injury and protection in living cells and tissues at low temperatures" in 'Current trends in cryobiology', Smith, A.U., Ed. p.139-152, Plenum Press, New York, 1970.
5. Mazur, P., "Basic problems in cryobiology" in 'Advances in cryogenic engineering' Vol. 9, p.28-37. Timmerhaus, K. D., Ed. Plenum Press, New york, 1964.
6. Meryman, H.T., "Review of biological freezing" in 'Cryobiology', p.2-106, Meryman, H.T., Ed. Academic Press, London, 1966,
7. Kavanau, J.L., 'Water and solute-water interactions', San Francisco: Holden-Day. 1964.
8. Stephenson, J.L., "Fundamental physical problems in the freezing and drying of biological materials" in 'Recent research in freezing and drying', p.121-145, Parkes, A.S.

and Smith, A.U. Eds. Blackwell, Oxford, 1960.

9. Walton, A.G., "Nucleation of crystals from solution". Science 148, p.601, 1965.

10. Fletcher, N.H., 'The chemical physics of ice'. Cambridge Univ. Press, London, 1970.

11. Adamson, A.W., 'A text book of physical chemistry', 2nd Ed. Academic Press, New York, 1979.

12. Franks, F., "Biophysics and biochemistry at low temperatures". Cambridge Univ. Press, Cambridge, 1985.

13. Giese, A.G., 'Cell physiology', 5th Ed. W.B. Sauders Company, Philadelphia, 1979.

14. Douzou, P. 'Cryobiochemistry-An Introduction' Academic Press, London, 1977.

15. Karow, A.M. Jr., "Biophysical and chemical considerations in cryopreservation" in 'Organ preservation for transplantation' 2nd. Ed., p.113-141, Karow, A.M. and Pegg, D.E. Eds., Marcel Dekker Inc., New York, 1981.

16. Dowell, L.G., and Rinfret, A.P., 'Low temperature forms of ice as studied by X-ray diffraction'. Nature 188, p.1144, 1960.

17. Luyet, B.J. "Phase transitions encountered in the rapid freezing of aqueous solutions", Annals of the New York academy of sciences 125, p.502-521, 1965.

18. Luyet, B.J. and Gehenio, P.M., "Effect of the rewarming velocity on the preservation of rapidly frozen blood". Biodynamica 7, p.273, 1955.

19. Grout, B.W.W. and Morris, G.J., "Freezing and cellular

organization" in 'The effects of low temperatures on biological systems'. Grout, B.W.W. and Morris, G.J. Eds. Edward Arnold, London, 1987.

20. Mazur, P., Leibo, S.P. and Chu, E.H.Y., "A two-factor hypothesis of freezing injury: evidence from chinese hamster tissue culture cells". Exp. cell research 71, 345-355, 1972.
21. Mazur, P., "Fundamental cryobiology and preservation of organ by freezing" in 'Organ preservation for transplatation'. 2nd, ED., Karow, A.M. and Pegg, D.E. Eds., Marcel Dekker Inc. New York, 1981.
22. Lovelock, J.E., "The denaturation of lipid-protein complexes as a cause of damage by freezing". Proc. Roy. Soc. Lond. Ser. B. 147, p.427-434, 1957.
23. Smith, A.U., "Effects of low temperature on living cells and tissue" in 'Biological applications of freezing and drying", Harris, R.J.C., Ed., Academic Press, New York, 1954.
24. Meryman, H.T., "The exceeding of a minimum tolerable cell volume in hypertonic suspension as a cause of freezing injury" in 'The frozen cell' Wolstenholme, G.E. W. and O'Connor, M., Eds., Cida Foundation Symposium, J & A Churchill, London, 1970.
25. Williams, R.J., "The mechanisms of cryoprotection in the intestinal mollusk mytilus". Cryobiology 4, p.250, 1979.
26. Levitt, J., "A sulfhydryl disulphide hypotheses of frost injury and resistance in plants". J. Theoret. Biol. 3,

p.355, 1962.

27. Kendrew, J.C., "Myollobin and the structure of proteins" , Science 139, p.1259.
28. Karow, A.M. adn Webb, W.R., "Tissue freezing: a theory for injury and survival." Cryobiology 2, p. 99-108, 1965.
29. Rall, W.F., Mazur, P. and Hiroshi, S., "physical-chemical basis of the protection of slowly frozen human erythrocytes by glycerol." Bilphys. J. 23, p.101-123, 1978.
30. Fishbein W.M. and Winkert, J.W., "Parameters of biological freezing damage in simple solutions: catalase 11 demonstration of an optimum recovery cooling rate curve in a membraneless system". Cryobiology 15, p.168, 1978.
31. Wiest, S.C. and Steponkus, P.L., "The osmometric behavior of human erythrocytes. Cryobiology 16, p.101, 1979.
32. Micronescu, S. and Seed, T.M., "Hyperosmotic injury in mammalian cells 2. surface alterations of CHO cells in unprotected & DMSO-treated cultures." Cryobiology 14, p.575, 1977.
33. Griffiths, J.B., "Effect of hypertonic stress on mammalian cell lines and its relevance to freeze-thaw injury" , Cryobiology 15, p.517, 1978.
34. Kruuv, J., Lepick, J.R., and Keith, A.D., "The effect of fluidity of membrane lipids on freeze-thaw survival of yeast." Cryobiology 15, p.73, 1978.
35. Mironescu, S., "Hyperosmotic injury in mamalian cells 3 , volume and alkali cation alteration in CHO cells in

unprotected and DMSO-treated cultures." Cryobiology 15, p.178, 1978.

36. Fahy, G.M., "Analysis of solution effects injury, equations for calculating phase diagram information for the ternary systems NaCl-Dimethysulfoxide-Water and NaCl-glycerol-water", Biophys. J. 32, p.837-850, 1980.
37. Leibo, S.P. and Mazur, P., "Survival of frozen-thawed mouse embryos as a function glycerol permeation. " Cryobiology 11, p.559, 1974.
38. Mazur, P., "Causes of injury in frozen and thawed cells" Fed. Proc. 24, Supp. No. 15, p.175, 1965.
39. Bank, H. and Mazur, P., "Visualization of freezing damage." J. Cell. Biol. 57, p.729, 1973.
40. Smith, A.U., Polge, C. and Smiles, J., "Microscopic observations of living cells during freezing and thawing." J.R. Micro. Soc. 71, p.186, 1951.
41. Rapatz, G. and Luyet, B.J., "Effects of cooling rates on the preservation of erythrocytes in frozen blood containing various protective agents." Biodynamica 9, p.333, 1965.
42. Mazur, P., "The role of intracellular freezing in the death of cells cooled at supraoptimal rates". Cryobiology 14, p.251-272, 1977.
43. Fujikawa, S., "Freeze-fracture and etching studies on membrane damage on human erythrocytes caused by formation of intracellular ice". Cryobiology 17, p.351-362, 1980.

44. Mazur, P., "The freezing of biological systems". Science 168, p.939, 1976.

45. Leibo, S.P., McGrath, J.J. and Cravalho, E.G., "Microscopic observation of intracellular ice formation in unfertilized mouse ova as a function of cooling rate". Cryobiology 15, p.257-265, 1978.

46. Farrant, J., Walter, C.A., Lee, H. and McGann, L.E., "Use of two-step cooling procedures to examine factors influencing cell survival following freezing and thawing." Cryobiology 14, p.273, 1977.

47. Mazur, P. and Schmidt, J., "Interactions of cooling velocity, temperature, and warming velocity on the survival of frozen and thawed yeast." Cryobiology 5, p.1, 1968.

48. Nei, T., " Mechanism of hemolysis of erythrocytes by freezing with special reference to freezing at near-zero temperatures" in 'The frozen cells'. Wolstenholme, G.E.W. and O'connor, M., Eds. J. and A. Churchill, London, 1970.

49. Nei, T., "Freezing injury to erythrocytes, I: Freezing patterns and post-thaw hemolysis". Cryobiology 13, p.278 -286, 1976.

50. Nei, T., "Freezing injury to erythrocytes, II: Morphological alterations of cell membranes". Cryobiology 13, p.287-294. 1976.

51. Mazur, P. Rall, W.F. and Rigopoulos, N., "Relative contributions of the fraction of unfrozen water and of

salt concentration to the survival of slowly frozen human erythrocytes". Biophysical J. 36, p.653-675, 1987.

52. Pegg, D.E. and Diaper, M.P., "The effect of cooling rate and warming rate on the packing effect in human erythrocytes frozen and thawed in the presence of 2M glycerol". Cryobiology 21, p.491-502, 1984.

53. Pegg, D.E., "The effect of cell concentration on the recovery of human erythrocytes after freezing and thawing in the presence of glycerol". Cryobiology 18, p.221-228, 1981.

54. Rubinsky, B., cravalho, E.G. and Nikic, B., "Thermal stresses in frozen organs." Cryobiology 17, p.66.

55. Gupta, K.C., "The mechanism of cryohemolysis: by direct observation with the cryomicroscope and the electron microscope". Cryobiology 12, p.417-426, 1975.

56. Bank, H., "Visualization of freezing damage, II: structural alterations during warming". Cryobiology 10, p.157-170, 1973.

57. Fujikawa, S. and Miura, K., "Plasma membrane ultrastructural changes caused by mechanical stress in the formation of extracellular ice as a primary cause of slow freezing injury in fruit-bodies of basidiomycetes". Cryobiology 23, p.371-382, 1986.

58. Hornblower, M. and Meryman, H.T., "Influence of the container material on the hemolysis of glycerolized red cells after freezing and thawing". Cryobiology 11, P.317-323, 1974.

59 Morris, G.J. and McGrath, J.J., "Intercellular ice nucleation and gas bubble formation in spirogyra". Cryoletters 2, p341-352, 1987.

60. Penninckx, F., "Erythrocyte swelling after rapid dilution of cryoprotectants and its prevention". Cryobiology 21, p.25-32, 1984.

61. Fahy, G.M., "The relevance of cryoprotectant toxicity to cryobiology". Cryobiology 24, p.1-13, 1986.

62. Fahy, G.M. and Hirsch, A., "Prospects for organ preservation by vitrification" in 'Organ preservation: Basic and applied aspects". p.399-404, Pegg, D.E., Jacobson, J.A. and Halasz, N.A. Eds., MTP press limited, Lancaster, 1982.

63. Onuchic, L.F. and Vieira, L., "Glycerol-induced baroprotection in erythrocyte membranes". Cryobiology 22, p.438 -445, 1985.

64. Zimmermann, U., Bechers, F. and Coster, H.G.L., "The effect of pressure on the electrical breakdown in the membranes of Valonia utricularis". Biochim. Biophys. Acta 464, p.399-416, 1977.

65. Hall, A.C., Ellory, J.C. and Klein, R.A., "Pressure and temperature effect on human red cell cation transport". J. Membr. Biol. 68, p.47-56, 1982.

66. Luyet, B.J. and Gehenio, P.M., 'Life and death at low temperatures.' Normandy, Missouri: Biodynamica, 1940.

67. Meryman, H.T., "Cryoprotective agents". Cryobiology 8, p.173-183, 1971.

68. Shlafer, M., "Pharmacological considerations in cryopreservation" in 'Organ preservation for transplantation'. Karow, A.M. and Pegg, D.E. Eds. Marcel Dekker Inc. New York, 1981.

69. Lovelock, J.E., "The mechanism of the protective action of glycerol against hemolysis by freezing and thawing." Biochim. Biophys. Acta 11, p.28, 1953.

70. Lovelock, J.E. and Bishop, M.W.H., "Prevention of freezing damage to living cells by dimethylsulfoxid." Nature (Lond.) 183, p.1394, 1959.

71. Meryman, H.T., "Modified model for the mechanism of freezing injury in erythrocytes." Nature (Lond.) 218, p.333, 1968.

72. Rasmussen, D.M. and Mackenzie, A.P., "Phase diagram for the system water-dimethylsulfoxide. Nature 220, p.1315.

73. Luyet, B.J. and Keane, J.K., "On the role of osmotic dehydration in the protective action of glycerol against freezing injury." Biodynamica 7, p.141.

74. Mazur, P., Miller, R.H., and Leibo, S.P., "Survival of frozen thawed bovine red cells as function of the penetreation of glycerol and sucrose." J. Membrane Biol. 15, p.137, 1974.

75. Mazur, P., Miller, R.H., "Survival of frozen-thawed human red cells as a function of the permeation of glycerol and sucrose." Cryobiology 13, p.523, 1976.

76. Taylor, R., Adams, G.D.J., Boardman, C.F.B. and Wallis, R.G., "Cryoprotection: permeant vs non-permeant addi-

tives." Cryobiology 11, p.430, 1974.

77. Leibo, S.P., Mazur, P. and Jackowski, S.C., "Factors affecting survival of mouse embryos during freezing and thawing." Exp. Cell Res. 89, p.79, 1974.

78. McGann, L.E., "Differing actions of penetrating and non-penetrating cryoprotective agents." Cryobiology 15, p.382, 1978.

79. Keane, J.F., "Comparative efficiency of some compounds containing the amido group in protecting tissues against freezing injury." Biodynamica 7, p.157, 1953.

80. Karow, A.M., "Cryoprotectants: A new class of drugs." J. Pharm. Pharmac. 21, p.209, 1969.

81. Farrant, J., "Mechanisms of injury and protection in living cells and tissues at low temperatures" in 'Current trends in cryobiology'. Smith, A.U. Ed., Plenum Press, New York, 1970.

82. Ashwood-Smith, M.J., "Low temperature preservation of cells, tissues and organs" in 'Low temperature preservation in medicine and biology", Ashwood-Smith, M.J. and Farrant, J. Eds., University Park Press, Baltimore, p.19 -25, 1980.

83. Korber, C. and Scheiwe, M.W., "The cryoprotective properties of hydroxyethyl starch investigated by means of differential thermal analysis." Cryobiology 17, p.54, 1980.

84. Mackenzie, A.P., "Non-equilibrium freezing behavior of aqueous systems". Phil. Trans.Roy. Soc. London ser. B278 p.167-188, 1977.

85. Doebbler, G.F. and Rinfret, A.P., "The influence of protective compounds and cooling and warming conditions on hemolysis of erythrocytes by freezing and thawing." Biochim. Biophys. Acta. 58, p.449, 1962.

86. Doebbler, G.F., "Cryoprotective compounds." Review and discussion of structure and function. Cryobiology 3, p.2 -10, 1966.

87. Doebbler, G.F., and Rinfret, A.P., "Rapid freezing of human blood: Physical and chemical considerations of injury and protection." Cryobiology 2, p.205, 1965.

88. Miller, J.S., Cornwell, D.G., "The role of cryoprotective agents as hydroxy radical scavengers." Cryobiology 15, p.585, 1978.

89. Williams, R.j. and Harris, D., "The distribution of cryoprotive agents into lipid interfaces." Cryobiology 14, p.670, 1977.

90. Barnett, R.E., "The effects of dimethysulfoxide and glycerol on Na^+, K^+ -ATPase and membrane structure." Cryobiology 15, p.227, 1978.

91. Farrant, J. and Woolgar, A.E., "Red cells under hypertonic conditions: a model for investigating freezing damage. 1. Sodium chloride." Cryobiology 9, p.9, 1972.

92. Farrant, J. and Woolgar, A.E., "Red cells under hypertonic conditions: a model for investigating freezing damage. 3. DMSO." Cryobiology 9, p.131, 1972.

93. Lawrie, J.W. 'Glycerol and glycols: production, properties and analysis'. The chemical catalog company, New

York, 1928.

94. Lehninger, A.L., 'Principles of biochemistry'. Worth Publishers Inc. New York, 1982.

95. Chen, R.T. Hua, Z., "A comparative study of the cryo-preservation techniques of human semen." Chinese J. of Biomedical Engineering 7, p.20-26, 1988.

96. Darnell, J. Lodish, H. and Baltimore, D., 'Molecular cell biology', Scientific American Books Inc. New York, 1986.

97. Evans, E. and Fung, Y-C., "Improved measurements of the erythrocyte geometry". Microvasc. Res. 4, p335-347, 1972.

98. Elgsaeter, A., "The molecular basis of erythrocyte shape". Science 234, p1217-1223, 1986.

99. Branton, D., "Interaction of cytoskeletal proteins on the human erythrocyte membrane". Cell 24,p.24-32, 1981.

100. Rand, R.P., "Mechanical properties of the red cell membrane: II. Viscoelastic breakdown of the membrane". Biophysics J. 4, p.303-316, 1964.

101. Hochmuth, R.M., "Measurement of the elastic modulus for a red cell membrane using a fluid mechanical technique" . Biophysics J. 13, p.747-762, 1973.

102. Hochmuth, R.M., "red cell relaxation and the determination of membrane viscosity". Biophysics J. 26, p.111-114, 1979.

103. Sutera, S.P., "Brief reviews: flow-induced trauma to blood cells". Circ. Res. 41(1), p.2-8, 1977.

104. Hochmuth, R.M., "Brief communication: temperature dependence of the viscoelastic recovery of red cell membrane". Biophysics J. 29, p.177-182, 1980.

105. Box, G.E.P., Hunter, W.G. and Hunter, J.S., 'Statistics for experimenters.' Wiley, New York, 1978.

106. Daniel, C., 'Applications of statistics to industrial experimentation.' Wiley, New York, 1976.

107. Zen, Q.C., 'Statistical methods of technology." 2nd Ed. Anhui Press of Science and Technology, Anhui, China, 1983.

108. Dacie, J.V. and Lewis, S.M., 'Practical hematology' 5th Ed. Churchill Livingstone, New York, 1984.

109. Zar, J.H., 'Biostatistical analysis." Prentice-Hall, Englewood Cliffs, N.J., 1984.

110. Foreman, J. and Pegg, D.E., "Cell preservation in a programmed cooling machine: the effect of variations in supercooling." Cryobiology 16, p.315-321, 1979.

111. Luyet, B. and Rapatz, G., "Mode of distribution of the ice and of the non-frozen phase in frozen aqueous solutions." Biodynamica 10, p.293-317, 1969.

112. Mathias, S.F., Franks, F. and Frafford, K., "Nucleation and growth of ice in deeply undercooled erythrocytes." Cryobiology 20, p.123-132, 1984.

113. Fahy, G.M., Mac Farane, D.R., Angell, C.A. and Merymen, H.T., "Vitrification as an approach to cryopreservation." Cryobiology 21, p.407-426, 1984.

114. Frank, F., Mathias, S.F. Galfre, P. and webster, S.D.,

"Ice nucleation and freezing in undercooled cells." Cryobiology 20, p.298-309, 1983.

115. Mazur, P. and Cole, K.W., "Influence of cell concentration on the contribution of unfrozen fraction and salt concentration to the survival of slowly frozen human erythrocytes." Cryobiology 22, p.509-536, 1985.

116. Pegg, D.E., Diaper, M.P., "The packing effect in erythrocyte freezing." Cryo-Letters 4, p.129-136, 1983.

117. Miller R.H. and Mazur, P., "Survival of frozen-thawed human red cells as a function of cooling and warming velocities." Cryobiology 13, p.404-414, 1976.

118. Boley, B.A. and Weiner, J.H., 'Theory of Thermal Stress', J. Wiley, 1962.

119. Riley, D.S., Smith, F.T., and Poots, D., "The inward solidification of sphere and circular cylinders." Int. J. Heat Transfer, Vol.17, p. 1507-1516, 1974.

120. Dantl,G., "Elastic moduli of ice" in 'Physics of ice', Plenum Press, 1969.

121. Michel, B., 'Ice Mechanics', LES PRESSES DE L'UNIVERSITE LAVAL, Montreal, 1978.

122. Duval, P. and Maitre, M., Manouvrier, A., Marec, G. and Jay, J.C., "Primary creep and experimental method for testing ice in various conditions of strain rates and stress", Proceedings of international symposium on ice, Vol. 11, p.112-123, 1981.

123. Higashi, A., "Mechanical properties of ice single crystal" in 'Physics of ice', Plenum Press, 1969.

124. Nakamura, T. and Jones, S.J., "Mechanical properties of impure ice crystal" in 'Physics and Chemistry of Ice', The Royal Society of Canada, University of Toronto Press, 1973.

125. Kuon, L.G. and Jonas, J.J., "Effect of strain rate and temperature on the microstructure of polycrystalline ice" in 'Physics and Chemistry of ice'. The Royal Society of Canada, University of Toronto Press, 1973.

126. Michel, B., "The strength of polycrystalline ice," Can. J. of Civil Eng. Vol.5, No.3, p.285-300, 1980.

127. Hornbeck, R. H., 'Numerical method', McGraw Hill, 1982.

128. Murray, W.D. and Landis, F., J. Heat Transfer, (Trans. ASME) 81, p.106-112, 1959.

129. Mazur, P., "Slow-freezing injury in mammalian cells" in 'The Freezing of Mammalian Embryos', Elliot, k. and Whelan, J. Eds., Elsevier, Amsterdam, 1977.

130. Gao, D.Y., Lin, S., Kornblatt, J.A., and Guttman, F.M. "A study of separate effects of influence factors and their coupled interactions on cryoinjury of human erythrocytes." Cryobiology 26, p.355-368, 1989.

131. Luyet, B. and Rasmussen, D., "Study by differential thermal analysis of the temperatures of instability of rapidly cooled solutions of glycerol, ethylene glycol, sucrose, and glucose", Biodynamica 10(211), p.167-191, 1968.

132. Jochem, M. and Korber, CH., "Extended phase diagrams for the ternary solutions H_2O-NaCl-Glycerol and H_2O-

NaCl-Hes determined by DSC." Cryobiology 24, p.513-536 , 1987.

133. Rubinsky, B., "Solidification processes in saline solutions", J. Crystal Growth 62, p.513-522, 1983.

134. Flemings, M.C., 'Solidificaiton process', McGraw-Hill Bood Company, New York, 1974.

135. Sharp, R.M. and Hellawell, A., "Solute distributions at non-planar, solid-liquid growth fronts, I. steady-state conditions", J. Crystal Growth 6, p.253-260, 1970.

136. Sharp, R.M. and Hellawell, A., "Solute distributions at non-planar, solid-liquid growth fronts, II. steady-state and transient conditions: no liquid stirring", J. Crystal Growth 6, p.334-340, 1970.

137. Jones, S.J. and Glen, J.W., "Impurity effects on the plasticity of ice and their explanation in terms of hydrogen reorientation" in 'Physics of ice', Plenum Press, New York, 1969.

138. Sha'afi, R.I., "Water and small nonelectrolyte permeation in red cells" in 'Membrane transport in red cells" , Ellory, J.C. and Lew, V.L. Eds., Academic Press, London, 1977.

139. Trauble, H., "Phase transitions in lipis" in 'Biomembranes' Vol. 3, Kreuzer, F. and Slegers, J.F.G., Eds., Plenum Press, New York, 1972.

140. Sha'afi, R.I. and Feinstein, M.B., "Membrane water channels and SH-groups", Advances in Experimental

Medicine and Biology 84, p.67-80, 1976.

141. Macey, R.I. and Farmer, R.E.L., "Inhibitions of water and solute permeability in human red cells", Biochimicaet Biophysica Acta 211, p.104-106, 1970.

142. Naccache, P. and Sha'afi, R.I., "Effect of PCMBS on water transfer across biological membranes", J. Cellular Physiology 83, p.449-456, 1974.

143. Benga, Gh. Pop, V.I. Ionescu, M., Holmes, R.P. and Popescu, O., "Irreversible inhibition of water transport in erythrocytes by fluoresceimercuric acetate", Cell Biology Int. Rep. Vol. 6, No. 8, p.775-781, 1982.

144. Miner, C.S., 'Glycerol', Reinhold Publishing Corporation, New York, 1953.

145. Moore, W.J., 'Physical chemistry', 4th Ed, Prentice-Hall, Inc. Englewood Cliffs, N.J. 1974.

146. Thomas, K.S., 'Mass transfer', McGraw Hill, New York, 1975.

147. Thom, F. and Matthes, G., "Deformation of the cell membrane at low temperatures, I. a crycmicroscopical technique", Cryo-letters 9, p.300-307, 1988.

148. Thom, F. and Matthes, G., "Deformation of the cell membrane at low temperatures, II. elastical deformability of the erythrocyte membrane", Cryo-letters 9, p.308-315, 1988.

149. Kraus, H., "Thin elastic shell', John Wiley and Sons, Inc., New York, 1967.

150. Flugge, W., 'Stress in shells', Springer Verlay,

Berlin, 1962.

151. Fung, Y.C., "Theoretical consideration of the elasticity of red cells and small blood vessels", Fed. Proc. 25, p.1761-1772, 1966.

152. Tsutsayeva, A.R., Pushkar, N.S., Markova, V.M., Itkin, Y.A., Markovsky, A.L., Gavrilova, I.I., Ivanov, L.V., Moiseyev, V.A. and Medvedyeva, G.G., "The mechanism of action of low temperature and cryoprotective agents on immunoproteins". Cryobiology 15, p.403-411, 1978.

APPENDIX 1

Computer Programs for the Simulation of Freezing Process of Water in the Cylindrical Test Tube and the Thermal Stress Analysis

LEGEND

SR1	Radial component of stress in the tube
SR2	Radial component of stress in the ice
SZ1	Axial component of stress in the tube
SZ2	Axial component of stress in the ice
ST1	Circumferential component of stress in the tube
ST2	Circumferential component of stress in the ice
ER1	Radial component of stain in the tube
ER2	Radial component of stain in the ice
EZ1	Axial component of stain in the tube
EZ2	Axial component of stain in the ice
ET1	Circumferential component of stain in the tube
ET2	Circumferential component of stain in the ice
D1	Radial component of displacement in the tube
D2	Radial component of displacement in the ice
R	Radial coordinates
R1	Outer radius of the tube
R2	inner radius of the tube
T1	Temperature in the tube
T2	Temperature in the ice
TB	Boundary temperature

V1	Poisson's ratio of the tube material
V2	Poisson's ratio of the ice
E1	Young's modulus of the tube material
E2	Young's modulus of the ice
TF	Freezing point of water
ALAW	Latent heat of water freezing
DENW	Density of water
AK1	Thermal conductivity of the tube material
AK2	Thermal conductivity of the ice
AF1	Linear thermal expansion coefficient of the tube
AF2	Linear thermal expansion coefficient of the ice

MAIN PROGRAM

```
/FILE 2 NAME(GA06.PRN) NEW(REPLACE) RLSE SPACE(1000)
/LOAD FORTG
/SYS REG=500
      DIMENSION  SR1(11),SR2(11),SZ1(11),SZ2(11),ST1(11),ST2(11),
     .ER1(11),ER2(11),ET1(11),ET2(11),D1(11),D2(11),T2(11),R(11),
     .STT1(11),STT2(11),DSTT2(11),SR2O(11),DSR2(11),
     .DET2(11),ET2O(11)
C     FF=0.999
      TB=-9.
      TF=0.
      R1=10.2/2.*0.01
      R2=9.54/2.*0.01
      ALAW=333.84E3
      DENW=999.8
      AK2=2.
      N=11
      AK1=52.0
      E1=15.E6*6894.76
      V1=0.36
      V2=0.31
      AF2=55.E-6
      AF1=16.E-6
      P=101325.
      TIME1=0.0
      FFF=0.0
```

```
      DO  1     J=1,9
      FFF=1.0-FLOAT(J)/10.0
      E2=9.94E9
      X=R2*FFF
      AM1=1./R2**2+(1.-2.*V1)/R1**2
      AM3=E1*(1./R1**2-1./R2/R2)/(1.+V1)
      AM4=E2*(1./R2**2-1./X/X)/(1.+V2)
      AM2=1./R2/R2+(1.-2.*V2)/X/X
      F1=-E1*AF1*TB*(R1*R1-R2*R2)/2./(1.-V1)/R1/R1
      A=(TB-TF)/ALOG(R2/X)
      B1=(TF*ALOG(R2)-TB*ALOG(X))/ALOG(R2/X)
      B=B1+0.03/AF2
      F2=-E2*AF2/(1.-V2)/R2/R2*(A*(R2*R2/2.*ALOG(R2)-R2*R2/4.)
     .+B/2.*R2*R2
     .-A*(X*X*ALOG(X)/2.-X*X/4.)-B/2.*X*X)
      F3=(1.+V2)/(1.-V2)*AF2/R2*(A*(R2*R2/2.*ALOG(R2)-R2*R2/4.)+
     .B/2.*R2*R2-A*(X*X/2.*ALOG(X)-X*X/4.)-B/2.*X*X)
      H=F3/R2+F1*(1.+V1)*(1.-2.*V1)/E1+P*(1.+V2)*(1.-2.*V2)/E2
      AI=F1+F2+P
      C4=(AI*AM1-H*AM3)/(AM4*AM1+AM2*AM3)
      C2=(H+AM2*C4)/AM1
      C3=(E2*C4/(1.+V2)/X/X+P)*(1.+V2)*(1.-2.*V2)/E2
      C1=(E1*C2/(1.+V1)/R1/R1-F1)*(1.+V1)*(1.-2.*V1)/E1
      AA=1.+V1
      BB=1.-V1
      CC=1.+V2
      DD=1.-V2
      EE=1.-2.*V1
      FF=1.-2.*V2
      TIME2=(X*X/2.*(ALOG(R2/X)+0.5)-R2*R2/4.)*DENW*ALAW/AK2/(TB-TF)
      WRITE(2,10) TIME2,X
      DT=TIME2-TIME1
      TIME1=TIME2
      DO  100  I=1,N
      R(I)=FLOAT(I-1)*(R1-R2)/FLOAT(N-1)+R2
      D1(I)=AA/BB*AF1*TB/R(I)/2.*(R(I)*R(I)-R2*R2)+C1*R(I)+C2/R(I)
      SR1(I)=E1/AA*(-AA/BB*AF1*TB/R(I)/R(I)/2.*(R(I)*R(I)-R2*R2)
     .+C1/EE-C2/R(I)/R(I))
      ER1(I)=AF1*AA*TB/2./BB*(R2*R2/R(I)/R(I)+1.)+C1-C2/R(I)/R(I)
      ET1(I)=D1(I)/R(I)
      ST1(I)=E1/AA*(BB/EE*ET1(I)+V1/EE*ER1(I))-AF1*E1/EE*TB
      SZ1(I)=E1*V1/AA/EE*(ER1(I)+ET1(I))-AF1*E1/EE*TB
100   CONTINUE
C     WRITE(2,12) (R(I),D1(I),ER1(I),ET1(I),I=1,11)
C     WRITE(2,12)(R(I),ST1(I),SR1(I),SZ1(I),I=1,11)
      DO  200 I=1,N
      R(I)=FLOAT(I-1)*(R2-X)/FLOAT(N-1)+X
      AN=A*(R(I)*R(I)/2.*ALOG(R(I))-R(I)*R(I)/4.)+B/2.*R(I)*R(I)
     .-A*(X*X/2.*ALOG(X)-X*X/4.)
     .-B/2.*X*X
      D2(I)=CC/DD*AF2/R(I)*AN+C3*R(I)+C4/R(I)
      ER2(I)=CC/DD*AF2*(-AN/R(I)/R(I)+A*ALOG(R(I))+B)+C3-C4/R(I)/R(I)
```

```
      ET2(I)=D2(I)/R(I)
      DET2(I)=(ET2(I)-ET20(I))/DT
      ET20(I)=ET2(I)
      T2(I)=A*ALOG(R(I))+B
      ST2(I)=E2/CC*(DD/FF*ET2(I)+V2/FF*ER2(I))-AF2*E2/FF*T2(I)
      SZ2(I)=E2*V2/CC/FF*(ET2(I)+ER2(I))-AF2*E2/FF*T2(I)
      SR2(I)=E2/CC*(-CC/DD*AF2/R(I)/R(I)*AN+C3/FF-C4/R(I)/R(I))
      DSR2(I)=(SR2(I)-SR20(I))/DT
      IF(ST2(I).GT.SR2(I))STT2(I)=(ST2(I)-SR2(I))*0.5
      IF(SR2(I).GT.ST2(I))STT2(I)=(SR2(I)-ST2(I))*0.5
      DSTT2(I)=(STT2(I)-STT1(I))/DT
      SR20(I)=SR2(I)
      STT1(I)=STT2(I)
      T2(I)=T2(I)-0.03/AF2
200   CONTINUE
C     WRITE(2,11)  (R(I),D2(I),ER2(I),ET2(I),T2(I),I=1,11)
C     WRITE(2,11)(R(I),ST2(I),SR2(I),SZ2(I),STT2(I),I=1,11)
      WRITE(2,10)(R(I),DET2(I),I=1,11)
 15   FORMAT(3E12.4)
  1   CONTINUE
C     ************************************************************
C     DO 300  I=1,1000
C     X=R2-FLOAT(I-1)*R2/1000.
C300   CONTINUE
C     ************************************************************
 11   FORMAT(5E12.4)
 12   FORMAT(4E12.4)
 10   FORMAT(2E12.4)
      STOP
      END
```

APPENDIX 2

Computer Program for the 3-D Finite Element Analysis of the Research Model of the Ice-Cell Interaction during Freezing Process

The finite element analysis of the research model of the ice-cell interaction was conducted by using the software code, ABAQUS (Hibbitt, Karlsson, Sorensen Inc.). The following program was used (1) to generate the finite element grids and nodes for the cell membrane and (2) to submit all information required for the 3-D finite element analysis to the ABAQUS. Please see manuals of the ABAQUS for the detailed information concerning the ABAQUS program.

```
*HEADING
RBCSA
*NODE,SYSTEM=C
1,0.0,0.0,0.405D-4
2,6.8571429D-5,0.0,5.1048686D-5
9,6.8571429D-5,-315.0,5.1048686D-5
10,1.3714286D-4,0.0,7.8427701D-5
25,1.3714286D-4,-337.5,7.8427701D-5
26,1.8857143D-4,0.0,1.0288926D-4
57,1.8857143D-4,-348.75,1.0288926D-4
58,2.4D-4,0.0,1.2239424D-4
89,2.4D-4,-348.75,1.2239424D-4
90,2.9714286D-4,0.0,1.269954D-4
121,2.9714286D-4,-348.75,1.269954D-4
122,3.914285714D-4,0.0,4.4088808D-5
153,3.914285714D-4,-348.75,4.4088808D-5
154,4.0D-4,0.0,0.0
185,4.0D-4,-348.75,0.0
186,0.0,0.0,-0.405D-4
187,6.8571429D-5,0.0,-5.1048686D-5
```

```
194,6.8571429D-5,-315.0,-5.1048686D-5
195,1.3714286D-4,0.0,-7.8427701D-5
210,1.3714286D-4,-337.5,-7.8427701D-5
211,1.8857143D-4,0.0,-1.0288926D-4
242,1.8857143D-4,-348.75,-1.0288926D-4
243,2.4D-4,0.0,-1.2239424D-4
274,2.4D-4,-348.75,-1.2239424D-4
275,2.9714286D-4,0.0,-1.269954D-4
306,2.9714286D-4,-348.75,-1.269954D-4
307,3.914285714D-4,0.0,-4.4088808D-5
338,3.914285714D-4,-348.75,-4.4088808D-5
*NGEN,SYSTEM=C,LINE=C
2,9,1,,0.0,0.0,5.1048686D-5,0.0,0.0,-1.0
10,25,1,,0.0,0.0,7.8427701D-5,0.0,0.0,-1.0
26,57,1,,0.0,0.0,1.0288926D-4,0.0,0.0,-1.0
58,89,1,,0.0,0.0,1.2239424D-4,0.0,0.0,-1.0
90,121,1,,0.0,0.0,1.269954D-4,0.0,0.0,-1.0
122,153,1,,0.0,0.0,4.4088808D-5,0.0,0.0,-1.0
154,185,1,,0.0,0.0,0.0,0.0,0.0,-1.0
187,194,1,,0.0,0.0,-5.1048686D-5,0.0,0.0,-1.0
195,210,1,,0.0,0.0,-7.8427701D-5,0.0,0.0,-1.0
211,242,1,,0.0,0.0,-1.0288926D-4,0.0,0.0,-1.0
243,274,1,,0.0,0.0,-1.2239424D-4,0.0,0.0,-1.0
275,306,1,,0.0,0.0,-1.269954D-4,0.0,0.0,-1.0
307,338,1,,0.0,0.0,-4.4088808D-5,0.0,0.0,-1.0
*ELEMENT,TYPE=STRI3
1,1,3,2
2,1,4,3
3,1,5,4
4,1,6,5
5,1,7,6
6,1,8,7
7,1,9,8
8,1,2,9
9,11,2,3
10,13,3,4
11,15,4,5
12,17,5,6
13,19,6,7
14,21,7,8
15,23,8,9
16,25,9,2
17,2,11,10
18,3,12,11
19,3,13,12
20,4,14,13
21,4,15,14
22,5,16,15
23,5,17,16
24,6,18,17
25,6,19,18
```

```
26,7,20,19
27,7,21,20
28,8,22,21
29,8,23,22
30,9,24,23
31,9,25,24
32,2,10,25
33,27,10,11
34,29,11,12
35,31,12,13
36,33,13,14
37,35,14,15
38,37,15,16
39,39,16,17
40,41,17,18
41,43,18,19
42,45,19,20
43,47,20,21
44,49,21,22
45,51,22,23
46,53,23,24
47,55,24,25
48,57,25,10
49,10,27,26
50,11,28,27
51,11,29,28
52,12,30,29
53,12,31,30
54,13,32,31
55,13,33,32
56,14,34,33
57,14,35,34
58,15,36,35
59,15,37,36
60,16,38,37
61,16,39,38
62,17,40,39
63,17,41,40
64,18,42,41
65,18,43,42
66,19,44,43
67,19,45,44
68,20,46,45
69,20,47,46
70,21,48,47
71,21,49,48
72,22,50,49
73,22,51,50
74,23,52,51
```

```
75,23,53,52
76,24,54,53
77,24,55,54
78,25,56,55
79,25,57,56
80,10,26,57
81,59,26,27
112,58,57,26
113,26,59,58
144,57,58,89
176,90,89,58
208,89,90,121
240,122,121,90
272,121,122,153
273,155,122,123
304,154,153,122
305,122,155,154
336,153,154,185
337,186,187,188
338,186,188,189
339,186,189,190
340,186,190,191
341,186,191,192
342,186,192,193
343,186,193,194
344,186,194,187
345,196,188,187
346,198,189,188
347,200,190,189
348,202,191,190
349,204,192,191
350,206,193,192
351,208,194,193
352,210,187,194
353,187,195,196
354,188,196,197
355,188,197,198
356,189,198,199
357,189,199,200
358,190,200,201
359,190,201,202
360,191,202,203
361,191,203,204
362,192,204,205
363,192,205,206
364,193,206,207
365,193,207,208
366,194,208,209
367,194,209,210
368,187,210,195
```

```
369,212,196,195
370,214,197,196
371,216,198,197
372,218,199,198
373,220,200,199
374,222,201,200
375,224,202,201
376,226,203,202
377,228,204,203
378,230,205,204
379,232,206,205
380,234,207,206
381,236,208,207
382,238,209,208
383,240,210,209
384,242,195,210
385,195,211,212
386,196,212,213
387,196,213,214
388,197,214,215
389,197,215,216
390,198,216,217
391,198,217,218
392,199,218,219
393,199,219,220
394,200,220,221
395,200,221,222
396,201,222,223
397,201,223,224
398,202,224,225
399,202,225,226
400,203,226,227
401,203,227,228
402,204,228,229
403,204,229,230
404,205,230,231
405,205,231,232
406,206,232,233
407,206,233,234
408,207,234,235
409,207,235,236
410,208,236,237
411,208,237,238
412,209,238,239
413,209,239,240
414,210,240,241
415,210,241,242
416,195,242,211
417,244,212,211
448,243,211,242
```

```
449,211,243,244
480,242,274,243
512,275,243,274
544,274,306,275
576,307,275,306
608,306,338,307
609,155,308,307
640,154,307,338
641,307,154,155
672,338,185,154
*ELGEN
81,31,1,1,3,32,64
113,31,1,1,3,32,64
273,31,1,1
305,31,1,1
417,31,1,1,3,32,64
449,31,1,1,3,32,64
609,31,1,1
641,31,1,1
*ELSET,ELSET=UP,GENERATE
1,336
*ELSET,ELSET=DOWN,GENERATE
337,672
*ELSET,ELSET=LOOK,GENERATE
1,208
*SHELL SECTION,ELSET=UP
7.0D-7
*SHELL SECTION,ELSET=DOWN
7.0D-7
*MATERIAL
*ELASTIC
1.0,0.5
**BOUNDARY
**RR,1
*PLOT
*DRAW
*DETAIL,ELSET=UP
*VIEWPOINT
1.0,1.0,0.5
*DRAW
*VIEWPOINT
1.0,1.0,-1.0
*DRAW
*DETAIL,ELSET=LOOK
*DRAW,ELNUB,NODENUB
*DETAIL,ELSET=DOWN
*DRAW,ELNUB,NODENUB
*VIEWPOINT
1.0,0.0,0.0
```

```
*DRAW
*VIEWPOINT
1.0,0.0,0.0
*DETAIL
-5.0D-4,-0.5D-5,-1.5D-4,5.0D-4,0.5D-5,1.5D-4
*DRAW
**STEP,LINEAR=NEW
**DLOAD
**PLOT
**DISPLACED
**DETAIL,ELSET=CORNER
**DISPLACED
**EL PRINT,COORDS,TEMPS,ELSET=TUBE
**EL PRINT,COORDS,TEMPS,ELSET=TUBSHE
**END STEP
```